Summer 8-15-2019

Understanding Excitation Energy Quenching in IsiA

Hui-Yuan Steven Chen
Washington University in St. Louis

WASHINGTON UNIVERSITY IN ST. LOUIS

McKelvey School of Engineering

Department of Energy, Environmental, and Chemical Engineering

Dissertation Examination Committee:
Himadri B. Pakrasi, Chair
Robert E. Blankenship
Michael L. Gross
Tae Seok Moon
Yinjie Tang
Fuzhong Zhang

Understanding Excitation Energy Quenching in IsiA

by

Hui-Yuan Steven Chen

A dissertation presented to
The Graduate School
of Washington University in
partial fulfillment of the
requirements for the degree
of Doctor of Philosophy

Aug 2019
St. Louis, Missouri

Table of Contents

List of Figures

List of Tables

Acknowledgments

I would like to thank my advisor, Dr. Himadri Pakrasi, for his support, patience and encouragement during the past five years. I still remember when he carefully went through my first monthly report with me and made sure that I understood what I wrote. As someone who had a chemical engineering background and barely heard anything about photosystems before, without his patient guidance, I could not come this far. My thanks also go to the members of my thesis committee, Drs. Robert Blankenship, Michael Gross, Tae Seok Moon, Yinjie Tang, Fuzhong Zhang for their insightful comments and some hard questions. I would like to acknowledge the Photosynthetic Antenna Research Center (PARC), an Energy Frontier Research Center funded by the U.S. Department of Energy, Office of Science, Office of Basic Energy Sciences under Award Number DE-SC 0001035 and DOE-BES grant from Chemical Sciences, Geosciences, and Biosciences Division, Office of Basic Energy Sciences, Office of Science, U.S. Department of Energy (grant no. DE-FG02-99ER20350 to Dr. Pakrasi), for supporting my research during the past five years.

I thank Dr. Daniel Weisz, the person helped me starting as a fresh biochemist, for not only training, but also valuable advice he gave me on how to survive graduate school. I would like to express my gratitude to Drs. Justin Ungerer, Michelle Liberton and Po-Cheng Lin for their assistance in studies on cyanobacterial cultivations, genome editing as well as physiological analysis.

I thank Dr. Anindita Bandyopadhyay for the helpful discussions and her assistance in cyanobacterial genome analysis while writing Chapter 1. The phylogenetic analysis in Chapter 1 and protein sequence alignment in Chapter 4 were performed by Dr. Anindita Bandyopadhyay. I

thank Dr. Dariusz Niedzwiedzki for his fantastic spectroscopy lessons, from which I benefitted greatly. The time-resolved spectroscopic analyses in Chapter 2 and 3 were performed by Dr. Dariusz Niedzwiedzki. We thank Ultrafast Laser Facility of Photosynthetic Antenna Research Center (PARC). I thank Dr. Jesús Barrera Roja for teaching me the hrCN-PAGE and 2D-SDS techniques and the results are shown in Appendix 1. I thank Drs. Hajime Wada and Hisako Kubota for kindly sharing the PsaF-His and PsaJ-His *Synechocystis* strains with us. I would also like to thank Dr. Gross and all the members in Gross lab. I enjoyed the group meetings and learned a lot about mass spectrometry. I am grateful to all the members of the Pakrasi lab. I really appreciate the exchange of brilliant ideas, fun conversations and the wonderful working environments.

Chaoran, my lovely wife, thank you for your love and support. I am the luckiest man in the world.

My special thanks go to my mother and sister. They are always supportive and have faith in me.

Hui-Yuan Steven Chen

Washington University in St. Louis

Aug 2019

In memory of my father,

the most brilliant and humorous man I have ever known.

Abstract of The Dissertation

Understanding Excitation Energy Quenching in IsiA

by

Hui-Yuan Steven Chen

Doctor of Philosophy in Energy, Environmental, and Chemical Engineering

Washington University in St. Louis, 2019

Professor Himadri B. Pakrasi, Chair

Cyanobacteria are photoautotrophic organisms that contribute a significant amount of global primary productivity. They are found in freshwater, marine and even some extremely severe environments. Among those environments, iron deficiency is one of the most common stress conditions in cyanobacterial habitats. To survive, cyanobacteria have evolved and developed several strategies to alleviate the damage caused by iron deficiency.

Iron stress-inducible protein (IsiA) is a chlorophyll-binding membrane protein found in cyanobacteria grown in iron-deficient conditions. During the past decades, considerable effort has been put on understanding how IsiA functions to help cyanobacteria survive iron deficiency. It was reported that IsiA forms various ring-shaped complexes with PSI (PSI_x-$IsiA_y$) or by itself (IsiA aggregate). While coupled with PSI (PSI_x-$IsiA_y$), the IsiA protein serves as an accessary antenna for PSI, which increases the absorption cross-section by 60% compared with the PSI trimer. IsiA aggregate, instead, dissipates excess light energy to prevent the cells from photodamage. Although these functions have been discovered and demonstrated *in vivo* and *in*

vitro, the detailed mechanisms, especially the non-photochemical quenching process in IsiA, were not well understood.

In this study, the excitation energy quenching process in IsiA was investigated by time-resolved spectroscopy, and we proposed that IsiA dissipates excitation energy via a cysteine-mediated quenching process. Site-directed mutagenesis was performed to replace this critical cysteine (C260) in IsiA with a valine. This single amino acid substitution in IsiA results in a defective IsiA, which no longer quenches excitation energy but still functions as light-harvesting antenna for PSI. Interestingly, this IsiA mutant grew faster than the wild type in the presence of iron under high light, suggesting a more efficient use of light energy owing to the abolishment of a photoprotective mechanism.

Sharing a similar structure with IsiA, CP43, an intrinsic antenna of PSII, has not been reported being involved in excitation energy quenching process. We attempted to introduce this cysteine-mediated quenching process into CP43 to provide directly photoprotection to the reaction center of PSII. The mutant CP43 phenotypes showed a 25% lower quantum efficiency of PSII and barely grew photoautotrophically, implying an inefficient energy transfer to the reaction center of PSII caused by the introduction of an extrinsic quenching process.

1. Chapter One: Introduction: Function, regulation and distribution of IsiA, a membrane bound chlorophyll *a*-antenna protein in cyanobacteria

This chapter was adapted from:

Chen H-Y, Bandyopadhyay A, Pakrasi H (2018) Function, regulation and distribution of IsiA, a membrane-bound chlorophyll *a*-antenna protein in cyanobacteria. *Photosynthetica* 56 (1):322-333

A.B. performed the phylogenetic analysis.

1.1 Abstract

IsiA is a membrane bound Chl *a*-antenna protein synthesized in cyanobacteria under iron-deficiency. Because iron-deficiency is a common nutrient stress in significant fractions of cyanobacterial habitats, IsiA is likely to be essential for some cyanobacteria. However, the role it plays in cyanobacteria is not fully understood. In this chapter, we summarize research efforts directed towards characterizing IsiA over the past three decades and attempt to bring all the pieces of the puzzle together to get a more comprehensive understanding of the function of this protein. Moreover, we analyzed the genomes of over 390 cyanobacterial strains available in the JGI/IMG database to assess the distribution of IsiA across the cyanobacterial kingdom. Our study revealed that only 125 such strains have an IsiA homolog, suggesting that the presence of this protein is a niche specific requirement, and cyanobacterial strains that lack IsiA might have developed other mechanisms to survive iron-deficiency.

1.2 Introduction

The Earth's atmosphere has undergone a gradual transformation into an oxidative environment since the great oxidation event in which photosynthetic organisms like cyanobacteria are thought to have played a major role (Lane 2002; Holland 2006). As the oxygen level increased, Fe (II) was oxidized to Fe (III), resulting in the formation of water-insoluble oxides of iron. This led to the low bioavailability of iron in aquatic environments despite it being the fourth most abundant element in the Earth's crust. The low bioavailability of iron in aquatic ecosystems (Vrede and Tranvik 2006; North *et al.* 2007; Martin and Fitzwater 1988; Moore *et al.* 2013) has been a challenge for cyanobacteria. Pronounced effects of iron stress in cyanobacteria are the decreased levels of chlorophyll-binding proteins, phycobilisomes (PBS), cytochromes and ferredoxins

(Guikema and Sherman 1984; Fitzgerald *et al.* 1977; Sherman and Sherman 1983). A strategy that cyanobacteria have evolved to overcome such negative effects, is replacing these proteins with functional homologs that demand no iron. For instance, a flavodoxin, encoded by *isiB* (iron stress-induced) gene, is synthesized by many cyanobacteria under iron-stress conditions. This flavodoxin acts as a functional homolog of ferredoxin and compensates for its loss (Fitzgerald *et al.* 1977; Guikema and Sherman 1984). Other remarkable changes observed in iron-starved cyanobacterial cells are the decrease of PSI and PSII contents, the increase of PSII/PSI ratios, as well as the synthesis of a chlorophyll-binding protein with the molecular weight of about 36 KD called CPVI-4 (Pakrasi *et al.* 1985a; Pakrasi *et al.* 1985b). With sufficient iron, PSI and PSII are the major chlorophyll-binding protein complexes in cyanobacteria (Pakrasi *et al.* 1985a; Pakrasi *et al.* 1985b). Under iron-deficient conditions, CPVI-4 protein becomes the dominant chlorophyll-binding protein (Burnap *et al.* 1993), which implies that the synthesis of CPVI-4 may be produced to compensate for the loss of photosystems, especially for PSI. CPVI-4 is a product of an iron-induced gene, *isiA* (Burnap *et al.* 1993). This gene was initially discovered as part of an iron-stress induced operon that includes a flavodoxin gene, *isiB* (Laudenbach and Straus 1988). It was later shown that *isiA* can be elsewhere in the genome and expressed independently of *isiB* (Leonhardt and Straus 1994).

Because iron-deficiency is a common nutrient stress in notable portions of cyanobacterial habitats (Bibby *et al.* 2009; Martin and Fitzwater 1988; North *et al.* 2007; Vrede and Tranvik 2006; Moore *et al.* 2013) and the production of IsiA is one of the most noticeable responses to iron-deficiency, it is reasonable to consider that the IsiA content in thylakoid membranes of cyanobacteria in certain environments is always maintained at high levels. In fact, it was reported that *isiA* was found in iron-limited oceanic environments (Bibby *et al.* 2009;

Behrenfeld *et al.* 2006; Schrader *et al.* 2011), demonstrating the significant role that IsiA plays in helping cyanobacteria survive in iron-deficient environments. The importance of IsiA in stressed cyanobacteria has drawn the attention of researchers over the past decades, and numerous hypotheses about the functions of IsiA have been proposed. Despite all the efforts, the pieces of the puzzle are yet to come together. In this chapter, we review the efforts directed towards elucidating the attributes of the IsiA protein over the past decades. We have also attempt to analyze the currently rich repertoire of sequenced cyanobacterial strains to assess the distribution of this protein across the cyanobacterial kingdom and hypothesize plausible roles for it in these organisms.

1.3 Characteristics of IsiA protein

The discovery of the IsiA protein dates to the early 1970's when Öquist reported altered spectral properties in iron-deficient cyanobacterial cells (Oquist 1971). Following this, in the early 80's, the Sherman lab demonstrated that cyanobacterial cells subjected to iron starvation for a prolonged period can undergo severe structural and functional alterations (Guikema and Sherman 1983a; Sherman and Sherman 1983). A blue-shift of Chl *a* absorbance from 685 nm to 673 nm and the presence of a sharp peak at ~685 nm in the 77 K fluorescence emission spectrum of cyanobacterial cells was observed in iron-starved cyanobacteria (Oquist 1971; Burnap *et al.* 1993; Falk *et al.* 1995). In addition, a significant decrease in the PSI and PSII contents of the cells and synthesis of CPVI-4 protein were observed under these conditions (Guikema and Sherman 1984, 1983b; Burnap *et al.* 1993; Pakrasi *et al.* 1985a). It was later demonstrated that the spectral changes in iron-starved cells was also associated with the presence of CPVI-4 protein (Pakrasi *et al.* 1985a; Guikema and Sherman 1983a; Pakrasi *et al.* 1985b). The nucleotide sequence analysis in *Anacystis*

nidulans R2 (*Synechococcus* sp. PCC7942) revealed that a gene, *isiA*, was in the same operon as *isiB* (which encodes for flavodoxin), right upstream of it (Laudenbach *et al.* 1988; Leonhardt and Straus 1992). A later report demonstrated that the CPVI-4 protein synthesized in iron-starved cells was encoded by the *isiA* gene (Burnap *et al.* 1993). The nucleotide sequence analysis showed that *isiA* is highly homologous to CP43 (Laudenbach and Straus 1988), a chlorophyll-binding membrane protein, which is a core antenna of PSII. Crystallographic analysis of PSII showed that CP43 has six-transmembrane helices and binds to 13 Chl *a* (Barber *et al.* 2000; Ferreira *et al.* 2004; Umena *et al.* 2011). The folding diagram of IsiA based on its nucleotide sequence in *Synechocystis* PCC 6803 and a hydropathy analysis suggested that IsiA also had six transmembrane helices and the histidine residues were conserved, implying that IsiA may bind to 13 Chl *a* (Bibby *et al.* 2001b; Feng *et al.* 2011). Later, a comparative study of the integrated absorption of PSI and IsiA, indicated that IsiA possesses 13~16 Chl *a* (Feng *et al.* 2011; Andrizhiyevskaya *et al.* 2002). Despite the similarity, a noticeable difference between CP43 and IsiA is that the large loop on the lumenal side joining helices V and VI in CP43 is missing in IsiA, thus resulting in the ~100 less amino acid residues in IsiA than in CP43 (Bibby *et al.* 2001b).

IsiA was found to form an antenna ring around PSI trimer under iron-deficient conditions (Boekema *et al.* 2001; Bibby *et al.* 2001a). Electron microscopy single-particle analysis revealed that the PSI-IsiA supercomplex consisted of 18 IsiA and a trimeric PSI (Boekema *et al.* 2001; Bibby *et al.* 2001a). Later reports showed that during prolonged iron-starvation, the number of IsiA and PSI monomers varied in the PSI-IsiA supercomplexes (Yeremenko *et al.* 2004). At times, empty IsiA rings were also detected under such conditions (Yeremenko *et al.* 2004; Chauhan *et al.* 2011). While IsiA was considered to be mainly associated with PSI, it was originally proposed to serve as an antenna for PSII to compensate the loss of phycobilisomes

during iron-starvation (Pakrasi *et al.* 1985b). A recent study reported the formation of IsiA-PSI-PSII supercomplex under iron-deficient as well as under high light conditions (Wang *et al.* 2010). In addition, the presence of IsiA in a complex containing PsaD, slr1128, and high light-inducible proteins (Hilps) under high light conditions were also reported (Wang *et al.* 2008; Daddy *et al.* 2015). However, this Hlip-containing complex could not be detected when Komenda and Sobotka (Komenda and Sobotka 2016) attempted to reproduce the above results. Therefore, whether IsiA is involved in the Hlip-containing complex remains unclear, and further investigation is needed.

Unlike *isiB* gene (Kutzki *et al.* 1998), *isiA* was shown to be an essential gene in iron-starved cyanobacteria by insertional mutagenesis (Burnap *et al.* 1993). Since it was reported that iron-deficiency is common in significant fractions of the habitats of cyanobacteria (Vrede and Tranvik 2006; North *et al.* 2007; Martin and Fitzwater 1988; Moore *et al.* 2013; Bibby *et al.* 2009) and *isiA* was detected in several model cyanobacteria, *isiA* was thought to be widespread in species across the cyanobacterial kingdom (Geiss *et al.* 2001a). However, later reports showed that some cyanobacterial strains including *Synechococcus* WH 8102 did not have *isiA* (Bailey *et al.* 2005). In addition, instead of IsiA, prochlorophytes including *Prochloron*, *Prochlorothrix,* and *Prochlorococcus* were found to have prochlorophyte chlorophyll *a/b* protein (Pcb), which is also a member of the six-transmembrane helices antenna super-family (La Roche *et al.* 1996). The field measurements conducted in the global ocean demonstrated that *isiA* is more prevalent in some iron-limiting oceanic regions, such as equatorial Pacific and Atlantic (Ryan-Keogh *et al.* 2012; Richier *et al.* 2012; Schrader *et al.* 2011). These facts conflict with the idea that *isiA* gene is commonly distributed in most cyanobacterial strains. Therefore, the physiological significance of IsiA and the role it plays in cyanobacteria need to be revisited.

1.4 Expression of IsiA

The transcripts of *isiAB* (iron stress-inducible) operon, encoding for IsiA protein and flavodoxin, was first identified when *Anacystis nidulans* R2 (*Synechococcus* sp. PCC7942) was grown under iron-deficient conditions (Laudenbach and Straus 1988; Laudenbach *et al.* 1988). However, later reports showed that *isiAB* operon could also be transcribed under other stressful conditions including high salt, heat shock (Vinnemeier *et al.* 1998), high light (Havaux *et al.* 2005), limiting light (Foster *et al.* 2007; Sandrini *et al.* 2016), and oxidative stress (Li *et al.* 2004; Yousef *et al.* 2003) conditions as well as in some mutants such as *psaFJ*-null mutant (Jeanjean *et al.* 2003) and cytochrome c_6-deficient mutant (Ardelean *et al.* 2002). However, it should be noted that the synthesis and integration of IsiA in thylakoid membranes were not observed under some of the conditions mentioned above.

The induction of *isiAB* operon as a function of the ammonium ferric citrate ($Fe(NH_4)$ citrate) concentration in *Synechocystis* 6803 was determined by monitoring the fluorescence signal of GFP fused with *isiAB* promoter in iron-starved cells at different $Fe(NH_4)$ citrate concentration (Geiss *et al.* 2001a). The results showed a noticeable increase in GFP fluorescence signal when the $Fe(NH_4)$ citrate concentration was below 0.77 μM (Geiss *et al.* 2001a), which again confirmed that the *isiAB* promoter is iron-responsive. Meanwhile, the mechanism of iron-responsive regulation controlling *isiAB* expression was studied (Kunert *et al.* 2003; Vinnemeier *et al.* 1998; Ghassemian and Straus 1996). One of the hypotheses is that the *isiAB* expression is controlled by the ferric uptake regulator (Fur) (Kunert *et al.* 2003; Vinnemeier *et al.* 1998; Ghassemian and Straus 1996), a repressor binding to a Fur box under iron-replete conditions to repress gene expression, which is commonly found in prokaryotes (Stojiljkovic and Hantke 1995). Under

nutrient-replete conditions, the Fur repressor binds to a Fur box upstream of *isiAB* operon and prevent the binding of RNA polymerase. On the other hand, under stressful conditions, the Fur repressor falls off, and the expression of *isiAB* becomes possible (Kunert *et al.* 2003; Vinnemeier *et al.* 1998). As expected, the Fur box consensus sequences were found upstream of *isiA* gene in some cyanobacteria (Kunert *et al.* 2003), and the de-repression of *isiAB* operon was observed in the strains with insertional mutagenesis of *fur* gene (Ghassemian and Straus 1996). To determine further the regulatory elements controlling *isiAB* expression, GFP-containing strains were constructed in which GFP was fused with truncated *isiAB* promoter fragments containing different compositions of regulatory elements, which include the A+T-rich region, inverted repeat (IR), and the Fur box (Kunert *et al.* 2003). Intriguingly, the truncation of the sequence between the A+T-rich and IR regions dramatically reduced the GFP fluorescence detected in iron-deficient conditions. This region was, therefore, considered to act as an unidentified positive regulatory element. Furthermore, a deletion of the Fur box also resulted in lower GFP fluorescence under iron-deficient conditions compared to iron-replete conditions, suggesting that an unrevealed mechanism is involved in repressing *isiAB* expression (Kunert *et al.* 2003). Besides the regulatory mechanism at transcriptional level, an antisense, IsrR (iron stress-repressed RNA), was identified to be involved in the posttranscriptional regulation of *isiA* expression (Duhring *et al.* 2006). IsrR is a cis-encoded antisense transcribed from the noncoding strand of *isiA* gene. It forms IsrR-*isiA* RNA heteroduplexes with *isiA* mRNA, and the heteroduplexes are targeted for selective degradation (Duhring *et al.* 2006). The inverse relationship between IsrR and *isiA* mRNA has been determined under oxidative stress, iron-deficient, and high light conditions (Duhring *et al.* 2006). It is likely that IsrR is also present under the stressful conditions mentioned above, but the accumulation of *isiA* mRNA exceeds the amount of IsrR, thus resulting in the production of IsiA

(Duhring *et al.* 2006). This regulatory machinery enables the cyanobacteria to respond instantly to the environmental signals and control the expression of *isiA*. No *isiA* mRNA was detected from the IsrR knock-down strain in iron-replete conditions, implying that IsrR regulatory mechanism was independent of the Fur mechanism (Duhring *et al.* 2006). However, this does not explain the expression/ de-repression of *isiA* in other stressful conditions.

To elucidate the factors responsible for the induction of the *isiAB* operon, stress conditions other than iron-deficiency were also studied, and the results suggested that cross-talks between multiple stress-induced genes existed (Michel and Pistorius 2004; Yousef *et al.* 2003; Jeanjean *et al.* 2003; Havaux *et al.* 2005). The production of reactive oxygen species (ROS) is inevitable in photosynthetic organism, thus resulting in the oxidative stress in cells. A strong and rapid induction of *isiAB* operon was determined when *Synechocystis* PCC 6803 was treated with 75 µM H_2O_2 (Yousef *et al.* 2003; Li *et al.* 2004). In addition, studies focusing on the responses of cyanobacterial cells to oxidative stress conditions suggested that the ROS may interfere with the binding of Fur or PerR with the DNA as ROS was known to extract their metal cofactors and, thus, de-repress the iron inducible genes (Li *et al.* 2004). Interestingly, it was reported that no *isiA* transcript was detected in cells grown in iron and manganese co-limiting conditions (Salomon and Keren 2015). Because manganese-depletion led to a decrease in the PSII content, resulting in the limited production of ROS, the absence of *isiA* transcript in the cells under these conditions revealed the connection between *isiA* expression and oxidative stress, which appears to be a superior trigger for *isiA* expression (Salomon and Keren 2015). Besides *isiAB*, researchers found that some other iron-inducible genes, such as *idiA* (iron-deficiency-induced), a gene encoding for a protein produced under stressful conditions involved in protecting PSII against the damage caused by ROS (Michel and Pistorius 2004; Michel *et al.* 1996), were also induced under oxidative

stress. Even though the expression of *isiA* and *idiA* were thought to be controlled independently by Fur and IdiB (Michel *et al.* 1996), respectively, the *idiB* deletion strain showed a decreased IsiA content under iron-deficient conditions, which implied the cross-talk between the iron inducible genes. Given that the stressful conditions inducing *isiAB* operon are either linked to oxidative stress or iron-deficiency, a strong relationship between iron homeostasis and oxidative stress in cyanobacterial cells was proposed (Yousef *et al.* 2003; Michel and Pistorius 2004). These findings explained the induction of *isiAB* operon under some stressful conditions, other than iron stress, and supported the hypothesis that the cross-talk among stress-inducible genes are involved in *isiAB* expression. However, the expression of *isiA* was also observed in the cells transitioning into stationary growth phase under normal physiological conditions without any stress imposed (Singh and Sherman 2006). Therefore, further investigation is needed to elucidate the entire story of the expression of *isiA*.

The time course studies on synthesis and integration of IsiA protein in thylakoid membranes under iron-deficient conditions (Pakrasi *et al.* 1985a; Fraser *et al.* 2013; Ma *et al.* 2017; Ryan-Keogh *et al.* 2012; Yeremenko *et al.* 2004) provided another aspect for understanding the dynamic changes of *isiA* expression. IsiA was first identified as CPVI-4 protein (Pakrasi *et al.* 1985b), isolated from *Synechococcus* sp. PCC7942 cells iron-starved for 4 to 5 days. In addition, the PSI-IsiA supercomplex with 18 IsiA and 1 trimeric PSI was also isolated and visualized from *Synechocystis* PCC 6803 and *Synechococcus* sp. PCC7942 cells after short-term iron-starvation (Boekema *et al.* 2001; Bibby *et al.* 2001a). It was later revealed that various other IsiA-associated supercomplexes can be formed within a few additional days of iron-starvation (Yeremenko *et al.* 2004; Kouril *et al.* 2005). Yeremenko *et al.* (2004) performed electron microscopy followed by particle analysis on protein complexes isolated from *Synechocystis* PCC 6803 cells grown under

conditions of prolonged iron-deficiency and visualized the IsiA ring structures with various compositions of IsiA and PSI (Yeremenko *et al.* 2004). Although the majority of PSI-IsiA supercomplexes found was PSI_3IsiA_{18}, with longer period of iron-deficiency, smaller ring structures consisting of 12~14 IsiA and 1 PSI monomer, larger ones comprised of double IsiA rings with PSI at the center, IsiA double rings without PSI, as well as partial ring structures were observed (Yeremenko *et al.* 2004). However, it is difficult to monitor the exact amount of all these supercomplexes during iron-starvation. To understand the dynamic changes of IsiA-associated ring structures during iron-starvation, others have attempted to track the amount of bound and unbound IsiA at different time points (Ryan-Keogh *et al.* 2012; Fraser *et al.* 2013). It was found that the amount of unbound IsiA increased as the iron-starvation was prolonged, and the growth of cells slowed after 72 hr (Ryan-Keogh *et al.* 2012; Fraser *et al.* 2013). Nevertheless, the spectroscopic results showed fluorescence quenching caused by unbound IsiA at the early iron-starvation stage (van der Weij-de Wit *et al.* 2007). A recent study showed the complexities of IsiA-associated supercomplexes while the thylakoid protein complexes were separated by sucrose gradient ultracentrifugation from cells after 1-15 days of iron-starvation (Ma *et al.* 2017). The protein fractions isolated from thylakoid membranes became more complicated as the iron-starvation was prolonged and revealed distinct fluorescence properties (Ma *et al.* 2017). These findings suggested that IsiA proteins in various ring structures assembled during iron-starvation, probably served distinct purposes to meet the need at different levels of iron-deficiency.

The nutrient availabilities and the expression of IsiA in the world's oceans were also studied. In oligotrophic water and high-nitrate low-chlorophyll (HNLC) regions, bioavailability of iron is the main factor that limits the growth of phytoplankton (North *et al.* 2007; Martin and Fitzwater 1988; Coale *et al.* 1996; Tsuda *et al.* 2003). The analysis of a dataset obtained from the

Global Ocean Sampling Project, has revealed the environmental diversity of chlorophyll-binding protein complexes (Bibby *et al.* 2009). The *pcb*/*isiA* gene family has a higher genetic diversity in the open-ocean regions, and the *isiA*-like gene was found predominately at the interface of two geographically defined ocean regions that are dominated by *pcb*-type and PBS-type light harvesting systems, respectively. It was suggested that *isiA*-like gene was restricted to a defined oceanic region, so that the detection of *isiA*-like gene could be used as a biomarker of iron-limitation in the ocean. Other studies suggested that 30% of the ocean is an HNLC region, in which the low F_v/F_m value was detected and attributed to the presence of uncoupled IsiA rings (Behrenfeld *et al.* 2006; Moore *et al.* 2013). Schrader *et al.* (2011) investigated *isiA* expression in *Synechocystis* PCC 6803 under iron and nitrogen co-limiting as well as high-nitrate low-iron conditions to mimic the natural environments (Schrader *et al.* 2011). Interestingly, the cells grown in co-limiting conditions showed low fluorescence emission and high F_v/F_m values similar to that of cells grown under nutrient-replete conditions (Schrader *et al.* 2011). On the other hand, cells grown in high nitrate and low iron, or HNLC, conditions showed high fluorescence emission and low energy-transfer efficiency (Schrader *et al.* 2011). In addition, cells grown under co-limiting conditions had limited IsiA, whereas under HNLC conditions, the cells possessed a huge IsiA pool that was not coupled with PSI (Schrader *et al.* 2011). These results suggest that the majority of IsiA produced under co-limiting conditions was well-coupled with PSI and served as an accessary antenna of PSI. The energy transfer from IsiA to PSI was efficient so that the IsiA did not contribute to the fluorescence emission. Under high-nitrate, low-iron conditions, a huge amount of IsiA antenna decoupled from PSI reaction center was produced, thus leading to the high fluorescence emission and low energy transfer efficiency (Schrader *et al.* 2011). The field studies conducted by collecting and analyzing the phytoplankton populations from HNLC, co-limiting

and nutrient-replete regions showed spectroscopic properties that were in agreement with laboratory experimental data (Schrader *et al.* 2011). The field data revealed the possible composition of photosynthetic proteins in cyanobacteria living in aquatic habitats with different nutrient availabilities. In nutrient-replete environments, cyanobacteria have PSI, PSII with phycobilisome and no IsiA; in co-limiting regions, cyanobacteria have decreased PSI, limited IsiA coupled with PSI and PSII with no phycobilisome; in HNLC environments, cyanobacteria have decreased PSI, IsiA coupled with PSI, IsiA rings decoupled from PSI, and PSII with phycobilisome attached (Figure 1.1). Furthermore, the results from field studies and laboratory experiments supported that up to half of total chlorophyll in HNLC existed in uncoupled IsiA complexes and remained *Photosynthetica*lly inactive (Schrader *et al.* 2011; Behrenfeld *et al.* 2006).

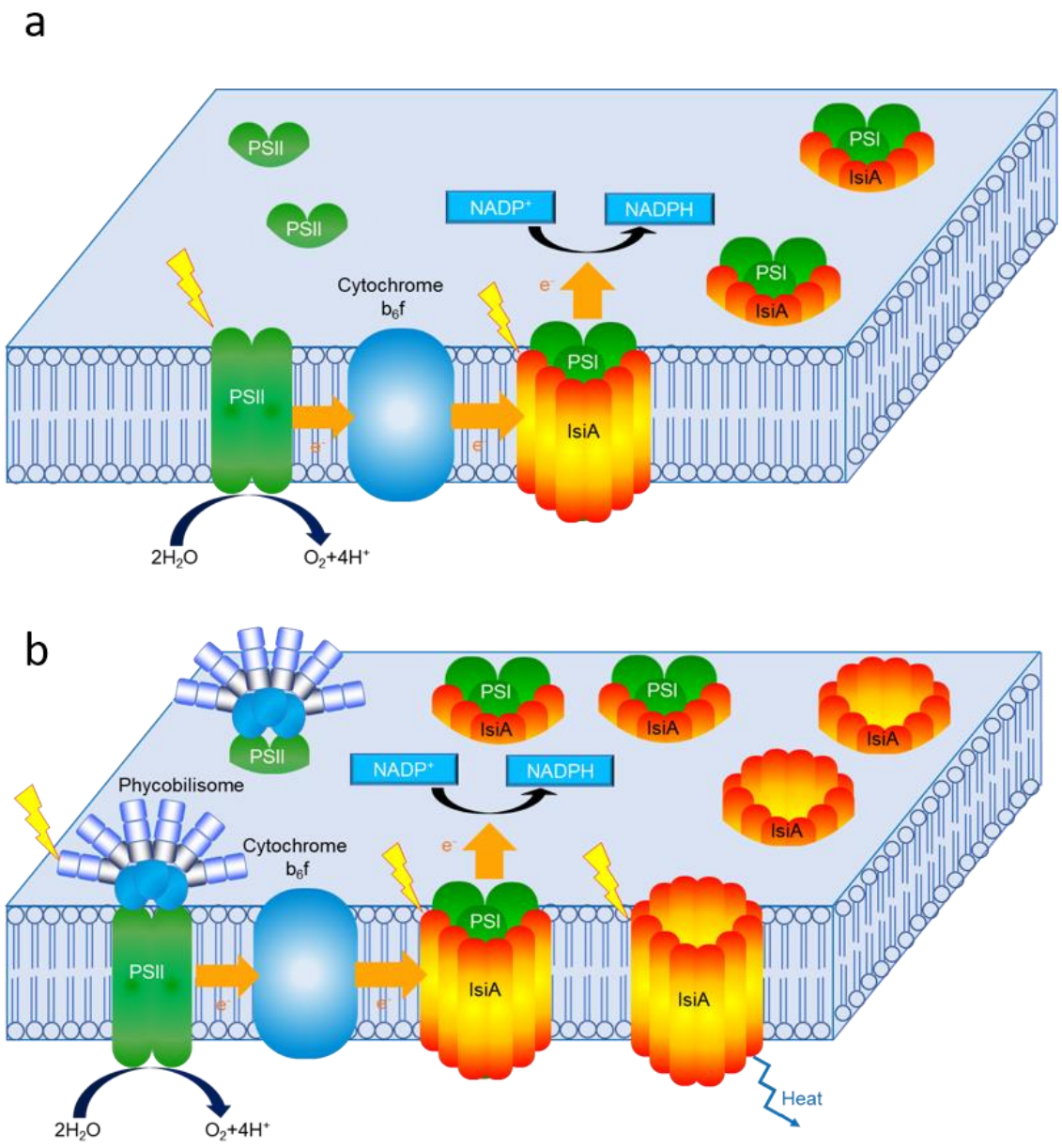

Figure 1.1 A schematic model of thylakoid membranes of cyanobacteria grown under (a) iron and nitrogen co-limiting and (b) HNLC conditions. Under co-limiting conditions, cyanobacterial thylakoid membranes contain PSI-IsiA and PSII without phycobilisomes. While under HNLC conditions, cyanobacterial thylakoid membranes have PSI-IsiA, IsiA rings and PSII with phycobilisomes attached.

1.5 Distribution and Phylogeny of IsiA

Earlier studies focused on IsiA have relied on molecular techniques as well as genome sequence data to evaluate its distribution across the cyanobacterial kingdom (Geiss *et al.* 2001a; Bibby *et al.* 2009; Shih *et al.* 2013). Although initially thought to be widespread among cyanobacteria (Geiss *et al.* 2001a), later studies with marine microbes indicated that the gene is not ubiquitous in cyanobacteria (Bailey *et al.* 2005; Bibby *et al.* 2009). Shih *et al.* (2013) studied the distribution of chlorophyll binding proteins (CBP's) and found them to be widely distributed (84 of the 126 strains studied) across the cyanobacterial phylum. In this analysis, *isiA* containing strains formed the largest clade of the CBP's (CBPIII). In the recent past, there has been an upsurge in the cyanobacterial gene sequence database, with the sequences of many ecologically and physiologically diverse strains becoming available. This provides us with a unique opportunity to assess the relevance of this protein across the cyanobacterial phylum.

We analyzed the genomes of ~ 390 cyanobacterial strains currently available in the JGI/IMG database for the presence of the *isiA* gene. A blastp search for IsiA across the available strains was performed, using *Synechocystis* 6803 IsiA, a 342 amino acid protein, as the template, and hits with ≥ 70% identity were designated as homologs of IsiA. In addition, some hits with lower percent identity but with proximity to the *isiB* gene in the genome and/or presence of a corresponding antisense RNA were also included as IsiA homologs for our analysis. The length of the protein identified in the above searches was also monitored to rule out non-specific selections. A hundred and twenty-five cyanobacterial strains were found to contain IsiA that complied with one or more of the above criteria. These included unicellular as well as filamentous cyanobacteria from diverse ecological niches, with distinct physiological traits. Prominent among the ~265 strains that lack *isiA* are the *Prochlorococcus* and the marine *Synechococcus* strains (~150 strains). In addition,

Planktothrix, *Tolypothrix* and the thylakoid-less *Gloeobacter* strains do not appear to have *isiA*. Several cyanobacterial genera include strains that do not harbor *isiA*. Examples are, the bloom-forming filamentous strains of *Microcystis* and *Anabaena* and unicellular diazotrophic strains like *Cyanothece* among others. The rationale for this variability among strains within a genus remains unclear. However, the variability is likely due to the presence of other low-iron responsive proteins or to the differences in their niches, which in turn determines their exposure to different environmental stresses. In accordance with the findings of Shih *et al.,* (2013), we also located *isiA* in the same gene cluster with other CBP proteins in several strains. This might be indicative of the parallel functions of these light harvesting proteins in some common pathway, and these genes may have been included in specific gene islands by horizontal transfer as an adaptive strategy to specific environmental needs.

The distribution of IsiA varied among symbiotic strains. Uncultivated unicellular N_2-fixing cyanobacteria of group A (UCYN-A) are known to be endosymbionts of prymnesiophytes. Both *UNYNA-1* and *UCYNA-2* contain genes for PSI but lack genes for PSII, resulting in the loss of photosynthetic ability. Our analysis revealed that this strain lacks IsiA. On the other hand, a photosynthetic symbiont of tunicates, *Prochloron didemni*, has the *isiA* gene (Figure 1.2) (Zehr *et al.* 2008; Donia *et al.* 2011). This suggests that the IsiA machinery is likely to be maintained when there is a need for increasing photosynthetic efficiency and/or for dissipation of excess light energy, both presumably unnecessary in UCYN-A.

Of the 125 strains containing *isiA* that were identified, 61 strains representing different cyanobacterial genera were selected for a phylogenetic analysis (Figure 1.2). In this study, the selection of the strains was not based on their ecology. Instead, strains representative of the diverse cyanobacterial genera that are commonly studied for their interesting physiology or ecology and

are currently present in the sequenced database were selected. The tree revealed that the IsiA of *Synechocystis* 6803 is closely related to that of *Spirulina major* 6313, and they both share a common ancestor with *Thermosynechococcus elongatus*, *Cyanothece* 7425 and *Synechococcus* 6312. The IsiA in the marine *Cyanothece* strains 51142 and 0110 grouped separately from the terrestrial strains *Cyanothece* 7425 and 7424 and appeared to have co-evolved with the closely related marine strain *Crocosphaera Watsonii*. Interestingly, the IsiA of 16 heterocystous cyanobacteria that were included in this study grouped together in a clade (highlighted in blue), implying the coevolution of this gene in these members of the specialized group of cyanobacteria. Some of these strains were found to have *isiA* in the same operon as *isiB* as opposed to *isiB* being separately expressed as reported for some heterocystous cyanobacteria (Geiss *et al.* 2001b; Geiss *et al.* 2001a). Some non-heterocystous anaerobic nitrogen fixers [except *Cyanothece* 7424 which was reported as both an anaerobic (Turner *et al.* 2001) and aerobic (Bandyopadhyay *et al.* 2011)] grouped together (highlighted in brown) and appear to have evolved from a common ancestor. The *pcb* containing *Prochlorothrix* and marine *Synechococcus* KORDI-100 grouped together with the *Prochlorococcus* strains (which also contain *pcb* genes) were used as an outlier in this study (highlighted in green).

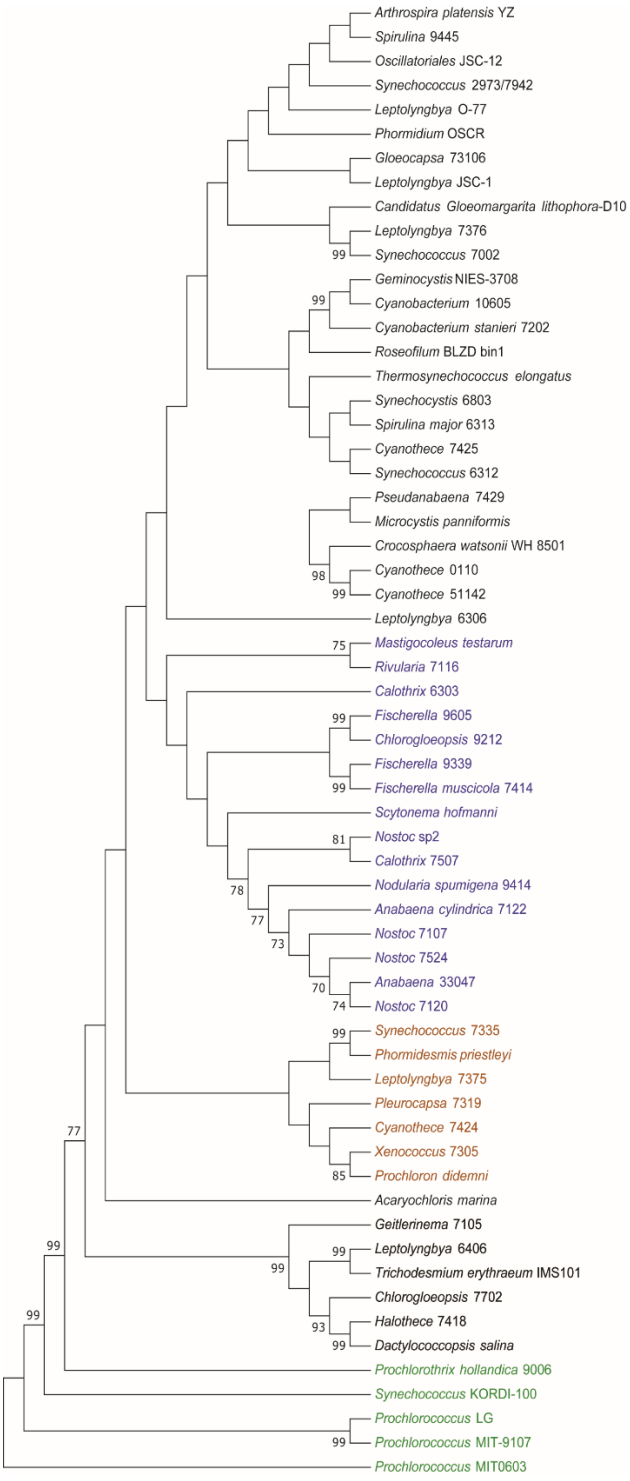

Figure 1.2 Phylogenetic tree of the IsiA protein from 61 sequenced representatives of diverse cyanobacterial species. IsiA protein sequences were obtained from the JGI/IMG microbial database and aligned with ClustalW within MEGA 7. The phylogenetic tree was generated using MEGA 7 (Neighbor-Joining method) (Saitou and Nei 1987). The percentage of replicate trees in

which the associated taxa clustered together in the bootstrap test (1000 replicates) are shown next to the branches (Felsenstein 1985). Only the nodes supported with a bootstrap of ≥ 70% are shown. All positions containing gaps and missing data were eliminated. Prochlorococcus strains containing the pcb genes were used to root the tree (green). The filamentous heterocystous cyanobacteria are shown in blue. The marine *Synechococcus* Kordi-100 strain and *Prochlorothrix hollandica* which also contain the pcb gene grouped together with the *Prochlorococcus*. Some anaerobic nitrogen fixers which contain the pigment phycoerythrin formed a distinct clade in the tree and are shown in orange color.

1.6 Discovery of IsiA functions

Although IsiA has been intensively studied for more than three decades, its functions are yet not fully understood. To elucidate the functions of IsiA, a comprehensive understanding of the factors that induce its expression and the physiological changes under these conditions is needed. As discussed in the previous section, most of the stressful conditions inducing *isiA* expression can be linked to oxidative stress or iron-deficiency. In iron-deficient conditions, the decrease of PSI contents and the loss of thylakoid membranes are two of the significant changes (Guikema and Sherman 1984; Sherman and Sherman 1983). Because IsiA protein is the major chlorophyll-binding protein produced under iron-deficient conditions, it is likely that the production of IsiA can compensate for the loss of the pigment-binding proteins. Therefore, the proposed hypotheses for IsiA function are: (1) a chlorophyll storage protein (Riethman and Sherman 1988); (2) an accessary antenna for PSI (Burnap *et al.* 1993); and (3) a dissipater to quench light energy (Park *et al.* 1999).

The analysis of chlorophyll-binding proteins in thylakoid membranes of *Synechococcus* sp. PCC 7942 during the recovery from iron-starvation showed a decrease in the IsiA content and a recovery of PSI and PSII levels within 24 h after the addition of iron (Pakrasi *et al.* 1985a). Moreover, experimental data showed that the addition of gabaculine, a chlorophyll

synthesis inhibitor, did not affect the spectral change at the early stage of recovery for iron-starvation (Guikema 1985). Therefore, IsiA has been thought to serve as a Chl *a* storage protein that maintains the Chl *a* content in cells under iron-deficient conditions, and releases Chl *a* for the synthesis of other chlorophyll-binding proteins, such as PSI, until the iron concentration gets back to normal levels. Additionally, unlike PSII, IsiA is mobile in thylakoid membranes (Sarcina and Mullineaux 2004) probably because of the loss of the huge loop on the lumenal side, which is the main difference between IsiA and CP43 (Burnap *et al.* 1993). Furthermore, the binding of Chl *a* to IsiA was considered not stable (Riethman and Sherman 1988), which suggests that IsiA is able to deliver Chl *a* during the recovery from iron-starvation. In HNLC environments, a huge pool of IsiA complexes were observed, which unlikely serve the purpose of photoprotection (Behrenfeld *et al.* 2006; Yeremenko *et al.* 2004; Ihalainen *et al.* 2005; Schrader *et al.* 2011). Instead, the IsiA complexes may be produced to maintain the Chl *a* content. It needs to be noted that atmospheric deposition of iron is an important iron source that episodically provides soluble iron to phytoplankton. The Chl *a* in IsiA can be rapidly released and used to produce PSI and PSII once their living environments receive iron pulses (Krishnamurthy *et al.* 2010; Schrader *et al.* 2011).

When IsiA was first identified in iron-starved *Synechococcus* sp. PCC 7942, it was thought as an intermediate antenna complex of PSII that absorbs light energy to compensate for the loss of phycobilisomes (Pakrasi *et al.* 1985b). The image of the PSI-IsiA supercomplex obtained by electron microscopy single-particle analysis provided abundant structural information that showed that IsiA was a peripheral membrane antenna associated with PSI (Bibby *et al.* 2001a; Boekema *et al.* 2001). Because a PSI trimer has 288 Chl *a* (Jordan *et al.* 2001) and an IsiA has 13 Chl *a*, according to the latest report (Feng *et al.* 2011), the IsiA ring surrounding the PSI trimer in a PSI_3IsiA_{18} supercomplex increases the theoretical absorption cross-section by 81%, which

suggests a great potential of IsiA for improving the light absorption capacities of PSI. The spectroscopic data showed multiple energy-transfer stages after the excitation of Chl *a* in PSI-IsiA supercomplexes, indicating the fast and efficient energy transfer between IsiA, within IsiA, and from IsiA to PSI (Melkozernov *et al.* 2003; Andrizhiyevskaya *et al.* 2004). In addition, a recent report showed that the electron throughput in PSI was enhanced while PSI was coupled with an IsiA ring (Sun and Golbeck 2015). Moreover, the mere 16% increase in exciton trapping time in PSI-IsiA$_{DR}$, the largest PSI-IsiA supercomplex isolated, compared with that in PSI timer, showed the well-coupled pigment network in PSI-IsiA supercomplex (Chauhan *et al.* 2011). The effective absorption cross-section of PSI (σ_{PSI}) in iron-starved *Synechocystis* sp. PCC6803 was measured *in vivo,* and a 60% increase in σ_{PSI} was observed with the accumulation of IsiA (Ryan-Keogh *et al.* 2012). Given the experimental data mentioned above, it was demonstrated that IsiA serves as a peripheral membrane antenna of PSI. However, because the available PSI-IsiA crystal structure is only at the resolution of ~20Å (Nield *et al.* 2003), it is impossible to simulate accurately the excitation energy transfer (EET) within the IsiA ring or from IsiA ring to PSI. The models of the EET in PSI-IsiA reported were constructed based on the positions of Chl *a* in CP43 and the relative positions between CP43 and PSII reaction center (Nield *et al.* 2003; Riley *et al.* 2006; Feng *et al.* 2011). It was proposed that the helices 5 and 6 of IsiA are facing the PSI trimer, and a well-defined path for EET from IsiA ring to PSI exists (Nield *et al.* 2003; Riley *et al.* 2006). Additionally, like the CP43's two lowest-energy states, which may play a role in the photoinhibitory and light-harvesting processes (Reppert *et al.* 2008), the analogous energy states identified in IsiA are likely to facilitate energy transfer from IsiA to PSI (Feng *et al.* 2011). Furthermore, Chl *a* 44 and 37, located in the proximity of PSI, were proposed to be the chlorophylls contributing to the lowest-

energy states A and B (Feng *et al.* 2011), which agrees with the structural model proposed by Nield *et al.* (2003).

Although IsiA was considered to improve the absorption cross-section of PSI and help capture light energy, some proposed that IsiA also functions as a non-photochemical quencher that protects PSII from photodamage (Park *et al.* 1999). This hypothesis was supported by the fact that the strain with the non-functional *isiA* gene (*isiA*$^{-}$), had a higher rate of oxygen evolution under modest illumination and was more sensitive to light intensity (Park *et al.* 1999). By overexpressing *isiA* in a *Synechococcus* sp. PCC 7942 strain, the photoinhibition of photosynthesis under high light conditions was eliminated, which again showed that IsiA was involved in photoprotection (Sandstrom *et al.* 2001). Moreover, blue light-induced fluorescence quenching was observed in iron-starved cells (Cadoret *et al.* 2004). However, it was not clear how a protein is able to function as a light-harvesting antenna as well as a non-photochemical quencher. This question was addressed in later studies in which the various IsiA-associated ring structures were identified and experimentally proved to play distinct roles in iron-starved cells (Yeremenko *et al.* 2004; Ihalainen *et al.* 2005). Intriguingly, later reports showed that the blue light-induced fluorescence quenching in the IsiA-deletion strain was similar to that in wild type, and instead, the orange carotenoid protein played the central role in this process, suggesting that IsiA is not involved in the blue light-induced non-photochemical quenching (NPQ) process (Wilson *et al.* 2006; Karapetyan 2007). This again questioned the mechanism of IsiA-mediated dissipation of light energy in iron-starved cells. Berera *et al.* (2009) proposed that energy in the Chl *a* pool was ultimately transferred to a quenching site, a carotenoid in IsiA (Berera *et al.* 2009; Berera *et al.* 2010), which is the same mechanism as the light-harvesting complex II in green plant and Hilp utilizes for energy dissipation (Ruban *et al.* 2007; Niedzwiedzki *et al.* 2016). Nevertheless, the direct evidence of

carotenoid involvement in this quenching process was missing. In addition, it was determined that the lifetime of excited Chl *a* fluorescence in IsiA is highly dependent on temperature (Chen *et al.* 2017), which is not shown in Hilp (Niedzwiedzki *et al.* 2016). Additionally, our previously published spectroscopic results showed that EET between Chl *a* and carotenoids in IsiA was absent, suggesting a novel quenching mechanism other than carotenoid quenching process in IsiA (Chen *et al.* 2017). Based on the spectroscopic results, we proposed that the quenching process was completed by a cysteine-mediated protein-pigment interaction that was previously demonstrated in the Fenna-Mathews-Olson (FMO) protein, a light harvesting protein in green sulfur bacteria (Orf *et al.* 2016).

1.7 Conclusion

During the past decades, considerable efforts were devoted to understanding the role that IsiA plays in cyanobacteria. Previous reports have shown that IsiA is required for growth of cyanobacteria under iron-deficient conditions (Burnap *et al.* 1993; Park *et al.* 1999). The hypothesis that IsiA stores Chl *a* under iron-deficient conditions and assimilates into photosynthetic proteins is supported by previous studies. Besides, the *in vitro* and *in vivo* measurements demonstrated that IsiA serves as an accessary antenna of PSI to increase the absorption cross section of PSI in PSI-IsiA supercomplex. Furthermore, it has been determined that IsiA dissipates excess light energy to prevent photosynthetic proteins from photodamage when IsiA is in an IsiA aggregate. However, the high-resolution crystal structure of IsiA is still unavailable, which makes it even more difficult to understand the processes and mechanisms of energy transfer from IsiA to PSI and the excited energy quenching in IsiA aggregate. In addition, the expression of *isiA* has been observed under various stressful conditions whereas the role of IsiA in these conditions is still unclear.

About 390 strains with available genomes in the JGI/IMG database were analyzed in this study. Surprisingly, only about one-third of these strains were found to have the *isiA* gene. The habitat of the strain may be a determining factor for the presence or absence of the *isiA* gene. The chances are that the strains without IsiA either live in iron-replete habitats or have developed other approaches to survive in iron-deficient conditions. Our study shows that *isiA* is ubiquitous among aquatic cyanobacterial strains that are likely to be subjected to iron deficiency under their natural growth conditions.

1.8 Dissertation overview

In this work, the excitation energy quenching process in IsiA was investigated by using time-resolved spectroscopy. In addition, site-directed mutagenesis was performed to obtain mutant phenotypes that were used to confirm the proposed quenching mechanism and to understand the physiological effects of the defective photoprotective mechanism in IsiA on cyanobacterial cells. Chapter 1 provides a comprehensive review of the role IsiA plays in cyanobacterial cells. Furthermore, more than 390 cyanobacterial genomes were analyzed to assess the distribution of the *isiA* gene, which informs the significance of IsiA among cyanobacterial kingdom.

By examining the pure IsiA-only protein complex by using time-resolved spectroscopy coupled with a femtosecond laser system, we were able to revisit the mechanism of excitation energy quenching in IsiA. Given the specific spectroscopic signature observed, we proposed that IsiA quenches light energy by a cysteine-mediated quenching process previously discovered in the Fenna-Matthews-Olson (FMO) protein from green sulfur bacteria.

In Chapter 3, several Cys-targeted *Synechocystis* sp. PCC 6803 mutants were prepared and used to examine the hypothesized cysteine-mediated quenching process in IsiA. The

spectroscopic results of the IsiA mutants clearly showed that IsiA can no longer quench light energy without this critical Cys residue. An IsiA mutant, C260V, was made in which the cysteine in motif AVFCAVN was replaced with a valine. This mutant was used to explore the physiological effects of the defective IsiA on the mutant cells. Under modest light, the C260V mutant appeared to grow as well as the wild type regardless of whether sufficient iron was present. Interestingly, with sufficient iron, the mutant grew better than the wild type under high light conditions. This suggests that the defective photoprotection may positively affect the biomass yield of cyanobacteria under certain growing conditions.

While sharing a similar structure with IsiA, CP43, an intrinsic antenna protein of PSII, has a valine instead of a cysteine at that critical position and, therefore, does not function in photoprotection. Inspired by the significant change in energy quenching due to a single amino acid substitution in IsiA, site-directed mutagenesis was performed to investigate the potential of photoprotective mechanisms in CP43. Although a thorough study on the CP43 mutant is needed, a 25% decrease in the PSII quantum yield compared with the wild type was determined, indicating the introduction of a quenching process in the mutant CP43.

Chapter 5 summarizes the findings in this work for understanding the role IsiA plays in cyanobacteria. In addition, Chapter 5 provides some insights on improving the understanding of IsiA in the future.

1.9 Reference

Andrizhiyevskaya EG, Frolov D, Van Grondelle R, Dekker JP (2004) Energy transfer and trapping in the photosystem I complex of *Synechococcus* PCC 7942 and in its supercomplex with IsiA. *Biochimica et biophysica acta* 1656 (2-3):104-113. doi:10.1016/j.bbabio.2004.02.002

Andrizhiyevskaya EG, Schwabe TM, Germano M, D'Haene S, Kruip J, van Grondelle R, Dekker JP (2002) Spectroscopic properties of PSI-IsiA supercomplexes from the cyanobacterium *Synechococcus* PCC 7942. *Biochimica et biophysica acta* 1556 (2-3):265-272

Ardelean I, Matthijs HC, Havaux M, Joset F, Jeanjean R (2002) Unexpected changes in photosystem I function in a cytochrome c_6-deficient mutant of the cyanobacterium *Synechocystis* PCC 6803. *FEMS Microbiology letters* 213 (1):113-119

Bailey S, Mann NH, Robinson C, Scanlan DJ (2005) The occurrence of rapidly reversible non-photochemical quenching of chlorophyll *a* fluorescence in cyanobacteria. *FEBS Lett* 579 (1):275-280

Bandyopadhyay A, Elvitigala T, Welsh E, Stöckel J, Liberton M, Min H, Sherman LA, Pakrasi HB (2011) Novel metabolic attributes of the genus *Cyanothece*, comprising a group of unicellular nitrogen-fixing cyanobacteria. *MBio* 2 (5):e00214-00211

Barber J, Morris E, Buchel C (2000) Revealing the structure of the photosystem II chlorophyll binding proteins, CP43 and CP47. *Biochimica et biophysica acta* 1459 (2-3):239-247

Behrenfeld MJ, Worthington K, Sherrell RM, Chavez FP, Strutton P, McPhaden M, Shea DM (2006) Controls on tropical Pacific Ocean productivity revealed through nutrient stress diagnostics. *Nature* 442 (7106):1025-1028. doi:10.1038/nature05083

Berera R, van Stokkum IH, d'Haene S, Kennis JT, van Grondelle R, Dekker JP (2009) A mechanism of energy dissipation in cyanobacteria. *Biophysical journal* 96 (6):2261-2267. doi:10.1016/j.bpj.2008.12.3905

Berera R, van Stokkum IH, Kennis JT, van Grondelle R, Dekker JP (2010) The light-harvesting function of carotenoids in the cyanobacterial stress-inducible IsiA complex. *Chemical Physics* 373 (1):65-70

Bibby TS, Nield J, Barber J (2001a) Iron deficiency induces the formation of an antenna ring around trimeric photosystem I in cyanobacteria. *Nature* 412 (6848):743-745. doi:10.1038/35089098

Bibby TS, Nield J, Barber J (2001b) Three-dimensional model and characterization of the iron stress-induced CP43'-photosystem I supercomplex isolated from the cyanobacterium *Synechocystis* PCC 6803. *The Journal of biological chemistry* 276 (46):43246-43252. doi:10.1074/jbc.M106541200

Bibby TS, Zhang Y, Chen M (2009) Biogeography of photosynthetic light-harvesting genes in marine phytoplankton. *PloS one* 4 (2):e4601. doi:10.1371/journal.pone.0004601

Boekema EJ, Hifney A, Yakushevska AE, Piotrowski M, Keegstra W, Berry S, Michel KP, Pistorius EK, Kruip J (2001) A giant chlorophyll-protein complex induced by iron deficiency in cyanobacteria. *Nature* 412 (6848):745-748. doi:10.1038/35089104

Burnap RL, Troyan T, Sherman LA (1993) The highly abundant chlorophyll-protein complex of iron-deficient *Synechococcus* sp PCC 7942 (CP43) is encoded by the *isiA* gene. *Plant Physiol* 103 (3):893-902. doi:Doi 10.1104/Pp.103.3.893

Cadoret JC, Demouliere R, Lavaud J, van Gorkom HJ, Houmard J, Etienne AL (2004) Dissipation of excess energy triggered by blue light in cyanobacteria with CP43' (*isiA*). *Biochimica et biophysica acta* 1659 (1):100-104. doi:10.1016/j.bbabio.2004.08.001

Chauhan D, Folea IM, Jolley CC, Kouril R, Lubner CE, Lin S, Kolber D, Wolfe-Simon F, Golbeck JH, Boekema EJ, Fromme P (2011) A novel photosynthetic strategy for adaptation to low-iron aquatic environments. *Biochemistry* 50 (5):686-692. doi:10.1021/bi1009425

Chen HS, Liberton M, Pakrasi HB, Niedzwiedzki DM (2017) Reevaluating the mechanism of excitation energy regulation in iron-starved cyanobacteria. *Biochimica et biophysica acta* 1858 (3):249-258. doi:10.1016/j.bbabio.2017.01.001

Coale KH, Johnson KS, Fitzwater SE, Gordon RM, Tanner S, Chavez FP, Ferioli L, Sakamoto C, Rogers P, Millero F (1996) A massive phytoplankton bloom induced by an ecosystem-scale iron fertilization experiment in the equatorial Pacific Ocean. *Nature* 383 (6600):495-501

Daddy S, Zhan J, Jantaro S, He C, He Q, Wang Q (2015) A novel high light-inducible carotenoid-binding protein complex in the thylakoid membranes of *Synechocystis* PCC 6803. *Scientific reports* 5:9480. doi:10.1038/srep09480

Donia MS, Fricke WF, Partensky F, Cox J, Elshahawi SI, White JR, Phillippy AM, Schatz MC, Piel J, Haygood MG (2011) Complex microbiome underlying secondary and primary metabolism in the tunicate-*Prochloron* symbiosis. *Proceedings of the National Academy of Sciences* 108 (51):E1423-E1432

Duhring U, Axmann IM, Hess WR, Wilde A (2006) An internal antisense RNA regulates expression of the photosynthesis gene *isiA*. *Proceedings of the National Academy of Sciences of the United States of America* 103 (18):7054-7058. doi:10.1073/pnas.0600927103

Falk S, Samson G, Bruce D, Huner NP, Laudenbach DE (1995) Functional analysis of the iron-stress induced CP 43' polypeptide of PS II in the cyanobacterium *Synechococcus* sp. PCC 7942. *Photosynthesis research* 45 (1):51-60. doi:10.1007/BF00032235

Felsenstein J (1985) Confidence-Limits on Phylogenies - an Approach Using the Bootstrap. *Evolution* 39 (4):783-791. doi:Doi 10.2307/2408678

Feng X, Neupane B, Acharya K, Zazubovich V, Picorel R, Seibert M, Jankowiak R (2011) Spectroscopic study of the CP43' complex and the PSI-CP43' supercomplex of the cyanobacterium *Synechocystis* PCC 6803. *The journal of physical chemistry B* 115 (45):13339-13349. doi:10.1021/jp206054b

Ferreira KN, Iverson TM, Maghlaoui K, Barber J, Iwata S (2004) Architecture of the photosynthetic oxygen-evolving center. *Science* 303 (5665):1831-1838. doi:10.1126/science.1093087

Fitzgerald MP, Husain A, Hutber GN, Rogers LJ (1977) Studies on the flavodoxins from a cyanobacterium and a red alga [proceedings]. *Biochem Soc Trans* 5 (5):1505-1506

Foster JS, Singh AK, Rothschild LJ, Sherman LA (2007) Growth-phase dependent differential gene expression in *Synechocystis* sp. strain PCC 6803 and regulation by a group 2 sigma factor. *Archives of Microbiology* 187 (4):265-279. doi:10.1007/s00203-006-0193-6

Fraser JM, Tulk SE, Jeans JA, Campbell DA, Bibby TS, Cockshutt AM (2013) Photophysiological and photosynthetic complex changes during iron starvation in *Synechocystis* sp. PCC 6803 and *Synechococcus* elongatus PCC 7942. *PloS one* 8 (3):e59861. doi:10.1371/journal.pone.0059861

Geiss U, Vinnemeier J, Kunert A, Lindner I, Gemmer B, Lorenz M, Hagemann M, Schoor A (2001a) Detection of the *isiA* gene across cyanobacterial strains: Potential for probing iron deficiency. *Appl Environ Microb* 67 (11):5247-5253

Geiss U, Vinnemeier J, Schoor A, Hagemann M (2001b) The iron-regulated *isiA* gene of *Fischerella muscicola* strain PCC 73103 is linked to a likewise regulated gene encoding a Pcb-like chlorophyll-binding protein. *FEMS Microbiology letters* 197 (1):123-129

Ghassemian M, Straus NA (1996) Fur regulates the expression of iron-stress genes in the cyanobacterium *Synechococcus* sp. strain PCC 7942. *Microbiology* 142 (Pt 6):1469-1476. doi:10.1099/13500872-142-6-1469

Guikema JA (1985) Fluorescence Induction Characteristics of Anacystis-Nidulans during Recovery from Iron-Deficiency. *J. Plant. Nutr.* 8 (10):891-908. doi:Doi 10.1080/01904168509363393

Guikema JA, Sherman LA (1983a) Chlorophyll Protein Organization of Membranes from the Cyanobacterium Anacystis-Nidulans. *Arch. Biochem. Biophys.* 220 (1):155-166. doi:Doi 10.1016/0003-9861(83)90396-X

Guikema JA, Sherman LA (1983b) Organization and function of chlorophyll in membranes of cyanobacteria during iron starvation. *Plant Physiol* 73 (2):250-256. doi:Doi 10.1104/Pp.73.2.250

Guikema JA, Sherman LA (1984) Influence of iron deprivation on the membrane composition of *Anacystis nidulans*. *Plant physiology* 74 (1):90-95

Havaux M, Guedeney G, Hagemann M, Yeremenko N, Matthijs HC, Jeanjean R (2005) The chlorophyll-binding protein IsiA is inducible by high light and protects the cyanobacterium *Synechocystis* PCC6803 from photooxidative stress. *FEBS letters* 579 (11):2289-2293. doi:10.1016/j.febslet.2005.03.021

Holland HD (2006) The oxygenation of the atmosphere and oceans. Philosophical transactions of the Royal Society of London Series B, *Biological Science*s 361 (1470):903-915. doi:10.1098/rstb.2006.1838

Ihalainen JA, D'Haene S, Yeremenko N, van Roon H, Arteni AA, Boekema EJ, van Grondelle R, Matthijs HC, Dekker JP (2005) Aggregates of the chlorophyll-binding protein IsiA (CP43') dissipate energy in cyanobacteria. *Biochemistry* 44 (32):10846-10853. doi:10.1021/bi0510680

Jeanjean R, Zuther E, Yeremenko N, Havaux M, Matthijs HC, Hagemann M (2003) A photosystem 1 *psaFJ*-null mutant of the cyanobacterium *Synechocystis* PCC 6803 expresses the *isiAB* operon under iron replete conditions. *FEBS letters* 549 (1-3):52-56

Jordan P, Fromme P, Witt HT, Klukas O, Saenger W, Krauss N (2001) Three-dimensional structure of cyanobacterial photosystem I at 2.5 Å resolution. *Nature* 411 (6840):909-917. doi:10.1038/35082000

Karapetyan NV (2007) Non-photochemical quenching of fluorescence in cyanobacteria. *Biochemistry Biokhimiia* 72 (10):1127-1135

Komenda J, Sobotka R (2016) Cyanobacterial high-light-inducible proteins--Protectors of chlorophyll-protein synthesis and assembly. *Biochimica et biophysica acta* 1857 (3):288-295. doi:10.1016/j.bbabio.2015.08.011

Kouril R, Arteni AA, Lax J, Yeremenko N, D'Haene S, Rogner M, Matthijs HC, Dekker JP, Boekema EJ (2005) Structure and functional role of supercomplexes of IsiA and photosystem I in cyanobacterial photosynthesis. *FEBS letters* 579 (15):3253-3257. doi:10.1016/j.febslet.2005.03.051

Krishnamurthy A, Moore JK, Mahowald N, Luo C, Zender CS (2010) Impacts of atmospheric nutrient inputs on marine biogeochemistry. *Journal of Geophysical Research: Biogeosciences* 115 (G1)

Kunert A, Vinnemeier J, Erdmann N, Hagemann M (2003) Repression by Fur is not the main mechanism controlling the iron-inducible *isiAB* operon in the cyanobacterium *Synechocystis* sp. PCC 6803. *FEMS Microbiology letters* 227 (2):255-262

Kutzki C, Masepohl B, Bohme H (1998) The *isiB* gene encoding flavodoxin is not essential for photoautotrophic iron limited growth of the cyanobacterium *Synechocystis* sp. strain PCC 6803. *FEMS Microbiology letters* 160 (2):231-235

La Roche J, van der Staay GW, Partensky F, Ducret A, Aebersold R, Li R, Golden SS, Hiller RG, Wrench PM, Larkum AW, Green BR (1996) Independent evolution of the prochlorophyte and green plant chlorophyll *a/b* light-harvesting proteins. *Proceedings of the National Academy of Sciences of the United States of America* 93 (26):15244-15248

Lane N (2002) Oxygen: the molecule that made the world. OUP Oxford,

Laudenbach D, Reith M, Straus N (1988) Isolation, sequence analysis, and transcriptional studies of the flavodoxin gene from *Anacystis nidulans* R2. *J. Bacteriol.*170 (1):258-265

Laudenbach DE, Straus NA (1988) Characterization of a cyanobacterial iron stress-induced gene similar to psbC. *Journal of bacteriology* 170 (11):5018-5026

Leonhardt K, Straus NA (1992) An iron stress operon involved in photosynthetic electron transport in the marine cyanobacterium *Synechococcus* sp. PCC 7002. *Journal of general Microbiology* 138 Pt 8:1613-1621. doi:10.1099/00221287-138-8-1613

Leonhardt K, Straus NA (1994) Photosystem II genes *isiA*, *psbDI* and *psbC* in *Anabaena* sp. PCC 7120: cloning, sequencing and the transcriptional regulation in iron-stressed and iron-repleted cells. *Plant molecular biology* 24 (1):63-73

Li H, Singh AK, McIntyre LM, Sherman LA (2004) Differential gene expression in response to hydrogen peroxide and the putative PerR regulon of *Synechocystis* sp. strain PCC 6803. *Journal of bacteriology* 186 (11):3331-3345. doi:10.1128/JB.186.11.3331-3345.2004

Ma F, Zhang X, Zhu X, Li T, Zhan J, Chen H, He C, Wang Q (2017) Dynamic changes of IsiA-containing complexes during long-term iron deficiency in *Synechocystis* sp. PCC 6803. *Molecular plant* 10 (1):143-154. doi:10.1016/j.molp.2016.10.009

Martin JH, Fitzwater SE (1988) Iron-deficiency limits phytoplankton growth in the northeast Pacific subarctic. *Nature* 331 (6154):341-343. doi:Doi 10.1038/331341a0

Melkozernov AN, Bibby TS, Lin S, Barber J, Blankenship RE (2003) Time-resolved absorption and emission show that the CP43' antenna ring of iron-stressed *Synechocystis* sp. PCC6803 is efficiently coupled to the photosystem I reaction center core. *Biochemistry* 42 (13):3893-3903. doi:10.1021/bi026987u

Michel KP, Pistorius EK (2004) Adaptation of the photosynthetic electron transport chain in cyanobacteria to iron deficiency: The function of IdiA and IsiA. *Physiologia plantarum* 120 (1):36-50. doi:10.1111/j.0031-9317.2004.0229.x

Michel KP, Thole HH, Pistorius EK (1996) IdiA, a 34 kDa protein in the cyanobacteria *Synechococcus* sp. strains PCC 6301 and PCC 7942, is required for growth under iron and manganese limitations. *Microbiology* 142 (Pt 9):2635-2645. doi:10.1099/00221287-142-9-2635

Moore C, Mills M, Arrigo K, Berman-Frank I, Bopp L, Boyd P, Galbraith E, Geider R, Guieu C, Jaccard S (2013) Processes and patterns of oceanic nutrient limitation. *Nature geoscience* 6 (9):701

Niedzwiedzki DM, Tronina T, Liu H, Staleva H, Komenda J, Sobotka R, Blankenship RE, Polivka T (2016) Carotenoid-induced non-photochemical quenching in the cyanobacterial chlorophyll synthase-HliC/D complex. *Biochimica et biophysica acta* 1857 (9):1430-1439. doi:10.1016/j.bbabio.2016.04.280

Nield J, Morris EP, Bibby TS, Barber J (2003) Structural analysis of the photosystem I supercomplex of cyanobacteria induced by iron deficiency. *Biochemistry* 42 (11):3180-3188. doi:10.1021/bi026933k

North R, Guildford S, Smith R, Havens S, Twiss M (2007) Evidence for phosphorus, nitrogen, and iron colimitation of phytoplankton communities in Lake Erie. Limnology and Oceanography 52 (1):315-328

Oquist G (1971) Changes in Pigment Composition and Photosynthesis Induced by Iron-Deficiency in Blue-Green-Alga Anacystis-Nidulans. Physiol Plantarum 25 (2):188-&. doi:DOI 10.1111/j.1399-3054.1971.tb01426.x

Orf GS, Saer RG, Niedzwiedzki DM, Zhang H, McIntosh CL, Schultz JW, Mirica LM, Blankenship RE (2016) Evidence for a cysteine-mediated mechanism of excitation energy regulation in a photosynthetic antenna complex. *Proceedings of the National Academy of Sciences of the United States of America* 113 (31):E4486-4493. doi:10.1073/pnas.1603330113

Pakrasi HB, Goldenberg A, Sherman LA (1985a) Membrane development in the cyanobacterium, *Anacystis nidulans*, during recovery from iron starvation. *Plant Physiol* 79 (1):290-295

Pakrasi HB, Riethman HC, Sherman LA (1985b) Organization of pigment proteins in the photosystem II complex of the cyanobacterium *Anacystis nidulans* R2. *Proceedings of the National Academy of Sciences* 82 (20):6903-6907

Park YI, Sandstrom S, Gustafsson P, Oquist G (1999) Expression of the *isiA* gene is essential for the survival of the cyanobacterium *Synechococcus* sp. PCC 7942 by protecting photosystem II from excess light under iron limitation. *Molecular Microbiology* 32 (1):123-129

Reppert M, Zazubovich V, Dang NC, Seibert M, Jankowiak R (2008) Low-energy chlorophyll states in the CP43 antenna protein complex: simulation of various optical spectra. II. *The journal of physical chemistry B* 112 (32):9934-9947. doi:10.1021/jp8013749

Richier S, Macey AI, Pratt NJ, Honey DJ, Moore CM, Bibby TS (2012) Abundances of iron-binding photosynthetic and nitrogen-fixing proteins of *Trichodesmium* both in culture and *in situ* from the north Atlantic. *PloS one* 7 (5):e35571. doi:10.1371/journal.pone.0035571

Riethman HC, Sherman LA (1988) Purification and characterization of an iron stress-induced chlorophyll-protein from the cyanobacterium *Anacystis nidulans* R2. *Biochim Biophys Acta* 935 (2):141-151

Riley KJ, Zazubovich V, Jankowiak R (2006) Frequency-domain spectroscopic study of the PS I-CP43' supercomplex from the cyanobacterium *Synechocystis* PCC 6803 grown under iron stress conditions. *The journal of physical chemistry B* 110 (45):22436-22446. doi:10.1021/jp063691f

Ruban AV, Berera R, Ilioaia C, van Stokkum IH, Kennis JT, Pascal AA, van Amerongen H, Robert B, Horton P, van Grondelle R (2007) Identification of a mechanism of photoprotective energy dissipation in higher plants. *Nature* 450 (7169):575-578. doi:10.1038/*Nature*06262

Ryan-Keogh TJ, Macey AI, Cockshutt AM, Moore CM, Bibby TS (2012) The cyanobacterial chlorophyll-binding-protein IsiA acts to increase the *in vivo* effective absorption cross-section of psi under iron limitation(1). Journal of phycology 48 (1):145-154. doi:10.1111/j.1529-8817.2011.01092.x

Saitou N, Nei M (1987) The neighbor-joining method - a new method for reconstructing phylogenetic trees. *Mol Biol Evol* 4 (4):406-425

Salomon E, Keren N (2015) Acclimation to environmentally relevant Mn concentrations rescues a cyanobacterium from the detrimental effects of iron limitation. *Environmental Microbiology* 17 (6):2090-2098. doi:10.1111/1462-2920.12826

Sandrini G, Tann RP, Schuurmans JM, van Beusekom SA, Matthijs HC, Huisman J (2016) Diel variation in gene expression of the CO_2-concentrating mechanism during a harmful cyanobacterial bloom. *Frontiers in Microbiology* 7:551. doi:10.3389/fmicb.2016.00551

Sandstrom S, Park YI, Oquist G, Gustafsson P (2001) CP43 ', the *isiA* gene product, functions as an excitation energy dissipator in the cyanobacterium *Synechococcus* sp PCC 7942. *Photochem. Photobiol.* 74 (3):431-437. doi:Doi 10.1562/0031-8655(2001)074<0431:Ctigpf>2.0.Co;2

Sarcina M, Mullineaux CW (2004) Mobility of the IsiA chlorophyll-binding protein in cyanobacterial thylakoid membranes. *The Journal of biological chemistry* 279 (35):36514-36518. doi:10.1074/jbc.M405881200

Schrader PS, Milligan AJ, Behrenfeld MJ (2011) Surplus photosynthetic antennae complexes underlie diagnostics of iron limitation in a cyanobacterium. *PloS one* 6 (4):e18753. doi:10.1371/journal.pone.0018753

Sherman DM, Sherman LA (1983) Effect of iron-deficiency and iron restoration on ultrastructure of *Anacystis nidulans*. *J. Bacteriol.*156 (1):393-401

Shih PM, Wu D, Latifi A, Axen SD, Fewer DP, Talla E, Calteau A, Cai F, De Marsac NT, Rippka R (2013) Improving the coverage of the cyanobacterial phylum using diversity-driven genome sequencing. *Proceedings of the National Academy of Sciences* 110 (3):1053-1058

Singh AK, Sherman LA (2006) Iron-independent dynamics of IsiA production during the transition to stationary phase in the cyanobacterium *Synechocystis* sp. PCC 6803. *FEMS Microbiology letters* 256 (1):159-164. doi:10.1111/j.1574-6968.2006.00114.x

Stojiljkovic I, Hantke K (1995) Functional Domains of the Escherichia-Coli Ferric Uptake Regulator Protein (Fur). *Mol. Gen. Genet.* 247 (2):199-205. doi:Doi 10.1007/Bf00705650

Sun J, Golbeck JH (2015) The presence of the IsiA-PSI supercomplex leads to enhanced photosystem I electron throughput in iron-starved cells of *Synechococcus* sp. PCC 7002. *The journal of physical chemistry B* 119 (43):13549-13559. doi:10.1021/acs.jpcb.5b02176

Tsuda A, Takeda S, Saito H, Nishioka J, Nojiri Y, Kudo I, Kiyosawa H, Shiomoto A, Imai K, Ono T (2003) A mesoscale iron enrichment in the western subarctic Pacific induces a large centric diatom bloom. *Science* 300 (5621):958-961

Turner S, Huang T-C, Chaw S-M (2001) Molecular phylogeny of nitrogen-fixing unicellular cyanobacteria. *Botanical Bulletin of Academia Sinica* 42

Umena Y, Kawakami K, Shen JR, Kamiya N (2011) Crystal structure of oxygen-evolving photosystem II at a resolution of 1.9 A. *Nature* 473 (7345):55-60. doi:10.1038/Nature09913

van der Weij-de Wit CD, Ihalainen JA, van de Vijver E, D'Haene S, Matthijs HC, van Grondelle R, Dekker JP (2007) Fluorescence quenching of IsiA in early stage of iron deficiency and at cryogenic temperatures. *Biochimica et biophysica acta* 1767 (12):1393-1400. doi:10.1016/j.bbabio.2007.10.001

Vinnemeier J, Kunert A, Hagemann M (1998) Transcriptional analysis of the *isiAB* operon in salt-stressed cells of the cyanobacterium *Synechocystis* sp. PCC 6803. *FEMS Microbiology letters* 169 (2):323-330

Vrede T, Tranvik LJ (2006) Iron constraints on planktonic primary production in oligotrophic lakes. Ecosystems 9 (7):1094-1105

Wang Q, Hall CL, Al-Adami MZ, He Q (2010) IsiA is required for the formation of photosystem I supercomplexes and for efficient state transition in *Synechocystis* PCC 6803. *PloS one* 5 (5):e10432. doi:10.1371/journal.pone.0010432

Wang Q, Jantaro S, Lu BS, Majeed W, Bailey M, He QF (2008) The high light-inducible polypeptides stabilize trimeric photosystem I complex under high light conditions in *Synechocystis* PCC 6803. *Plant Physiol* 147 (3):1239-1250. doi:10.1104/pp.108.121087

Wilson A, Ajlani G, Verbavatz JM, Vass I, Kerfeld CA, Kirilovsky D (2006) A soluble carotenoid protein involved in phycobilisome-related energy dissipation in cyanobacteria. *Plant Cell* 18 (4):992-1007. doi:10.1105/tpc.105.040121

Yeremenko N, Kouril R, Ihalainen JA, D'Haene S, van Oosterwijk N, Andrizhiyevskaya EG, Keegstra W, Dekker HL, Hagemann M, Boekema EJ, Matthijs HC, Dekker JP (2004) Supramolecular organization and dual function of the IsiA chlorophyll-binding protein in cyanobacteria. *Biochemistry* 43 (32):10308-10313. doi:10.1021/bi048772l

Yousef N, Pistorius EK, Michel KP (2003) Comparative analysis of *idiA* and *isiA* transcription under iron starvation and oxidative stress in *Synechococcus* elongatus PCC 7942 wild-type and selected mutants. *Archives of Microbiology* 180 (6):471-483. doi:10.1007/s00203-003-0618-4

Zehr JP, Bench SR, Carter BJ, Hewson I, Niazi F, Shi T, Tripp HJ, Affourtit JP (2008) Globally Distributed Uncultivated Oceanic $N(_2)$-Fixing Cyanobacteria Lack Oxygenic Photosystem II. *Science* 322 (5904):1110-1112. doi:10.1126/*Science*.1165340

2. Chapter Two: Reevaluating the mechanism of excitation energy regulation in iron-starved cyanobacteria

This chapter was adapted from:

Chen HS, Liberton M, Pakrasi HB, Niedzwiedzki DM (2017) Reevaluating the mechanism of excitation energy regulation in iron-starved cyanobacteria. *Biochimica et biophysica acta* 1858 (3):249-258.

M. L. created the IsiA-His strain and D. M. N. performed the experiments and analyses of time-resolved spectroscopy.

2.1 Abstract

This paper presents a spectroscopic investigation of IsiA, a chlorophyll *a*-binding membrane protein produced by cyanobacteria grown in iron-deficient environments. IsiA, when associated with photosystem I, supports photosystem I in light-harvesting by efficiently transferring excitation energy. However, while separated from photosystem I, IsiA exhibits considerable excitation quenching observed as a substantial reduction of protein-bound chlorophyll *a* fluorescence lifetime. Previous spectroscopic studies suggested that carotenoids are involved in excitation energy dissipation and additionally play a second role in this antenna complex by supporting chlorophyll *a* in light harvesting by absorbing in the spectral range inaccessible for chlorophyll *a* and transferring excitation energy to chlorophylls. However, this investigation does not support these proposed roles of carotenoids in this light-harvesting protein. This study shows that carotenoids do not transfer excitation energy to chlorophyll *a*. In addition, our investigations do not support the hypothesis that carotenoids are quenchers of the excited state of chlorophyll *a* in this protein complex. We propose that quenching of chlorophyll *a* fluorescence in IsiA is maintained by pigment-protein interactions that allow electron transfer from an excited chlorophyll *a* to a cysteine residue, an excitation quenching mechanism that was recently proposed to regulate the light harvesting capabilities of the bacteriochlorophyll *a*-containing Fenna-Mathews-Olson protein from green-sulfur bacteria.

2.2 Introduction

Cyanobacteria are oxygenic photosynthetic organisms that are responsible for a significant portion of global biomass production. They are genetically and morphologically diverse and are found in various environments across a wide range of altitudes and latitudes (De los Rios *et al.*

2007). Cyanobacteria have survived many geological and climatic changes on Earth during the past ~3.5 billion years, and have evolved to overcome severe environmental conditions, such as nutrient deficiencies (De Marais 2000). Iron deficiency is a common nutrient-deficient condition in cyanobacterial habitats. Although iron is one of the most abundant elements on Earth, it is usually found in the form of insoluble ferric oxides (Stumm and Morgan 1981; Lane 2002). Cyanobacteria need significant amounts of ferric iron (Fe^{3+}) for assembly of iron-sulfur complexes that are necessary for maintaining light-dependent photochemical reactions in protein complexes like photosystem I (PSI) (Reilly and Nelson 1988). If the environment lacks iron, cyanobacteria cannot produce sufficient levels of PSI or other essential iron-sulfur proteins, leading to lethal consequences.

IsiA is a chlorophyll *a* (Chl *a*)-binding protein produced by cyanobacteria living in iron-deficient conditions (Pakrasi *et al.* 1985). Given that iron limitation is common in natural environments, the IsiA protein is produced and associated with PSI (Bibby *et al.* 2001b, a; Boekema *et al.* 2001) under such conditions, where it participates in the process of light harvesting. IsiA is a 36 kDa membrane protein with high protein sequence homology to CP43, a core light-harvesting antenna protein of photosystem II (PSII) (Bibby *et al.* 2001b). A major difference between these proteins is their pigment content. Whereas CP43 binds 13 Chl *a* and three molecules of carotenoid β-carotene, IsiA contains between 13 and 16 Chl *a* and four carotenoids: three β -carotenes and one echinenone (Ihalainen *et al.* 2005; Andrizhiyevskaya *et al.* 2002). A high-resolution crystal structure of the IsiA protein is not available, but top view images obtained by electron microscopy analysis of single particles of PSI-IsiA supercomplexes showed that the PSI trimer is surrounded by 18 IsiA subunits forming a $(PSI)_3(IsiA)_{18}$ supercomplex (Bibby *et al.*

2001a). This ring-shaped supercomplex is a preferred formation adapted by $(PSI)_x(IsiA)_y$ supercomplexes (Yeremenko *et al.* 2004).

Since the identification of the IsiA protein in the 1980s (Pakrasi *et al.* 1985), several hypotheses were proposed to explain its biological function. IsiA is highly homologous with CP43 but is produced when the cyanobacterial cells are grown in iron-deficient environments where adequate quantities of PSI cannot be assembled (Ryan-Keogh *et al.* 2012). It was suggested that the protein is synthesized to compensate for the loss of PSI and maintain light-harvesting capacity. From this perspective, the IsiA rings formed around PSI may act as huge light harvesting antennae, similar to phycobilisomes associated with PSII (Gantt 1981). Owing to a high mobility of IsiA in thylakoid membranes and a large pigment capacity, another function in Chl *a* storage has been also proposed (Sarcina and Mullineaux 2004).

Studies using time-resolved optical spectroscopies (Andrizhiyevskaya *et al.* 2002; Melkozernov *et al.* 2003) suggested that in PSI-IsiA supercomplexes, IsiA very efficiently transfers the excitation energy of absorbed light to the PSI. However, the antenna proteins that are separated from PSI and freely float in the thylakoid membrane show a protective, dissipative mechanism that mitigates potential photo-oxidative damage. Excitation quenching has been clearly observed as a substantial shortening of the excited state lifetime of Chl *a* (Ihalainen *et al.* 2005). Further investigations proposed that a quenching mechanism based on non-photochemical quenching was present at the level of the protein monomer and maintained by carotenoids. It was argued that one of the carotenoids, preferentially echinenone, quenches the singlet excited state of Chl *a* via direct energy transfer from the Chl *a* Q_y state to the carotenoid S_1 state (Berera *et al.* 2010; Berera *et al.* 2009).

Efficient quenching of the Chl *a* excited state via the carotenoid S_1 state can compete with the intrinsic decay of the carotenoid S_1. If the pool of carotenoids excited to their S_1 state via chlorophyll-to-carotenoid energy transfer is populated faster than intrinsic decay of the S_1 state, the state can be detected by time-resolved absorption spectroscopy by recording the $S_1 \rightarrow S_n$ excited state absorption band. This provides direct evidence of carotenoid involvement in the quenching process. Recently, this spectroscopic method was used to demonstrate the involvement of a carotenoid in Chl *a* quenching in another class of cyanobacterial proteins called High-Light Inducible Proteins (Niedzwiedzki *et al.* 2016; Staleva *et al.* 2015). No such spectral signature of the carotenoid excited S_1 state has ever been experimentally observed for IsiA. An explanation is based on the hypothesis that the populating rate of the quencher (echinenone in the S1 state) is not fast enough to compensate for a subsequent, immediate decay of its excited state. The excited carotenoid will be only a "virtual" element in the excitation decay pathway. Thus, carotenoid involvement was simply anticipated and built into kinetic models of the Chl *a* excitation decay path (Berera *et al.* 2010; Berera *et al.* 2009).

Furthermore, the absorption spectrum of the IsiA sample used in the previous studies (Berera *et al.* 2010; Berera *et al.* 2009) showed the maximum absorption of the Chl *a* Q_y band to be shifted to 675 nm, which according to other spectroscopic studies is more characteristic of the IsiA-PSI supercomplex (Andrizhiyevskaya *et al.* 2002; Andrizhiyevskaya *et al.* 2004; Feng *et al.* 2011; Melkozernov *et al.* 2003). This is strongly suggestive of a sample that could be substantially contaminated by PSI or that contains a mixture of IsiA and IsiA-PSI supercomplexes. Because the effect of the quenching of Chl *a* fluorescence in the IsiA protein could be undermined by hypothetically possible IsiA-to-PSI energy transfer, this questions the conclusions of the previous studies.

The work presented here strongly indicates that carotenoids do not play a role in the energetics of this pigment protein complex, either as quenchers or supporters of Chl *a*. The results of this study strongly suggest that the quenching mechanism is merely governed by Chl *a*-protein interactions via electron transfer from an excited Chl *a* to a cysteine residue. Such a novel energy-quenching mechanism was very recently proposed to regulate the light harvesting capabilities of the bacteriochlorophyll *a*-containing Fenna-Mathews-Olson (FMO) protein from green sulfur bacteria (Orf *et al.* 2016). However, the current study suggests that this mechanism may be more broadly utilized by photosynthetic organisms.

2.3 Results and Discussion

2.3.1 Characterization and steady-state spectroscopy of the PSI-IsiA and IsiA complexes

The various protein complexes, including the pure IsiA and PSI-IsiA supercomplexes, in iron-starved cells were isolated and shown in Figure 2.1A. The top green band with the lowest mass density was targeted as a candidate for IsiA-only complexes. Further analysis of this band by western blotting (Figure 2.1B) confirmed the absence of the PSI core subunit PsaA. Furthermore, the strong band shown on the blot probed by the IsiA antibody showed the presence of IsiA, thus confirming that it contained IsiA-only complexes. On the other hand, the PSI-IsiA sample contained both PSI and IsiA as expected. Room temperature absorption spectra of the IsiA, PSI and PSI-IsiA samples are provided in Figure 2.1C, showing very distinctive differences in the Q_y band of Chl *a*. The Q_y absorption band appears at 670 nm in the IsiA sample but is shifted to longer wavelengths for the PSI complex (679 nm) and for the PSI-IsiA supercomplex (674 nm). Figure 2.1D shows absorption spectra taken at 77 K. As visualized by the green dashed line, the absorption

of the PSI-IsiA supercomplex was very adequately mimicked by the weighted sum of the individual spectra of the IsiA and PSI complexes.

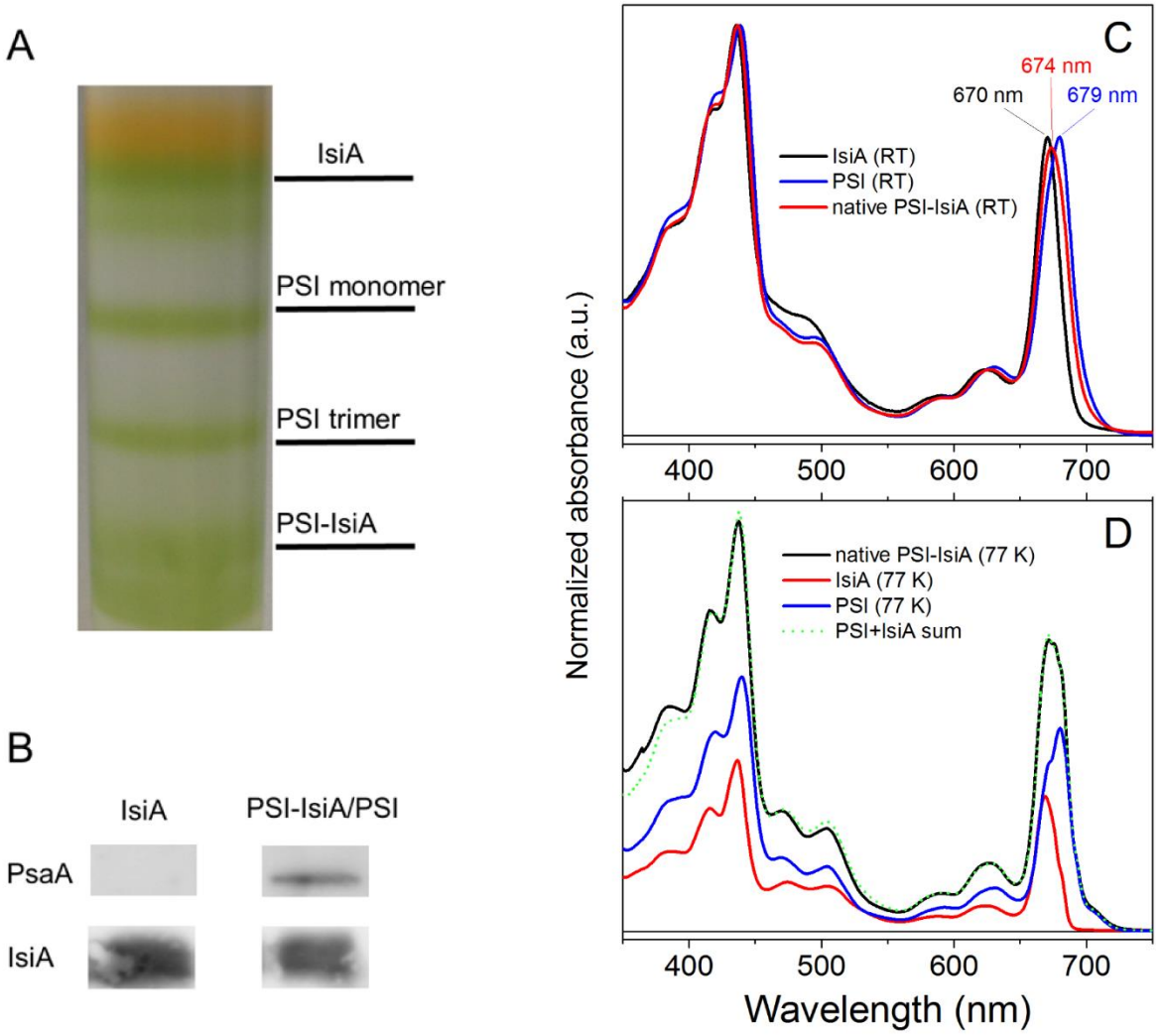

Figure 2.1 Purification and basic spectroscopic characterization of IsiA and PSI-IsiA. (A) Protein bands obtained from sucrose gradient ultracentrifugation, (B) PSI-IsiA complexes purified by nickel affinity chromatography and the IsiA band from ultracentrifugation probed by immunoblotting, (C) Room temperature and (D) 77 K absorption spectra of PSI-IsiA complexes and individual IsiA, PSI (with absorptions adjusted to relative contributions in the PSI-IsiA spectrum).

The good agreement of the spectral shapes of the native and reconstructed PSI-IsiA spectra indicated that there was no excitonic coupling between Chls from IsiA and PSI proteins, as that would affect the shape of the Q_y band. The near-identical spectral lines of native and mimicked absorption spectra suggest that there are no additional pigments (carotenoid, Chl *a*) that are weakly bound in the IsiA and PSI interface and that could be lost during separation of the supercomplex into individual complexes during detergent treatment.

Past studies reported that carotenoids transfer excitation energy to Chl *a* with an overall efficiency of ~25%, suggesting that those pigments also supplement Chl *a* in light harvesting in the IsiA complex (Berera *et al.* 2010). However, this hypothesis was based on kinetic modeling of transient absorption data, and additional support was not provided (Berera *et al.* 2010). Our fluorescence studies (Figure 2.2) clearly show that carotenoids are essentially not involved in supporting Chl *a* in light harvesting. The fluorescence excitation (Exc) spectrum did not show any evidence of a carotenoid absorption band, as seen in the absorbance (1 - T, where T is transmittance) spectrum. Assuming 100% energy transfer within Q_y (profiles are normalized there), carotenoid-to-Chl *a* energy transfer efficiency was essentially zero as there was no contribution in the Exc profile of IsiA that could be assigned to carotenoids (between 450 – 550 nm). There are no available prior results of Chl *a* fluorescence excitation of the IsiA protein for comparison. The profile recorded for a highly homologous protein CP43 shows that energy transfer from carotenoids to Chl *a* is very small in that protein (Alfonso *et al.* 1994), consistent with the results obtained for IsiA in this study.

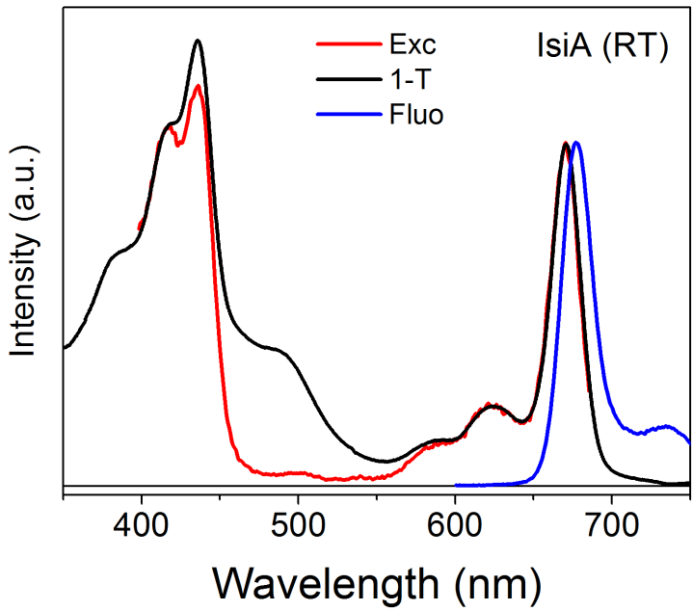

Figure 2.2 Fluorescence excitation, emission and absorptance spectral profiles of the IsiA complex at room temperature. Exc, excitation; Fluo, fluorescence emission; 1-T, T-transmittance, absorption.

2.3.2 Time-resolved fluorescence of PSI-IsiA and IsiA complexes

Figure 2.3 shows TRF results from PSI-IsiA and IsiA complexes recorded at RT and at 77 K. The two-dimensional pseudo-color profiles of TRF of the samples are given in panels A, C and E, and the corresponding global analyses of the datasets are shown in panels B, D and F. Cryogenic temperature essentially had no effect on IsiA-to-PSI energy transfer. As demonstrated in Figure 2. 3A, excitations populated initially on IsiA were promptly transferred to PSI. Target analysis of TRF data showed that transfer time could not be precisely defined, as it was shorter than the streak camera temporal resolution in this time window (FWHM of IRF is ~70 ps in a 1 ns time window). The spectral characteristics of other kinetic components strongly suggest that those are associated with excitation equilibration and followed excitation decay within the Chl *a* array in PSI.

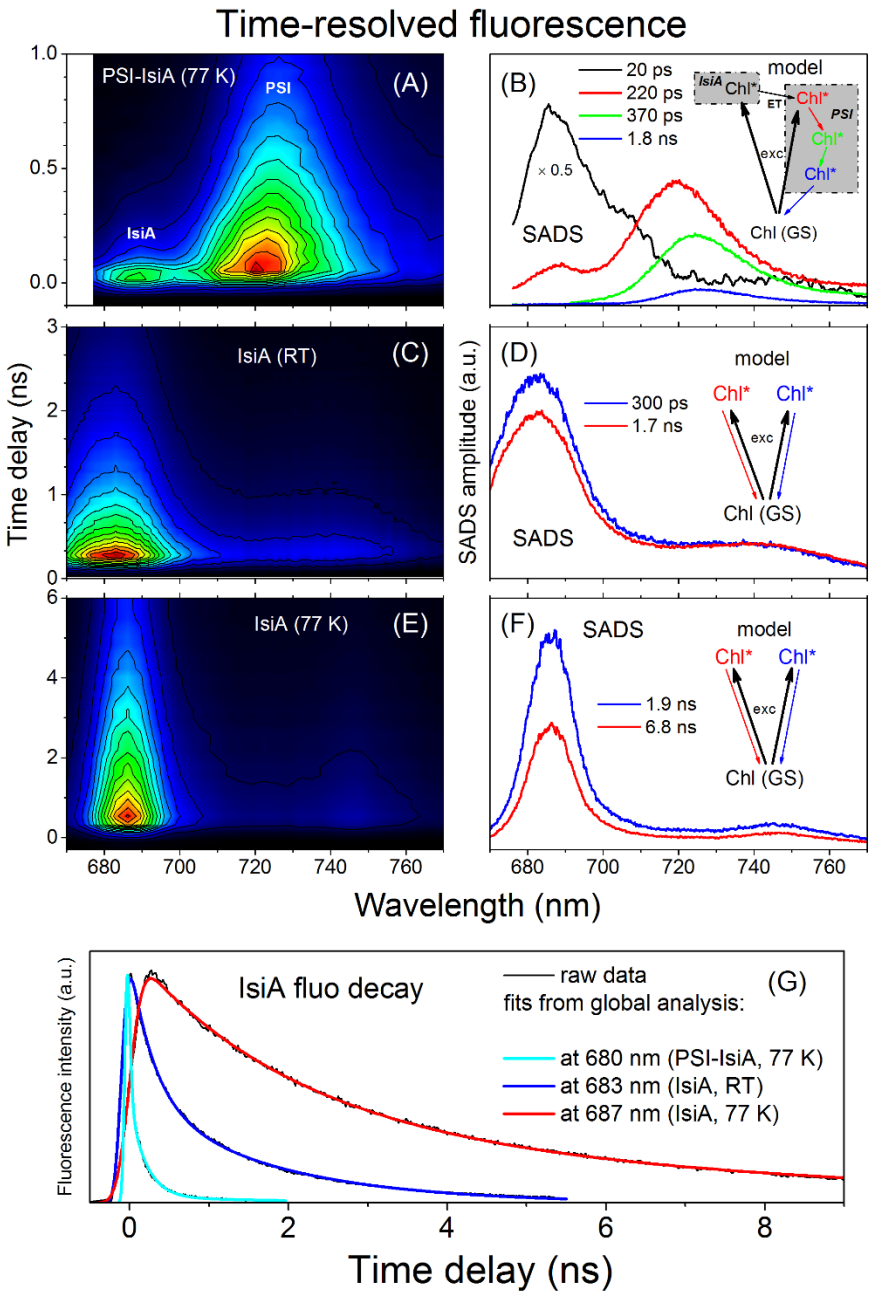

Figure 2.3 Time-resolved fluorescence of PSI-IsiA and IsiA complexes at RT and at 77 K. (A, C, E) Two-dimensional, pseudo-color fluorescence decay profiles of PSI-IsiA at 77 K, IsiA at RT and at 77 K, respectively. (B, D, F) Global analysis results of TRF datasets (SADS) with application of anticipated kinetic schemes of the excitation decay. The models are provided as insets. The legends contain effective lifetimes of spectro-kinetic components obtained from the analysis. (G) Representative traces of the IsiA fluorescence decay extracted for the datasets along with corresponding fits obtained from global analysis. exc - excitation, GS - ground state, ET - energy transfer, Chl – chlorophyll *a*, SADS – species associated decay spectra.

Global fitting of the RT TRF data of separate IsiA samples revealed two kinetic components with lifetimes of 300 ps and 1.7 ns. The fitting protocol assumed that both fractions were independently populated and decayed without interacting with each other. The spectral profiles of SADS showed identical line shapes. These lifetimes are comparable to those observed in the fluorescence decay of quenched IsiA aggregates in which a short kinetic component lifetime of ~200 ps dominates (Ihalainen *et al.* 2005). Interestingly, a substantial alteration of fluorescence lifetime distribution occurs if the IsiA protein is cooled to 77 K. Fitting results (Figure 2.3F) demonstrated that the lifetimes substantially lengthen to 1.9 ns and 6.8 ns, but the spectral lineshapes of both SADS remain identical although the fluorescence band is narrower and slightly red-shifted at 77 K. To assure that elongation of fluorescence lifetime is truly temperature dependent effect and is not simply due to presence of glycerol in the buffer, we compared the dynamics of Chl *a* fluorescence decay of the IsiA protein diluted only in the buffer and in the buffer-glycerol mixture, measured at RT. These results are given in supplementary information (Figure S2.1) and demonstrate that adding glycerol has negligible impact on IsiA fluorescence dynamics. Figure 2.3G shows the comparison of representative kinetic traces of fluorescence decay for IsiA-containing samples under different conditions: IsiA coupled with PSI at 77 K (cyan line), and IsiA aggregates at RT (blue line) and at 77 K (red line). Lifetime shortening of IsiA-bound Chl *a* fluorescence upon coupling to PSI is understandable and is associated with IsiA-PSI energy transfer; however, the substantial lengthening of the Chl *a* excited state lifetime in IsiA aggregates after cooling to cryogenic temperature is not easy to interpret and merits further investigation.

2.3.3 Time-resolved absorption spectroscopy of the IsiA complex

The strong dependence of the lifetime of excited Chl *a* in IsiA samples on temperature, as demonstrated in the time-resolved fluorescence studies, questions the idea that carotenoids are responsible for Chl *a* quenching. Previous studies on carotenoid-mediated Chl *a* quenching in another cyanobacterial chlorophyll protein from a family of High-Light Inducible Proteins (Hlips) clearly demonstrated that the quenching ability of the carotenoid is essentially not affected by low temperature (Niedzwiedzki *et al.* 2016) and lengthening of the effective lifetime of the quenched Chl *a* is not expected. In addition, at cryogenic temperature, the carotenoid reveals a very prominent electrochromic response to excited Chl *a*. An electrochromic response of carotenoid that interacts with either Chl *a* or BChls is not unusual; on the contrary, it is typically observed in many other photosynthetic proteins like PCP from dinoflagellates (Schulte *et al.* 2009) or LH2 and LH1 light harvesting complexes from purple bacteria (Herek *et al.* 2004; Herek *et al.* 1998; Ma *et al.* 2008; Zhang *et al.* 2001), particularly at cryogenic temperature. In those proteins, carotenoids play a role as either singlet energy donors or (B)Chls triplet quenchers. Both roles require that carotenoid and (B)Chl molecules are in close proximity, and thus carotenoid absorption should be similarly affected by the change in the surrounding electric field induced by (B)Chl excited state. We applied time-resolved absorption to test if the electrochromic effect on carotenoid absorption is also observed in IsiA. A negative result would indicate that carotenoids are likely not responsible for the Chl *a* quenching that is observed at RT, as the lack of electrochromic response to the excited Chl *a* would indicate that both pigments are not at a distance that allows energy transfer between them.

The results obtained for IsiA measured at 77 K are given in Figure 4. To test all possible outcomes, the sample was excited at wavelengths corresponding to absorption bands of all bound

pigments: β-carotene (at 505 nm), echinenone (at 535 nm) and Chl *a* (Q_y band, at 670 nm). Representative transient absorption spectra obtained after excitation of the carotenoid bands are given in Figures 4A and B. The spectra consist mostly of features associated with bleaching of the ground state absorption of the carotenoid (the negative region mirroring expected steady-state absorption of the carotenoid in IsiA) and associated positive excited state absorption, $S_1 \rightarrow S_n$, band. For β-carotene, this band peaks at 680 nm, for echinenone at 600 nm. Previous TA study of this protein suggested that instantaneous and prominent bleaching of Q_y band Chl *a* upon excitation of carotenoid band is a clear indication of carotenoid to Chl *a* energy transfer presumably via S_2 state. For echinenone, the quantum efficiency of the energy transfer process was ~40% (Berera *et al.* 2010). However, such interpretation of the TA results does not agree with fluorescence excitation that shows that carotenoid-to-Chl *a* energy transfer is negligible. The signal with apparent Chl *a* signatures must come from direct excitation of Chl *a* to a vibronic overtone of Q_y band. To elaborate further and prove that it is possible, we performed a TA study of Chl *a*- β-carotene mixture dissolved in n-hexane. The mixture closely mimicked absorption spectrum of the IsiA protein sample. In the mixture, energy transfer between pigments is negligible and upon excitation of the carotenoid band, any signal associated with Chl *a* should derive from its direct excitation. These results, shown in Figure S2.2 also support the idea of self-origin of Chl *a* signal in the IsiA sample upon carotenoid band excitation.

The TA data were fitted with anticipated models of the excitation decay path, and the resulting spectro-kinetic profiles (SADS) are given in Figure 2.4C and D. To simplify fitting, the spectral range comprising the Chl *a* Q_y band was not included. The SADS lifetimes of 10.5 and 6.6 ps associated with decay of the S_1 state indicate that both carotenoid pigments perform essentially as when in frozen solvent (for echinenone, 3'-hydroxyechinenone was used as a

benchmark) (Niedzwiedzki *et al.* 2006; Polivka *et al.* 2005), and binding to the protein does not induce any geometrical distortions, as that typically would affect those lifetimes.

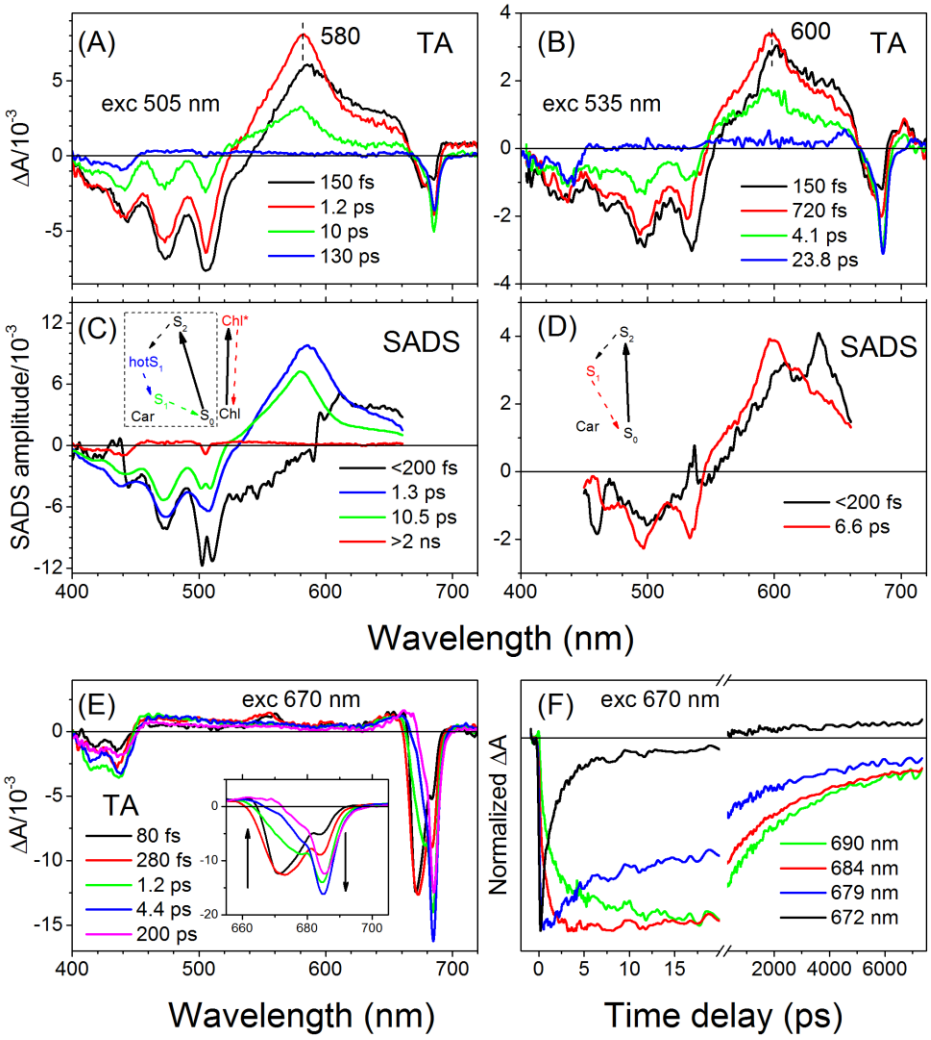

Figure 2.4 Time-resolved absorption of the IsiA complex at 77 K. (A, B) Representative TA spectra after selective excitation of the carotenoid absorption band: β-carotene (excitation at 505 nm) and echinenone (excitation at 535 nm). (C, D) Species associated difference spectra (SADS) resulting from global analysis of the TA datasets with application of the kinetic models provided in the graph inserts. (E) Representative TA spectra taken after excitation at the blue edge of the Chl *a* Q_y absorption band at 670 nm. (F) Representative kinetic traces of rise and decay of Q_y band probed at multiple wavelengths.

For early delay times, the spectra, 77 K transient absorption of IsiA upon excitation of the Q_y band of Chl *a* (Figure 2.4E), indicate rapid energy transfer within two different spectral forms of Chl *a*, as indicated by the split Q_y band (see insert). This intermolecular Chl *a*-Chl *a* energy flow is also well indicated in the kinetic traces provided in Figure 2.4F. More importantly, there is no signature of a carotenoid electrochromic response, either in β -carotene or echinenone. A bump appearing between 540 and 580 nm within the first 200 fs is also visible in blank buffer (not shown), indicating it is clearly associated with solvent response to the excitation.

More insight into the kinetic characteristics of Chl *a* in IsiA at 77 K is given in Figure 2.5. Figure 2.5A shows that rapid decay of the Chl *a* bleaching band at 671 nm is coupled with the rise of the bleaching of the band at 684 nm. The time constant of 1.3 ps obtained from fitting of the decay trace at 671 nm, matches very well with the rise constant of 1.1 ps observed in the 684 nm trace. This strongly indicates that none of the excitation initially localized on Chls absorbing at 670 nm is lost, but that it is essentially instantaneously passed on to low-energy Chls. This demonstrates that the Chl *a* array in this protein is very well optimized to minimize any potential loss of excitation during migration within IsiA.

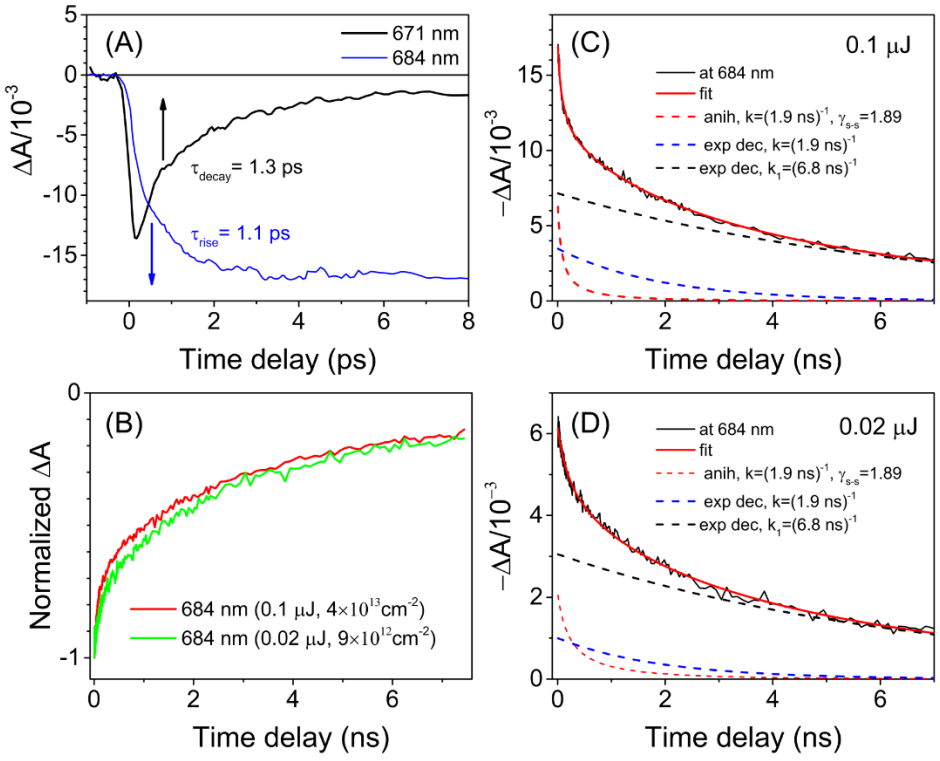

Figure 2.5 Temporal characteristics of recovery of the Chl *a* Q_y band of IsiA at 77 K. (A) Rise and decay of two Q_y sub-bands resolved by TA at 77 K. (B) Dependence of recovery dynamics on excitation intensity. (C, D) Fitting of kinetic traces according to equation 2.1.

On the other hand, recovery of the bleaching of the 684 nm Q_y band should temporarily show the same characteristics as the time-resolved fluorescence data because most likely the same pool of Chls is probed in both techniques. However, it should be noted that since an amplified laser excitation beam is used in transient absorption measurements, it is possible that multiple excitations are simultaneously populated within the Chl *a* exciton manifold and singlet-singlet annihilation will be unavoidable. Because the extent of this process is laser intensity dependent, it could be easily spotted by comparing the kinetic traces recorded upon vastly different excitation laser intensities. This is given in Figure 2.5B, which shows the recovery of the bleaching of the Chl *a* Q_y band at 684 nm for two substantially different excitation fluxes. Because both traces,

normalized at amplitudes, do not overlap, and the kinetic trace obtained at higher laser intensity initially decays faster, involvement of singlet-singlet annihilation is apparent. Consequently, an appropriate fitting model should account for an annihilation process. If it is assumed that the time of convoluting the Chl *a* transient signal (exciton generation) is negligible compared to the following decay, the 684 nm kinetic trace could be fitted according to the following equation that was adapted from (Zaushitsyn *et al.* 2007):

$$\Delta A(t) = \frac{\Delta A_1 e^{-kt}}{1+\Delta A_1 \gamma_{s-s} k^{-1}\left(1-e^{-kt}\right)} + \Delta A_2 e^{-kt} + \Delta A_2 e^{-k_1 t} \qquad (2.1)$$

where γ_{s-s} is the time-independent annihilation rate and *k* and k_1 are decay rates of Chl fractions that are not affected by singlet-singlet annihilation and should correspond to reciprocals of lifetimes obtained from time-resolved fluorescence. It was also assumed that the annihilation process would involve only the Chl *a* fraction that decays with a larger rate constant, *k*. The results of fitting of both traces (lower and higher laser intensity) are given in Figure 2.5C and D. Fitting demonstrates very good agreement with results obtained from time-resolved fluorescence.

2.3.4 Role of carotenoids in the IsiA protein

Previous investigations proposed that carotenoids play a dual role in the IsiA protein augmenting Chl *a* in light harvesting, and furthermore, if necessary, serving as quenchers of excited Chl *a* (Berera *et al.* 2009; Berera *et al.* 2010). However, our work does not support these suggested roles. The Chl *a* florescence excitation study shows that none of the two carotenoid species transfers absorbed light energy to the Chls. Time-resolved fluorescence experiments showed that the kinetic component (fast decay) that was previously targeted as a signal associated with the decay of quenched Chl *a* (Ihalainen *et al.* 2005) substantially lengthens at low temperature. This is difficult to explain because carotenoid-mediated quenching is often

independent of temperature (Niedzwiedzki *et al.* 2016), and the lifetime of quenched Chl *a* should not be affected. Moreover, cryogenic time-resolved absorption data revealed that none of the bound carotenoids show an electrochromic response to excited Chl *a*, a feature commonly seen in light harvesting proteins in which carotenoid and (B)Chl are bound in sufficient proximity to allow energetic interaction between them.

2.3.5 Toward a new quenching mechanism

A clue that a novel type of quenching mechanism may be present in the IsiA protein is that, upon lowering the temperature, Chl *a* fluorescence decay substantially elongates. A similar effect is well-known for another light harvesting protein, the Fenna-Matthews-Olson (FMO) protein from green sulfur bacteria. The FMO protein, which lacks carotenoids and comprises only BChl *a* pigments, if kept in oxygenated solution displays a very short BChl *a* fluorescence lifetime of ~60 ps, which is short enough to compete efficiently with energy transfer to the reaction center (RC) in the FMO-RC complex (Oh-Oka *et al.* 1998; Neerken *et al.* 1998; He *et al.* 2015). However, if conditions change from oxidizing to reducing, the BChl *a* fluorescence lifetime lengthens to ~2 ns, close to the intrinsic decay of the excited state of monomeric BChl *a* in solution (Niedzwiedzki and Blankenship 2010). However, a substantial elongation of fluorescence lifetime can also be achieved by freezing an oxidized FMO sample to cryogenic temperature (Orf *et al.* 2014). This appears to resemble the phenomenon seen for IsiA in this work. Even though the effect of reductant on BChl *a* fluorescence in the FMO protein was known for almost three decades, only very recently was it explained. It was demonstrated that in aerobic conditions the cysteine thiols are converted to thiyl radicals, and if those are in proximity to BChl *a*, they may quench the pigment excited state through electron-transfer photochemistry (Orf *et al.* 2016). It is not difficult to imagine that a similar quenching mechanism may be adopted by other photosynthetic organisms.

A

Species	Protein	UniProt ID	Sequence alignment
Synechocystis sp. (strain PCC 6803)	IsiA	Q55274	I F V G F L L I G G G I W ...G F V A A Y F **C** A V N T L A Y
Synechococcus elongatus (strain PCC 7942)	IsiA	P15347	V Y Y V G V M L I A G G I W ...G F V A A Y F **C** A V N T L A Y
Thermosynechococcus elongatus (strain BP-1)	IsiA	Q8DK20	I Y I A I L L I A G G I W ...G F V A A Y F **C** A V N T L A Y
Synechocystis sp. (strain PCC 6803)	CP43	P09193	I W I G L I **C** I S G G I W ... G F I A S V F V W F N N T A Y
Synechococcus elongatus (strain PCC 7942)	CP43	P11004	I W I G L I **C** I S G G I W ... G F I A S T M V W Y N N T V Y
Thermosynechococcus elongatus (strain BP-1)	CP43	Q8DIF8	I W I G L I **C** I A G G I W ...G F I A T **C** F V W F N N T V Y
Spinacia oleracea (spinach)	CP43	P06003	V W I G V I **C** I L G G I W ...G F I A **C C** F V W F N N T A Y

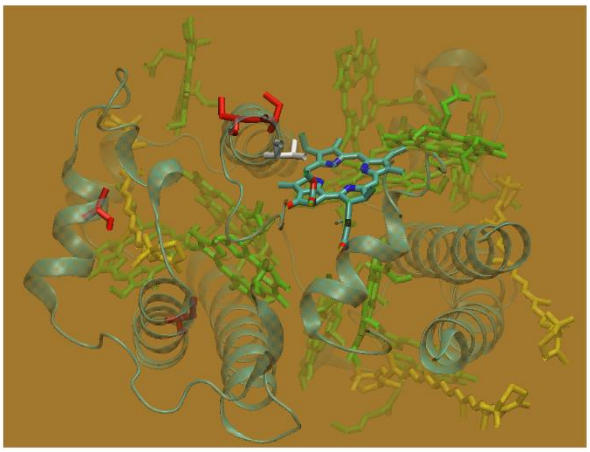

B

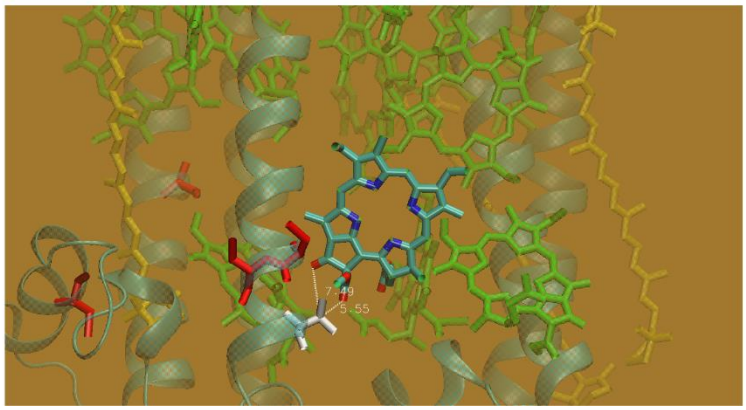

C

Figure 2.6 Cysteines in CP43 and IsiA structures. (A) Sequence alignment of IsiA and CP43 from three cyanobacterial species, along with the sequence from spinach for which the high resolution crystal structure of CP43 is known (PDB ID: 3JCU, (Wei *et al.* 2016)). A simplified view of the CP43 protein molecular structure from the (B) lumenal and (C) membrane side, which in IsiA will face toward PSI. For clarity, the large extrinsic lumenal loop domain E (Bricker and Frankel 2002) present in CP43 was removed. All possible cysteines present in various CP43 proteins across different organisms are marked in red. Valine 290, which in IsiA is replaced by cysteine and is fully conserved across multiple organisms, is marked in white.

Cyanobacteria, which are photosynthetic organisms living in oxidizing conditions and exposed to constant iron-starvation stress, are good candidates for adopting this protective mechanism and incorporating it into a light-harvesting antenna complex that is produced under challenging growth environments - IsiA. This mechanism would require the presence of cysteine in crucial places in the IsiA protein, preferentially in proximity to Chl(s) that may serve role(s) as so-called terminal emitter(s) (pass excitation to PSI) – most likely those pigments are responsible for observed fluorescence. In addition, a cysteine targeted as a quenching ligand should be quite unique, in that it must be present in IsiA but not in homologous proteins (such as CP43) that do not reveal similar Chl *a* fluorescence quenching.

To test this hypothesis, we compared the IsiA and CP43 protein sequences from three cyanobacterial species and also the CP43 protein sequence from spinach, which has a high-resolution crystallographic structure available (PDB ID: 3JCU) (Wei *et al.* 2016). The most relevant parts of the sequence alignment are given in Figure 2.6. This analysis demonstrated that cysteine is very scarce in cyanobacterial CP43 proteins, appearing only in two or three locations across the entire sequence, either on the protein side facing the membrane or not in proximity to any Chl *a*. This is consistent with the fact that CP43 does not show evidence of Chl *a* fluorescence quenching. However, the IsiA sequences have a unique cysteine that is fully conserved across the various IsiA proteins, whereas all CP43 sequences examined have valine (Val290) in this position. As shown in the simplified view of the CP43 crystal structure in Figures 2.5B and C, Val290 is in very close proximity to a Chl *a* molecule (Chl a_{34}), according to nomenclature used in the older PSII crystal structure (Loll *et al.* 2005). If replaced by cysteine, the distance between the amino acid and electron donating groups of Chl a_{34} would range between 5 and 7 Å, similar to distances observed between cysteine and BChl *a* in the FMO protein. According to the IsiA-PSI

supercomplex models (Feng *et al.* 2011; Nield *et al.* 2003), Chl a_{34} is the pigment that along with other nearby Chls (Chl $a_{37, 44, 41}$) could be involved in energy transfer to PSI. Importantly, the cysteine residues that are present in the sequence of CP43 from spinach, just two places away from Val290, if visualized on the structure (Figure 2.6B and C) appear on the opposite side of the helix and are essentially completely shielded from any Chls. Those cysteines may not be important because they are not conserved across different photosynthetic groups, which is clearly shown in the sequence alignment (Figure 2.6A). This structure-sequence analysis suggests that the IsiA protein has the capability of quenching the Chl *a* excited state through electron transfer photochemistry. Because cyanobacteria grow in aerobic conditions, the cysteine thiol in IsiA could be converted to a thiyl radical at any time and be capable of withdrawing an electron from a nearby excited Chl *a*. If this mechanism is behind the quenching of the excited state of Chl *a* in IsiA, the dynamics of protein fluorescence should be sensitive to the presence of reductant in the buffer, as was observed for FMO. Changes in the fluorescence decay dynamics of IsiA upon addition of sodium dithionite, a reductant that is typically used for FMO studies, are shown in Figure 2.7.

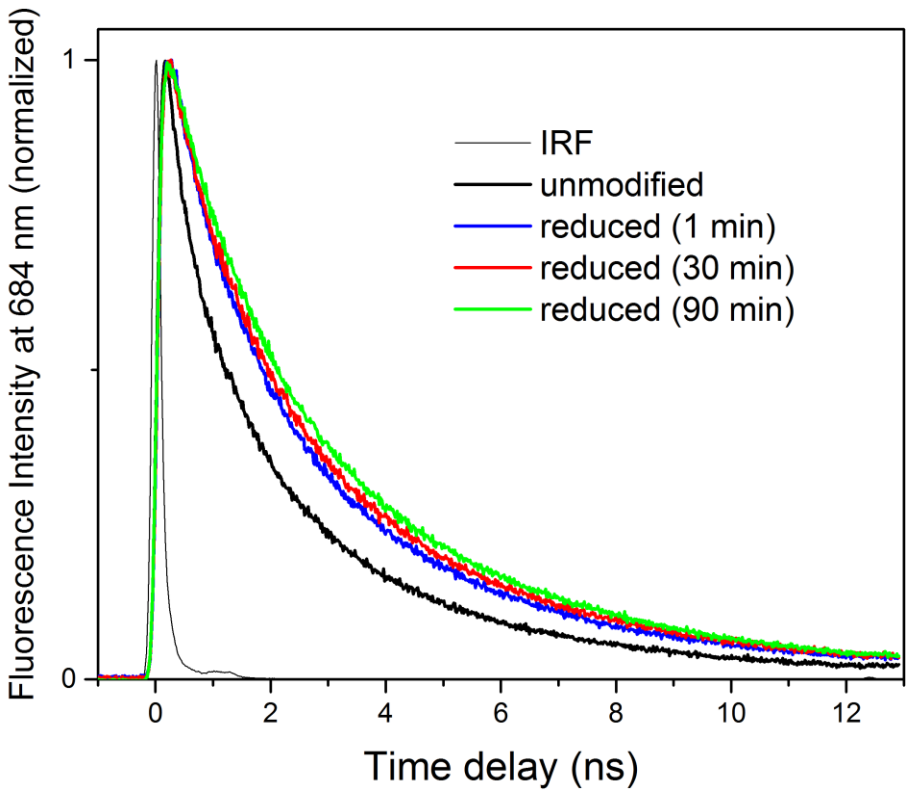

Figure 2.7 Temporal changes of IsiA-bound Chl *a* fluorescence decay upon addition of sodium dithionite (to a final 10 mM concentration) to the sample buffer. Fluorescence was recorded at 684 nm at RT. IRF – instrument response function.

To observe any changes in a more real-time fashion, a more sensitive TCSPC system was used. The fluorescence decay was measured at the maximum of the fluorescence emission spectrum (684 nm). The results show that the addition of reductant leads to a change in the temporal characteristics of fluorescence decay within a minute and that the effect is essentially maximized after ~90 min. It is apparent that the short-lived component considerably elongates. It is worth noting that sodium dithionite may not be most effective reductant as it is not physiologically relevant, and it is possible that other more natural, endogenous reductants (not tested here) may induce even more prominent effects on fluorescence decay dynamics.

Nonetheless, the observed effect is a strong indication of a cysteine-dependent excitation quenching mechanism in the IsiA protein, which was only very recently found in the FMO protein

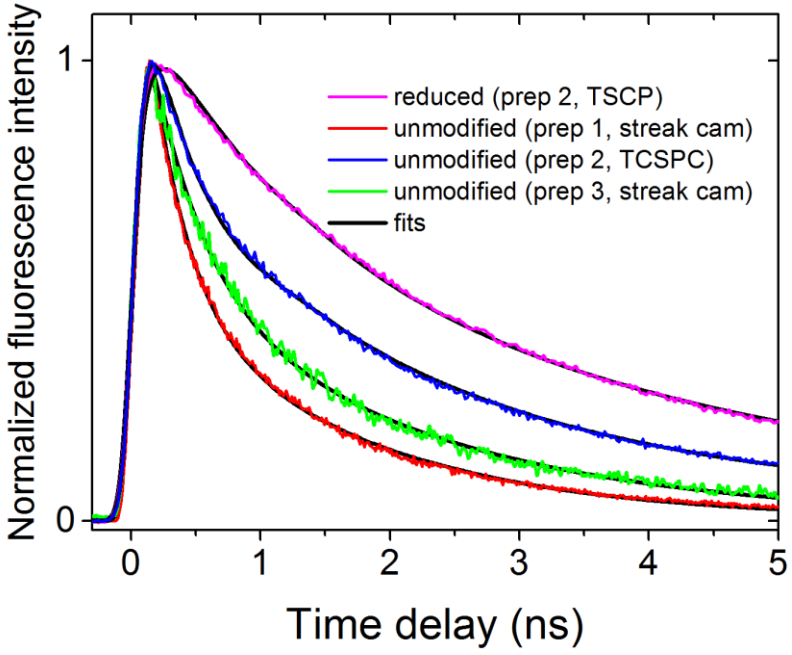

Figure 2.8 Variation of dynamics of Chl *a* fluorescence decay in the unmodified IsiA protein obtained from different purification experiments (prep 1, 2, 3) and effect of adding reductant. For more details on kinetic components refer to Table 2.1.

It should be noted that the fluorescence decay trace of the unmodified IsiA seems to be different from that obtained from the experimental setup based on the streak camera (Figure 2.3). Those two samples show common absorption spectra; however, they were obtained from different purification experiments. Additional TRF experiment performed on the unmodified IsiA protein from another (third) preparation demonstrated that every time, Chl *a* fluorescence kinetics of unmodified IsiA are somewhat different from each other (Figure 2.8). Further analysis (Table 2.1) demonstrated that all of them share similar kinetics components, however with different weights. Such variation in amplitudes of the decay components could be associated with fluctuation in natural levels of oxidation of cysteines; these levels may vary from preparation to preparation.

Table 2.1 Kinetic components obtained from fitting of Chl *a* fluorescence decay traces given in Fig 2.8.

Preparation	Sample†	τ_1 (ps)	A_1‡	τ_2 (ns)	A_2	τ_3 (ns)	A_3	Method§
1	U	280	0.62	1.6	0.38	n.e.		SC
2	U	300	0.43	1.6	0.40	4.5	0.17	TCSPC
2	R	n.e.		1	0.45	4.1	0.55	TCSPC
3	U	400	0.53	2.0	0.47	n.e.		SC

† U, unmodified IsiA; R, reduced IsiA
‡ $A_1+A_2+A_3=1$
§ SC, streak camera; n.e., not evident

2.4 Conclusions

In this study we revisited the mechanism of Chl *a* excitation quenching in the IsiA protein, which is a dominant light harvesting antenna complex produced by iron-starved cyanobacteria. In contrast to previous work relying on energetic interactions of the excited Chl *a* with carotenoids present in IsiA, our study indicates that quenching of excited Chl *a* may be cysteine-dependent, similar to the quenching mechanism recently revealed in FMO, a light harvesting protein from green sulfur bacteria. This finding opens many possibilities for more detailed studies of the quenching mechanism adapted by iron-starved cyanobacteria, including the influence of cysteine directed chemical modifications or cysteine directed mutations.

2.5 Materials and Methods

Strain growth and thylakoid membrane preparation

The IsiA-His strain of *Synechocystis* sp. PCC 6803 was constructed by oligonucleotide-directed mutagenesis to introduce six histidyl codons at the carboxy terminus of *isiA*. IsiA-His cells were grown phototrophically in BG11 medium containing kanamycin at 30 ℃. The liquid cultures were shaken in Erlenmeyer flasks at 60 rpm with illumination of 30 μmol photons m^{-2} s^{-}

[1]. After 5 days of growth, cells were washed with YBG11-Fe (Shcolnick *et al.* 2007) medium three times, and inoculated into 1 L YBG11-Fe medium. After about 2 weeks, the cells were then harvested and broken by bead-beating as described previously (Kashino *et al.* 2002). Thylakoid membranes were resuspended in Buffer A (50 mM HEPES-NaOH [pH 7.8], 10 mM $MgCl_2$, 5 mM $CaCl_2$, 25% glycerol). Membranes were solubilized by addition of β-D-dodecyl maltoside (DDM) to a final concentration of 1%. After incubation on ice in dark for 30 minutes, the solubilized membranes were separated from the insoluble material by centrifugation at gradually increasing speed from 120 × g to 27,000 × g at 4 ℃ for 20 minutes. The solubilized membranes were then stored at -80 ℃ for future use.

IsiA protein purification

The IsiA and PSI-IsiA complexes were purified using nickel affinity chromatography (Kubota *et al.* 2010) with some modifications. Ni-NTA slurry was precharged with 50 mM nickel sulfate overnight and loaded into an open column. The resin was washed with 25 column volumes of water, and then twice with 5 column volumes of Buffer A plus 0.04% DDM and 5 mM histidine to remove ethanol and nickel sulfate. After continuous mixing of the washed resin with the previously prepared solubilized membranes at 4 ℃ for 2 hours, the flow through material was collected. The resin was then washed with 1 column volume Buffer A plus 0.04% DDM and 5 mM histidine. To remove all other unbound proteins, 12 column volumes of Buffer A plus 0.04% DDM was used to wash the resin. The eluents were collected and absorption was measured using a DW2000 spectrophotometer (OLIS, USA) to verify that any residual unbound chlorophyll-containing proteins had been washed from the column. The target proteins, PSI-IsiA supercomplexes and IsiA proteins, were eluted with 6 column volumes of buffer A plus 0.04% DDM and 100 mM histidine. To concentrate the proteins, 80% (v/v) PEG8000 in 30 mM HEPES-

NaOH (pH 7.8) was added into the elution, and the proteins were precipitated by centrifugation at 31,000 × g for 15 minutes. The precipitated proteins were resuspended in Buffer A plus 0.04% DDM.

Sucrose gradient ultracentrifugation was used to obtain highly purified IsiA aggregates that do not contain PSI. The PEG-concentrated protein sample was diluted in glycerol-free Buffer A plus 0.04% DDM and then loaded on the top of a 10 – 35% sucrose gradient in glycerol-free Buffer A plus 0.04% DDM. Centrifugation was performed using a swinging bucket type Beckman-Coulter SW41 rotor at 4 ℃ and relative centrifugal force of 186,000 × g. After 18 hours of ultracentrifugation, green bands were collected. The first green band from the top of the gradient was determined spectroscopically to contain only IsiA, and was stored at -80 ℃ until future use.

SDS-PAGE and immunoblot analysis

SDS-PAGE was performed by loading the isolated PSI-IsiA supercomplexes and IsiA protein samples (adjusted to Chl *a* mass weight of 0.75 μg) on 12.5% acrylamide resolving gel. After transfer of the proteins onto a PVDF membrane, IsiA and PsaA were detected by using specific antisera. Bands were visualized using chemiluminescence reagents (EMD Millipore, Billerica, MA, USA) with an ImageQuant LAS-4000 imager (GE Healthcare).

Spectroscopic techniques

For all low-temperature spectroscopic measurements, the IsiA or IsiA-PSI samples were mixed with glycerol in 1:1 (v/v) ratio, placed in 1 cm square plastic cuvettes and frozen in a VNF-100 liquid nitrogen cryostat (Janis, USA). Steady-state absorption measurements were performed using a Shimadzu UV-1800 spectrophotometer. Fluorescence and fluorescence-excitation spectra

were recorded at room temperature using a Horiba-Spex Nanolog fluorometer. The spectra were recorded at 90o to excitation and corrected for the instrument spectral response. The excitation and detection bandwidths were 2– 4 nm. To avoid front-face and inner-filter effects, the samples were adjusted to an absorbance ≤0.1 at the excitation and emission wavelengths.

Time-resolved fluorescence (TRF) experiments were carried out using two different setups. Hamamatsu universal streak camera setup described in detail previously (Niedzwiedzki *et al.* 2013) was used to obtain multi-wavelength decay profiles. The frequency of the excitation pulses was set to 8 MHz, corresponding to ~120 ns between subsequent pulses. The excitation beam set to 630 nm, with photon intensity of ~10^{10} photons/cm^2 per pulse was depolarized and focused on the sample in a circular spot of ~1 mm diameter. The sample absorbance was adjusted to ~0.1 at the Q_y band of Chl *a* in a 1 cm cuvette. The emission was measured at a right angle to the excitation beam. To minimize the detection of scattered light from the excitation beam a long-pass 665 nm filter was placed at the entrance slit of the spectrograph. The integrity of the samples was examined by observing the photon counts in real-time over the time course of the experiment. These were constant, which indicated the absence of sample photodegradation. Single wavelength decay measurements were performed using a standalone Simple-Tau 130 time-correlated single photon counting (TCSPC) setup from Becker&Hickl (Germany) coupled to an ultrafast laser system (Spectra-Physics, USA) described in detail previously (Dilbeck *et al.* 2016). The IsiA complexes were resuspended to an absorbance of ≤0.1 at the Chl *a* Q_y band and the emission signal was recorded at a right angle with respect to the excitation beam.

Transient absorption (TA) measurements of the IsiA protein were performed using a Helios TA spectrometer (UltrafastSystems LCC, Sarasota, FL, USA) coupled to a Spectra-Physics femtosecond laser system described previously in detail (Greco *et al.* 2016). The white light

continuum probe was generated by a 3 mm thick CaF_2 plate. The pump beam with energy set to 0.1 µJ (670 nm, Chl *a*) or 0.2 µJ (505 nm, carotenoids) was focused to a spot size of 1 mm in diameter, corresponding to intensity of ~ 4–6 × 10^{13} photons/cm^2. The sample was adjusted to an absorbance of 0.4 at the Chl *a* Q_y band (1 cm path length).

Data Analysis and Fitting

Dispersion in TA datasets was corrected using Surface Xplorer, a software provided by Ultrafast Systems, by applying a dispersion correction. Directed kinetic modeling, referred to as target analysis, of the TRF and TA results was performed using CarpetView, a data viewing and analysis software for ultrafast spectroscopy measurements (Light Conversion Ltd., Vilnius, Lithuania). The fitting procedures used the kinetic models with anticipated realistic decay pathways following excitation of a carotenoid or Chl *a*. If the underlying assumptions are correct, targeted kinetic analysis separates spectral components such as excited state absorption (ESA) of the specific excited states of molecules, etc. The results are commonly abbreviated as SADS - Species Associated Decay Spectra (van Stokkum *et al.* 2004). We have adapted this nomenclature to the fitting results of both TA and TRF datasets. For fitting purposes, the instrument response function (IRF) was assumed to have a Gaussian-like shape with the full width at half maximum (FWHM) of ~200 fs for TA and 70 ps, 180 ps and 320 ps for TRF in 1, 5 and 10 ns time windows, respectively. This parameter was fixed in the fitting procedures.

2.6 References

Alfonso M, Montoya G, Cases R, Rodriguez R, Picorel R (1994) Core antenna complexes, CP43 and CP47, of higher-plant photosystem-II - spectral properties, pigment stoichiometry, and amino-acid-composition. *Biochemistry* 33 (34):10494-10500. doi:DOI 10.1021/bi00200a034

Andrizhiyevskaya EG, Frolov D, van Grondelle R, Dekker JP (2004) Energy transfer and trapping in the Photosystem I complex of *Synechococcus* PCC 7942 and in its supercomplex with IsiA. *BBA-Bioenergetics* 1656 (2-3):104-113. doi:10.1016/j.bbabio.2004.02.002

Andrizhiyevskaya EG, Schwabe TM, Germano M, D'Haene S, Kruip J, van Grondelle R, Dekker JP (2002) Spectroscopic properties of PSI-IsiA supercomplexes from the cyanobacterium *Synechococcus* PCC 7942. *Biochim Biophys Acta* 1556 (2-3):265-272

Berera R, van Stokkum IHM, d'Haene S, Kennis JTM, van Grondelle R, Dekker JP (2009) A mechanism of energy dissipation in cyanobacteria. *Biophys. J.* 96 (6):2261–2267

Berera R, van Stokkum IHM, Kennis JTM, van Grondelle R, Dekker JP (2010) The light-harvesting function of carotenoids in the cyanobacterial stress-inducible IsiA complex. *Chem. Phys.* 373 (1–2):65–70

Bibby TS, Nield J, Barber J (2001a) Iron deficiency induces the formation of an antenna ring around trimeric photosystem I in cyanobacteria. *Nature* 412 (6848):743-745. doi:10.1038/35089098

Bibby TS, Nield J, Barber J (2001b) Three-dimensional model and characterization of the iron stress-induced CP43'-photosystem I supercomplex isolated from the cyanobacterium *Synechocystis* PCC 6803. *J. Biol. Chem.* 276 (46):43246-43252. doi:10.1074/jbc.M106541200

Boekema EJ, Hifney A, Yakushevska AE, Piotrowski M, Keegstra W, Berry S, Michel KP, Pistorius EK, Kruip J (2001) A giant chlorophyll-protein complex induced by iron deficiency in cyanobacteria. *Nature* 412 (6848):745-748. doi:10.1038/35089104

Bricker TM, Frankel LK (2002) The structure and function of CP47 and CP43 in Photosystem II. *Photosynth. Res.* 72 (2):131-146. doi:Doi 10.1023/A:1016128715865

de los Rios A, Grube M, Sancho LG, Ascaso C (2007) Ultrastructural and genetic characteristics of endolithic cyanobacterial biofilms colonizing Antarctic granite rocks. *FEMS Microbiol Ecol* 59 (2):386-395

De Marais DJ (2000) Evolution. When did photosynthesis emerge on Earth? *Science* 289 (5485):1703-1705

Dilbeck PL, Tang Q, Mothersole DJ, Martin EC, Hunter CN, Bocian DF, Holten D, Niedzwiedzki DM (2016) Quenching capabilities of long-chain carotenoids in light harvesting-2 complexes from *Rhodobacter sphaeroides* with an engineered carotenoid synthesis pathway. *J. Phys. Chem. B.* 120 (24):5429–5443. doi:10.1021/acs.jpcb.6b03305

Feng X, Neupane B, Acharya K, Zazubovich V, Picorel R, Seibert M, Jankowiak R (2011) Spectroscopic study of the CP43′ complex and the PSI–CP43′ supercomplex of the cyanobacterium *Synechocystis* PCC 6803. *J. Phys. Chem. B.* 115 (45):13339-13349

Gantt E (1981) Phycobilisomes. *Annu. Rev. Plant Physiol.* 32 (1):327-347

Greco JA, LaFountain AM, Kinashi N, Shinada T, Sakaguchi K, Katsumura S, Magdaong NC, Niedzwiedzki DM, Birge RR, Frank HA (2016) Spectroscopic investigation of the carotenoid

deoxyperidinin: Direct observation of the forbidden S0 ®S1 transition. *J. Phys. Chem. B.* 120 (10):2731-2744. doi:10.1021/acs.jpcb.6b00439

He GN, Niedzwiedzki DM, Orf GS, Zhang H, Blankenship RE (2015) Dynamics of energy and electron transfer in the fmo-reaction center core complex from the phototrophic green sulfur bacterium Chlorobaculum tepidum. *J. Phys. Chem. B.* 119 (26):8321-8329. doi:10.1021/acs.jpcb.5b04170

Herek JL, Polivka T, Pullerits T, Fowler GJS, Hunter CN, Sundstrom V (1998) Ultrafast carotenoid band shifts probe structure and dynamics in photosynthetic antenna complexes. *Biochemistry* 37 (20):7057–7061. doi:DOI 10.1021/bi980118g

Herek JL, Wendling M, He Z, Polivka T, Garcia-Asua G, Cogdell RJ, Hunter CN, van Grondelle R, Sundstrom V, Pullerits T (2004) Ultrafast carotenoid band shifts: Experiment and theory. *J. Phys. Chem. B.* 108 (29):10398–10403. doi:10.1021/jp040094p

Ihalainen JA, D'Haene S, Yeremenko N, van Roon H, Arteni AA, Boekema EJ, van Grondelle R, Matthijs HCP, Dekker JP (2005) Aggregates of the chlorophyll-binding protein IsiA (CP43') dissipate energy in cyanobacteria. *Biochemistry* 44 (32):10846–10853

Kashino Y, Lauber WM, Carroll JA, Wang Q, Whitmarsh J, Satoh K, Pakrasi HB (2002) Proteomic analysis of a highly active photosystem II preparation from the cyanobacterium *Synechocystis* sp. PCC 6803 reveals the presence of novel polypeptides. *Biochemistry* 41 (25):8004-8012

Kubota H, Sakurai I, Katayama K, Mizusawa N, Ohashi S, Kobayashi M, Zhang P, Aro E-M, Wada H (2010) Purification and characterization of photosystem I complex from *Synechocystis* sp. PCC 6803 by expressing histidine-tagged subunits. *BBA-Bioenegetics* 1797 (1):98-105

Lane N (2002) Oxygen: the molecule that made the world. OUP Oxford,

Loll B, Kern J, Saenger W, Zouni A, Biesiadka J (2005) Towards complete cofactor arrangement in the 3.0 angstrom resolution structure of photosystem II. *Nature* 438 (7070):1040-1044. doi:10.1038/*Nature*04224

Ma F, Kimura Y, Zhao XH, Wu YS, Wang P, Fu LM, Wang ZY, Zhang JP (2008) Excitation dynamics of two spectral forms of the core complexes from photosynthetic bacterium *Thermochromatium tepidum*. *Biophys. J.* 95 (7):3349-3357. doi:DOI 10.1529/biophysj.108.133835

Melkozernov AN, Bibby TS, Lin S, Barber J, Blankenship RE (2003) Time-resolved absorption and emission show that the CP43' antenna ring of iron-stressed *Synechocystis* sp. PCC6803 is efficiently coupled to the photosystem I reaction center core. *Biochemistry* 42 (13):3893-3903. doi:10.1021/bi026987u

Neerken S, Permentier HP, Francke C, Aartsma TJ, Amesz J (1998) Excited states and trapping in reaction center complexes of the green sulfur bacterium *Prosthecochloris aestuarii*. *Biochemistry* 37 (30):10792-10797

Niedzwiedzki DM, Blankenship RE (2010) Singlet and triplet excited state properties of natural chlorophylls and bacteriochlorophylls. *Photosynth. Res.* 106 (3):227–238. doi:10.1007/s11120-010-9598-9

Niedzwiedzki DM, Jiang J, Lo CS, Blankenship RE (2013) Low-temperature spectroscopic properties of the peridinin−chlorophyll *a*−protein (PCP) complex from the coral symbiotic dinoflagellate *Symbiodinium*. *J. Phys. Chem. B.* 117:11091–11099

Niedzwiedzki DM, Sullivan JO, Polivka T, Birge RR, Frank HA (2006) Femtosecond time-resolved transient absorption spectroscopy of xanthophylls. *J. Phys. Chem. B.* 110 (45):22872–22885. doi:Doi 10.1021/Jp0622738

Niedzwiedzki DM, Tronina T, Liu H, Staleva H, Komenda J, Sobotka R, Blankenship RE, Polivka T (2016) Carotenoid-induced non-photochemical quenching in the cyanobacterial chlorophyll synthase-HliC/D complex. *BBA-Bioenegetics* 1857 (9):1430–1439. doi:10.1016/j.bbabio.2016.04.280

Nield J, Morris EP, Bibby TS, Barber J (2003) Structural analysis of the photosystem I supercomplex of cyanobacteria induced by iron deficiency. *Biochemistry* 42 (11):3180-3188. doi:10.1021/bi026933k

Oh-Oka H, Kamei S, Matsubara H, Lin S, van Noort PI, Blankenship RE (1998) Transient absorption spectroscopy of energy-transfer and trapping processes in the reaction center complex of *Chlorobium tepidum*. *J. Phys. Chem. B.* 102 (42):8190-8195

Orf GS, Niedzwiedzki DM, Blankenship RE (2014) Intensity dependence of the excited state lifetimes and triplet conversion yield in the Fenna-Matthews-Olson antenna protein. *J. Phys. Chem. B.* 118 (8):2058-2069

Orf GS, Saer RG, Niedzwiedzki DM, Zhang H, McIntosh CL, Schultz JW, Mirica LM, Blankenship RE (2016) Evidence for a cysteine-mediated mechanism of excitation energy regulation in a photosynthetic antenna complex. *P. Natl. Acad. Sci. USA* 113 (31):E4486-4493. doi:10.1073/pnas.1603330113

Pakrasi HB, Goldenberg A, Sherman LA (1985) Membrane development in the cyanobacterium, *Anacystis nidulans*, during recovery from iron starvation. *Plant Physiol* 79 (1):290-295

Polivka T, Kerfeld CA, Pascher T, Sundstrom V (2005) Spectroscopic properties of the carotenoid 3 '-hydroxyechinenone in the orange carotenoid protein from the cyanobacterium *Arthrospira maxima*. *Biochemistry* 44 (10):3994-4003

Reilly P, Nelson N (1988) Photosystem I complex. *Photosynth. Res.* 19 (1-2):73-84. doi:10.1007/BF00114570

Ryan-Keogh TJ, Macey AI, Cockshutt AM, Moore CM, Bibby TS (2012) The Cyanobacterial chlorophyll-binding-protein IsiA acts to increase the *in vivo* effective absorption cross-section of psi under iron limitation1. *J. Phycol.* 48 (1):145-154

Sarcina M, Mullineaux CW (2004) Mobility of the IsiA chlorophyll-binding protein in cyanobacterial thylakoid membranes. *J. Biol. Chem.* 279 (35):36514-36518. doi:10.1074/jbc.M405881200

Schulte T, Niedzwiedzki DM, Birge RR, Hiller RG, Polivka T, Hofmann E, Frank HA (2009) Identification of a single peridinin sensing Chl *a* excitation in reconstituted PCP by crystallography and spectroscopy. *P. Natl. Acad. Sci. USA* 106 (49):20764-20769

Shcolnick S, Shaked Y, Keren N (2007) A role for mrgA, a DPS family protein, in the internal transport of Fe in the cyanobacterium *Synechocystis* sp. PCC6803. *BBA-Bioenegetics* 1767 (6):814-819

Staleva H, Komenda J, Shukla MK, Slouf V, Kana R, Polivka T, Sobotka R (2015) Mechanism of photoprotection in the cyanobacterial ancestor of plant antenna proteins. *Nat. Chem. Biol.* 11 (4):287–291. doi:10.1038/nchemnio.1755

Stumm W, Morgan J (1981) Aquatic chemistry 2nd ed. John Wiley & Sons, New York,

van Stokkum IHM, Larsen DS, van Grondelle R (2004) Global and target analysis of time-resolved spectra. *BBA-Bioenergetics* 1657 (2–3):82–104. doi:http://dx.doi.org/10.1016/j.bbabio.2004.04.011

Wei XP, Su XD, Cao P, Liu XY, Chang WR, Li M, Zhang XZ, Liu ZF (2016) Structure of spinach photosystem II-LHCII supercomplex at 3.2 angstrom resolution. *Nature* 534 (7605):69-+. doi:10.1038/nature18020

Yeremenko N, Kouril R, Ihalainen JA, D'Haene S, van Oosterwijk N, Andrizhiyevskaya EG, Keegstra W, Dekker HL, Hagemann M, Boekema EJ, Matthijs HC, Dekker JP (2004) Supramolecular organization and dual function of the IsiA chlorophyll-binding protein in cyanobacteria. *Biochemistry* 43 (32):10308-10313. doi:10.1021/bi048772l

Zaushitsyn Y, Jespersen KG, Valkunas L, Sundstrom V, Yartsev A (2007) Ultrafast dynamics of singlet-singlet and singlet-triplet exciton annihilation in poly(3-2 '-methoxy-5 '-octylphenyl)thiophene films. *Phys. Rev. B.* 75 (19). doi:ARTN19520110.1103/PhysRevB.75.195201

Zhang JP, Nagae H, Qian P, Limantara L, Fujii R, Watanabe Y, Koyama Y (2001) Localized excitations on the B850a and B850b bacteriochlorophylls in the LH2 antenna complex from *Rhodospirillum molischianum* as probed by the shifts of the carotenoid absorption. *J. Phys. Chem. B.* 105 (30):7312-7322. doi:DOI 10.1021/jp004360k

2.7 Supplemental results

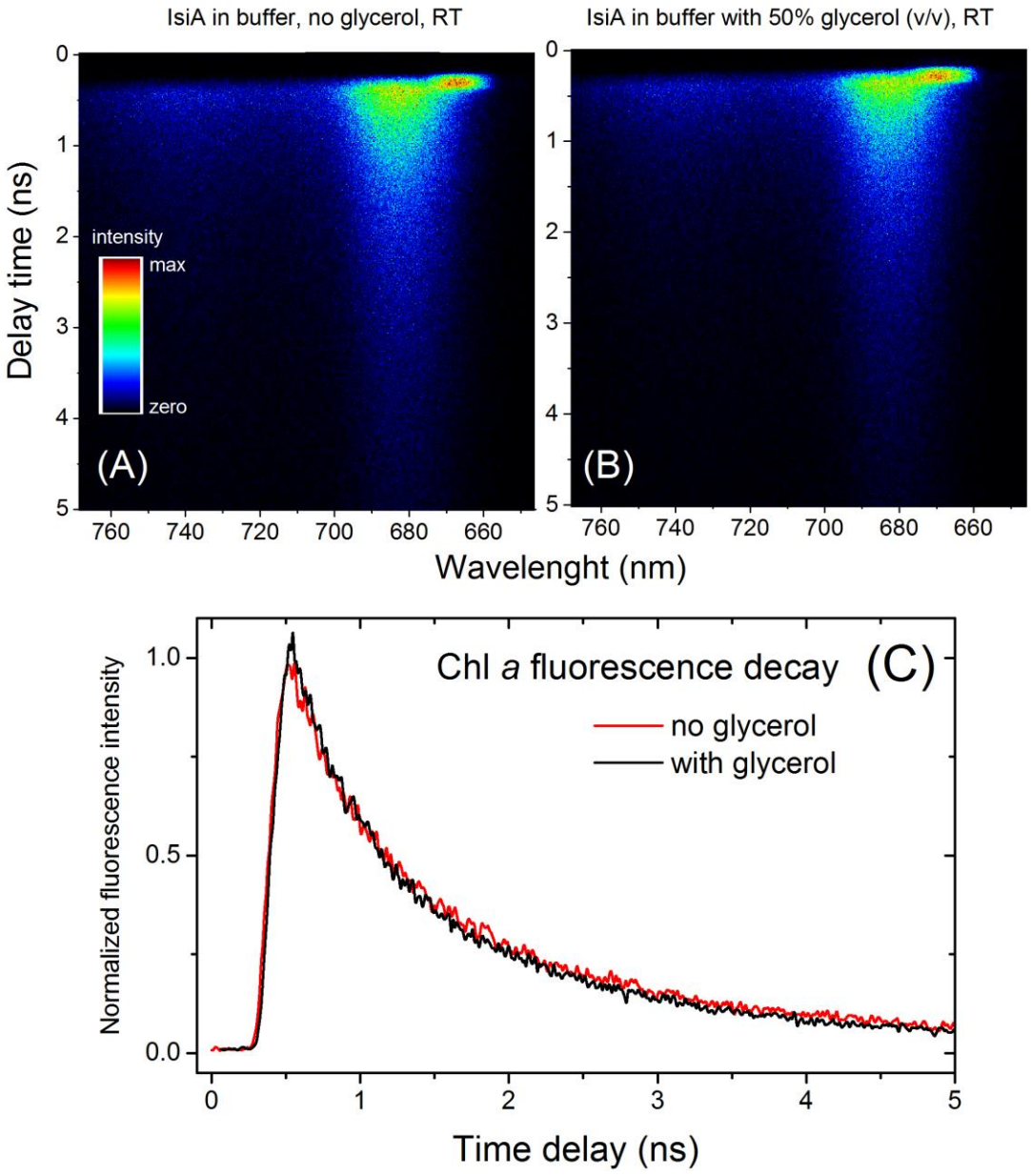

Figure S2.1 Time-resolved fluorescence of IsiA protein diluted in (A) buffer and (B) buffer/glycerol mixture (50% glycerol, v/v) at room temperature. (C) Chl *a* fluorescence decay traces extracted from both streak camera images (A, B).

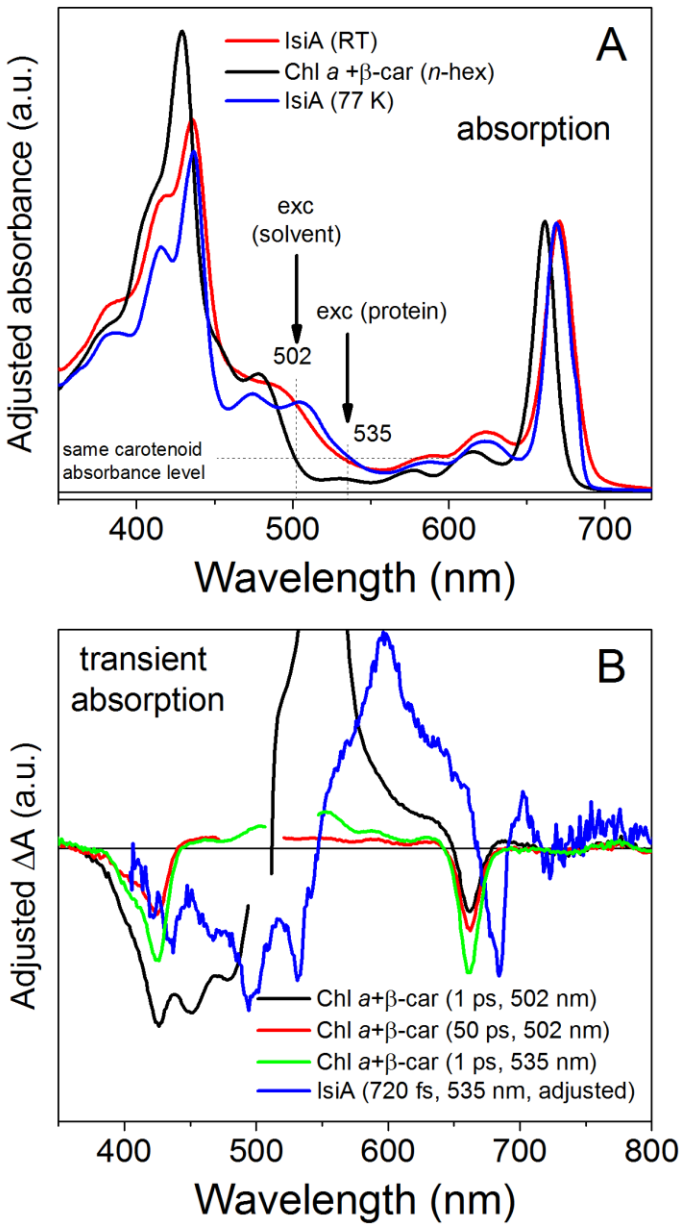

Figure S2.2 (A) Absorption spectra of IsiA at RT and at 77 K overlaid with absorption spectra of Chl *a*-β-carotene mixture in *n*-hexane (with small addition of pyridine to prevent Chl *a* aggregation) mimicking pigment absorption bands in the protein. (B) Transient absorption spectra of Chl *a*-β-carotene mixture compared with TA spectrum of IsiA at 77 K. The IsiA sample was excited at 535 nm, and the pigment mixture sample was excited at 502 nm, the wavelength at which the mixture shows a comparable level of carotenoid absorbance (to IsiA at 535 nm). Since the mixture sample gave a larger signal (due to being more concentrated), the TA spectrum of IsiA was adjusted (multiplied by a constant value) to match the amplitude of bleaching of the carotenoid band in the mixture sample. It is clear that bleaching of Chl *a* absorption bands in both samples will show comparable amplitudes.

3. Chapter Three: Excitation energy quenching by a cysteine-mediated process in IsiA in cyanobacteria

This chapter was adapted from:

Chen HYS, Niedzwiedzki DM, Bandyopadhyay A, Pakrasi HB. Excitation energy quenching by a cysteine-mediated process in IsiA in cyanobacteria. (in preparation)

A. B. performed the protein sequences alignment and D. M. N. performed the experiments and analyses of time-resolved spectroscopy.

3.1 Abstract

Iron stress-induced protein A (IsiA) is a chlorophyll (Chl) *a*-binding membrane protein expressed by cyanobacteria in iron-deficient, strong light, and other stress conditions. IsiA forms a PSI-IsiA supercomplex and serves as an accessary antenna complex for PSI. Although IsiA functions as an independent protein complex (IsiA aggregate), it dissipates excitation energy manifested as shortening of decay time of Chl *a* fluorescence. In chapter 2, we proposed that IsiA uses the cysteine-mediated process to quench excitation energy, and it was the first report of the cysteine-mediated excitation energy quenching process in a photoautotrophic organism. In this chapter, the specific site-directed mutagenesis was performed, abolishing the excitation energy quenching in IsiA and providing the direct evidence of IsiA using this cysteine-mediated process to quench excitation energy. In addition, with only one amino acid substitution, a significant decrease in photosynthetic protein content in the C260V mutant was observed, and the mutant was more light-sensitive in iron-deficient conditions, suggesting that the mutant IsiA is not capable of serving a complete photoprotection function without this critical Cys amino acid residue. Besides, a faster growth in the C260V mutant was observed, implying that the use of light energy is more efficient in the mutant in the iron-replete condition under high light.

3.2 Introduction

Iron deficiency is a common nutrient stress in the habitats of cyanobacteria (Martin and Fitzwater 1988; Moore *et al.* 2013; Vrede and Tranvik 2006; North *et al.* 2007; Bibby *et al.* 2009). In iron-depleted environments, some physiological changes were observed in cyanobacteria including the decrease of chlorophyll (Chl)-binding proteins, phycobilisomes as well as other

proteins containing iron as a co-factor (Sherman and Sherman 1983; Laudenbach and Straus 1988; Laudenbach *et al.* 1988). In response to iron-deficiency, cyanobacteria have evolved strategies to survive in such environments, and these strategies include the induction of the iron stress-induced protein A (IsiA) (Pakrasi *et al.* 1985; Laudenbach and Straus 1988).

IsiA is a Chl *a*-binding membrane protein that was first found in cyanobacteria grown in iron-free media (Laudenbach and Straus 1988; Pakrasi *et al.* 1985). Later reports showed that IsiA can be induced by other stress conditions including oxidative stress, high salt, heat stress, and high light (Yousef *et al.* 2003; Li *et al.* 2004; Havaux *et al.* 2005; Vinnemeier *et al.* 1998). IsiA belongs to a six-transmembrane helices antenna superfamily (La Roche *et al.* 1996), and is highly homologous with CP43, an intrinsic antenna protein of photosystem II (PSII). Unlike CP43, IsiA is being mainly associated with PSI, and forms PSI_3-$IsiA_{18}$ supercomplexes (Boekema *et al.* 2001; Bibby *et al.* 2001a). Time-resolved spectroscopic studies showed that the energy transfer from IsiA to PSI and between IsiA copies in PSI-IsiA supercomplexes is fast and efficient (Melkozernov *et al.* 2003; Andrizhiyevskaya *et al.* 2002a). Because one IsiA binds to 13 Chl *a* (Feng *et al.* 2011a) and one PSI monomer binds to 96 Chl *a* (Jordan *et al.* 2001), the outer IsiA ring can theoretically increase the absorption cross-section of the PSI_3-$IsiA_{18}$ supercomplex by ~81% compared with a PSI trimer. It was later demonstrated *in vivo* that IsiA increased the effective absorption cross-section of PSI by ~60% (Ryan-Keogh *et al.* 2012). These results demonstrated that in the PSI_3-$IsiA_{18}$ supercomplex, IsiA serves as an accessary antenna for PSI.

Besides the PSI_3-$IsiA_{18}$ supercomplex, other PSI_x-$IsiA_y$ supercomplexes and the IsiA-only aggregate were also found in cyanobacterial cells after prolonged growth in iron-depleted conditions (Yeremenko *et al.* 2004). Whereas IsiA functions as a light-harvesting antenna in PSI-IsiA supercomplexes, it was suggested that IsiA, as an IsiA-only aggregate, may be involved in

non-photochemical quenching processes (Park *et al.* 1999). Studies showed that the *isiA* deletion strain is more light-sensitive, suggesting that IsiA plays a significant role in providing photoprotection (Park *et al.* 1999; Havaux *et al.* 2005; Ihalainen *et al.* 2005). However, although it has been determined by time-resolved spectroscopy that the accumulation of IsiA results in a strongly quenched state in cells, suggesting the photoprotective purpose IsiA serves (Ihalainen *et al.* 2005; van der Weij-de Wit *et al.* 2007), the mechanism of IsiA excitation quenching was not fully understood. Original explanations of the quenching mechanism in IsiA assume that carotenoids present in the proteins are solely responsible for quenching of the excited state of Chl *a* (Berera *et al.* 2009; Berera *et al.* 2010).

However, recently this hypothesis was questioned and alternative quenching mechanism, a cysteine-mediated mechanism, first found in the Fenna-Matthews-Olson (FMO) protein in green sulfur bacteria (Orf *et al.* 2016) was proposed (Chen *et al.* 2017). According to it, in an FMO complex under oxidizing conditions, the excitation energy is quenched during the process of electron transfer between the excited bacteriochlorophyll *a* and the thiyl radical at the cysteine radical (Orf *et al.* 2016). The rate of photosynthesis is then reduced, protecting the photosynthetic proteins from photodamage. On the other hand, under reducing conditions, the thiyl radical is converted to a thiol group (or thiolate) and, therefore, no energy quenching takes place in FMO under such conditions (Orf *et al.* 2016). As a result, in green sulfur bacteria, efficiency of excitation energy transfer from the light-harvesting chlorosomes to bacterial reaction centers can be flexibly regulated, depending on prevailing environmental conditions. In our previous study, the spectroscopic signatures, including the increase in Chl *a* fluorescence lifetime in IsiA samples with the addition of reducing agents, showed that IsiA may also use the cysteine-mediated quenching process to quench excitation energy (Chen *et al.* 2017).

In the IsiA protein, the unique cysteine, C260, was identified to play the critical role in the excitation energy quenching process (Chen *et al.* 2017). Intriguingly, sharing a highly similar structure, CP43 does not have this cysteine at the same motif. As an intrinsic antenna protein of PSII, which passes the excitation energy to the reaction center, CP43 has not been reported to quench excitation on its own. Instead of cysteine, CP43 has a valine at this motif in the end of the fifth transmembrane helix. According to the proposed cysteine-mediated mechanism (Chen *et al.* 2017), having a valine at that position cannot facilitate the quenching process and, therefore, no excitation energy quenching takes place in CP43. In this study, site-directed mutagenesis was performed to construct the C260V and C260V-His *Synechocystis* sp. PCC 6803 (thereafter *Synechocystis*) strains, in which the unique cysteine in IsiA is replaced with a valine. To investigate further the significance of this cysteine in excitation energy quenching in IsiA, time-resolved spectroscopy was used to study fluorescence quenching in the C260V IsiA. In addition, we investigated the physiological changes in the C260V mutant cells caused by the single amino acid substitution. We determined that, with only this single amino acid change, C260V, the C260V mutant IsiA is unable to quench excitation energy although it is still capable of serving as a light-harvesting antenna for PSI. Furthermore, we demonstrated that the C260V mutant is more light-sensitive in strict iron-depleted conditions, but has a higher growth rate compared with the wild type cells in iron-replete conditions under high light.

3.3 Results

3.3.1 Construction of C260V and C260V-His *Synechocystis* strains

The mutation in the C260V strain was introduced with the CRISPR/Cpf1 system (Ungerer and Pakrasi 2016) to the wild type (WT) *Synechocystis* strain. The resulting mutant, the C260V

strain, is a marker-less mutant with the least changes needed to replace the cysteine with a valine. All the physiological comparisons in this study were done with this mutant and wile type *Synechocystis*. On the other hand, for the biophysical and biochemical studies, the pure IsiA and PSI-IsiA supercomplexes were needed. The histidine tagged IsiA was used to purify the protein complex and the PSI-IsiA supercomplex in the previous study (Chen *et al.* 2017). In this study, the C260V mutation was introduced into the IsiA-His strain via double homologous recombination. The resulting strain, C260V-His strain, was grown in iron-depleted conditions that induce *isiA* expression. The mutant IsiA and PSI-IsiA supercomplexes were purified from C260V-His strain by affinity chromatography followed by rate-zonal centrifugation.

3.3.2 Purification and basic spectroscopic characterization of mutant PSI-IsiA and IsiA protein complexes.

To answer the question of how this single amino acid mutation, C260V, affects the biophysical properties of the mutant PSI-IsiA and IsiA, the pure C260V IsiA and PSI-IsiA supercomplexes were needed. The results from ultracentrifugation are shown in Figure 3.1. The top green band (band 1) and the thick green band near to the bottom (band 4) were analyzed by immunoblotting. The proteins in both bands were fractionated by SDS-PAGE and visualized by antisera specifically against PsaA and IsiA (Figure 3.1B). These results show that the top green band contains the IsiA-only protein without PSI contamination, and the bottom thick green band contains PSI-IsiA supercomplex. These samples are termed C260V IsiA and PSI-C260V IsiA in this study. Sample purity can also be confirmed in absorption properties of both IsiA preparations. Room-temperature absorption spectra of both IsiA complexes (Figure 3.1C) show that both complexes have essentially identical Chl *a* Q_y bands with maximum at 670.8 nm, showing no PSI contamination, as was demonstrated in previous studies in which shifts Chl *a* Q_y band position by

few nanometers to longer wavelengths were observed (Chen *et al.* 2017; Andrizhiyevskaya *et al.* 2002b; Andrizhiyevskaya *et al.* 2004; Feng *et al.* 2011b). It is also demonstrated in Figure 3.1D, which highlights room temperature absorption spectra of PSI-IsiA complexes for WT and C260V mutant preparations.

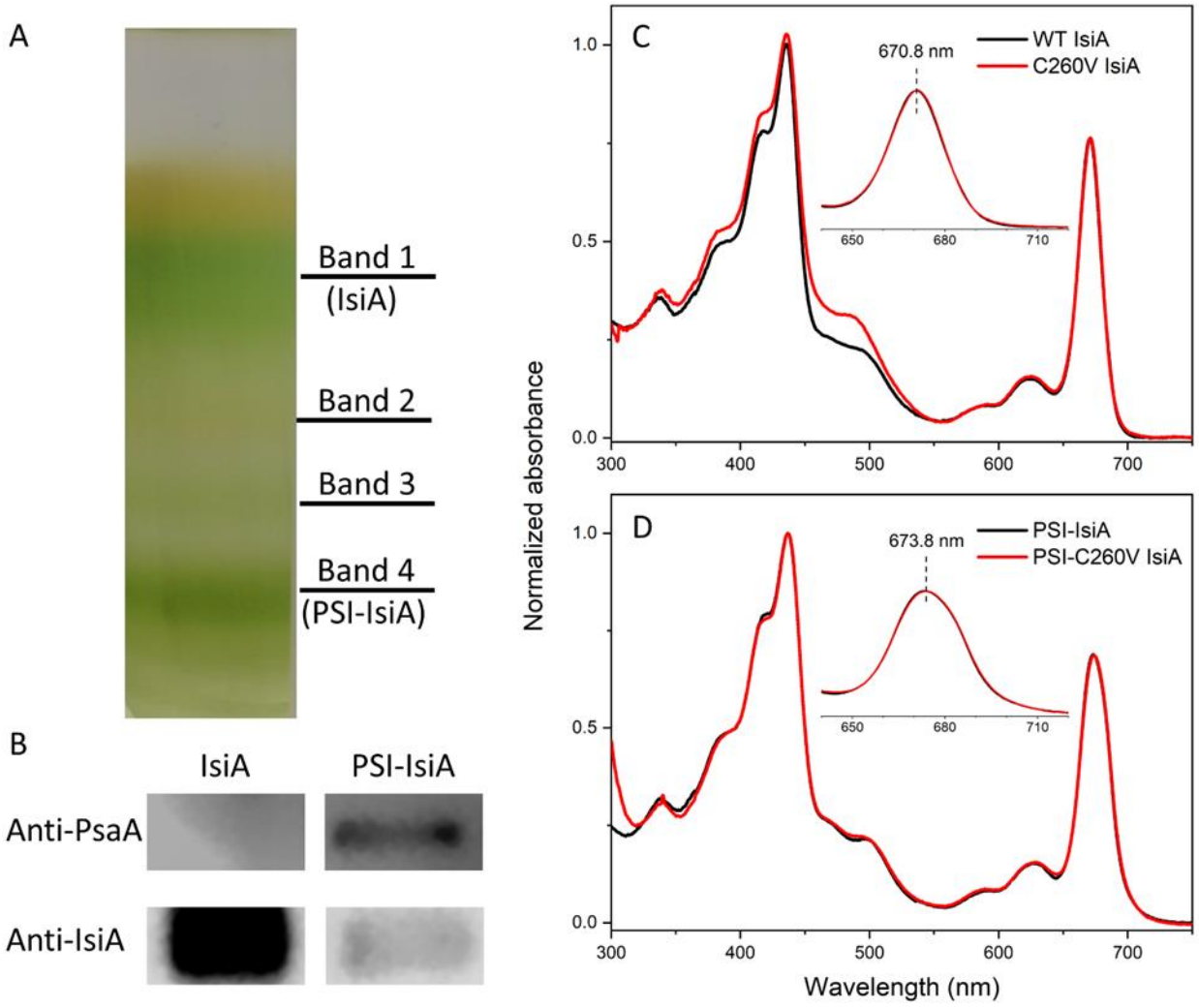

Figure. 3.1 Purification of mutant C260V IsiA and PSI-C260V IsiA from C260V-His tagged strain and basic spectroscopic characterization of protein complexes. (A) Protein bands obtained from sucrose gradient ultracentrifugation with IsiA and PSI-IsiA bands indicated, (B) Analysis of IsiA sample purity by immunoblotting probing by antisera against PsaA and IsiA, (C) room temperature absorption spectra of WT and C260V IsiA and (D) WT and C260V PSI-IsiA supercomplexes.

3.3.3 Fluorescence dynamics of Chl *a* in WT and C260V IsiA

Our previous studies of Chl *a* fluorescence decay in the WT IsiA demonstrated that fluorescence lifetime is sensitive to the presence of a reducing agent, sodium dithionite, in the sample buffer (Chen *et al.* 2017). We suggested that lifetime extension was associated with shutting down the cysteine-mediated excitation quenching mechanism similar to one proposed to explain redox dependent fluorescence decay of bacteriochlorophyll *a* in FMO photosynthetic antenna complex from green sulfur bacteria (Orf *et al.* 2016). In the C260V IsiA, the unique cysteine, which most likely is involved in the quenching mechanism, is replaced with a valine. Therefore, it is expected that even under oxidizing condition, C260V IsiA will reveal longer Chl *a* florescence decay as the quenching mechanism should be significantly obstructed or even completely absent. Comparison of fluorescence decay of Chl *a* in both WT and C260V IsiA (Figure 3.2) shows that the Chl *a* fluorescence lifetime of mutant IsiA is even longer than that of the reduced wild type IsiA, indicating the abolishment of excitation energy quenching done by replacing the cysteine with a valine.

The time-resolved fluorescence spectra of wild-type IsiA, wild type PSI-IsiA and mutant PSI-IsiA (Figure 3.3) clearly shows that energy transfer from the mutant IsiA to PSI is still fast and efficient. It suggests that with the C260V mutation, the mutant IsiA still possesses the capability of serving as an accessary antenna of PSI.

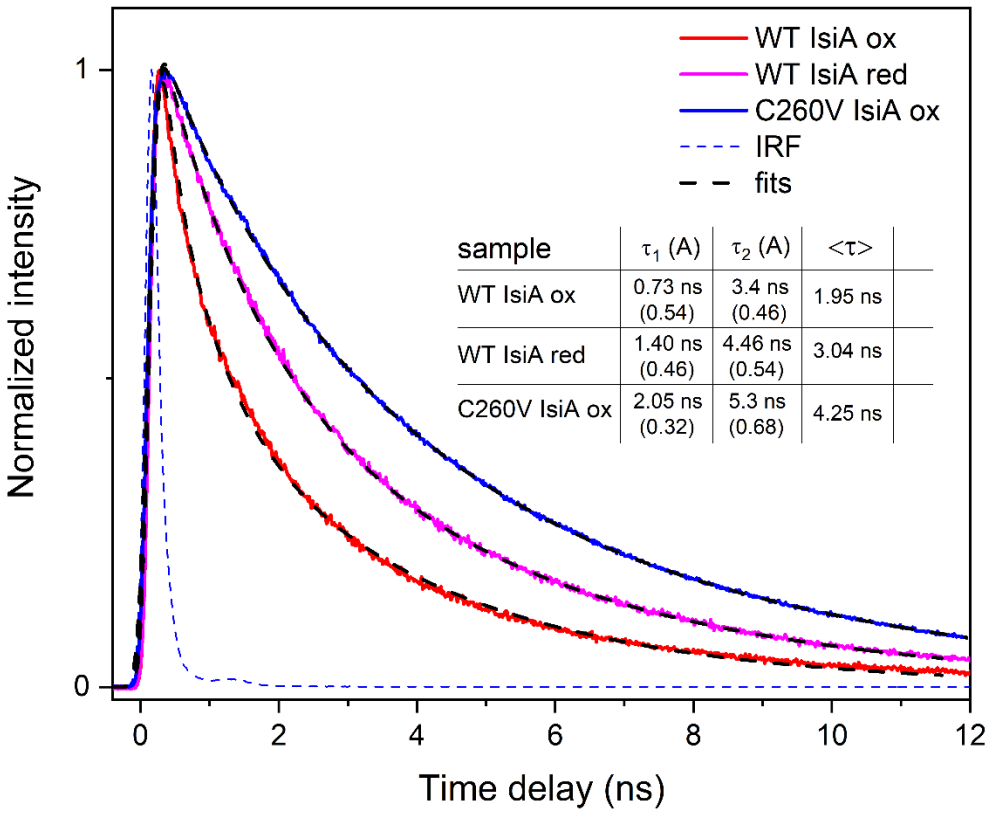

Figure 3.2 Exemplary fluorescence decay dynamics of IsiA-bound Chl *a* in WT and C260V IsiA, under oxidative (ox, buffer as is) and reducing (red, after addition of 10 mM sodium dithionite) conditions. Fluorescence decay was recorded at 684 nm at room temperature. IRF – instrument response function. The insert table shows fitting results with lifetimes and amplitudes of contributing kinetic components as well amplitude weighted lifetime <τ>. The signals were normalized for better comparability.

Both WT and C260V IsiA proteins, if assembled into supercomplexes with PSI, show substantial and equal shortening of Chl *a* fluorescence decay, demonstrating that antenna complexes are equally capable to transfer efficiently excitation energy to PSI. Figures 3.3A and B show two-dimensional pseudo-color fluorescence decay profiles recorded for both supercomplexes. Measurements of time-resolved fluorescence were performed at 77 K, at cryogenic temperature that allows the recording of fluorescence from PSI (720 nm band). Figures 3.3C and D show time-integrated fluorescence spectra that are integration of all time-resolved

spectra of time domain and, in principle, should be equal to expected steady-state fluorescence of a supercomplex. Fluorescence decay traces of Chl *a* associated with IsiA and with PSI, normalized to unity to maxima (Figure 3.3E), show that fluorescence decay of IsiA-bound Chl *a* is equal for both WT and C260V IsiA, therefore both IsiA equally well serve PSI as light harvesting antenna and excitation donors. Note that at 77 K standalone IsiA even in oxidizing conditions has Chl *a* fluorescence lifetime of ~4 ns (Chen *et al.* 2017).

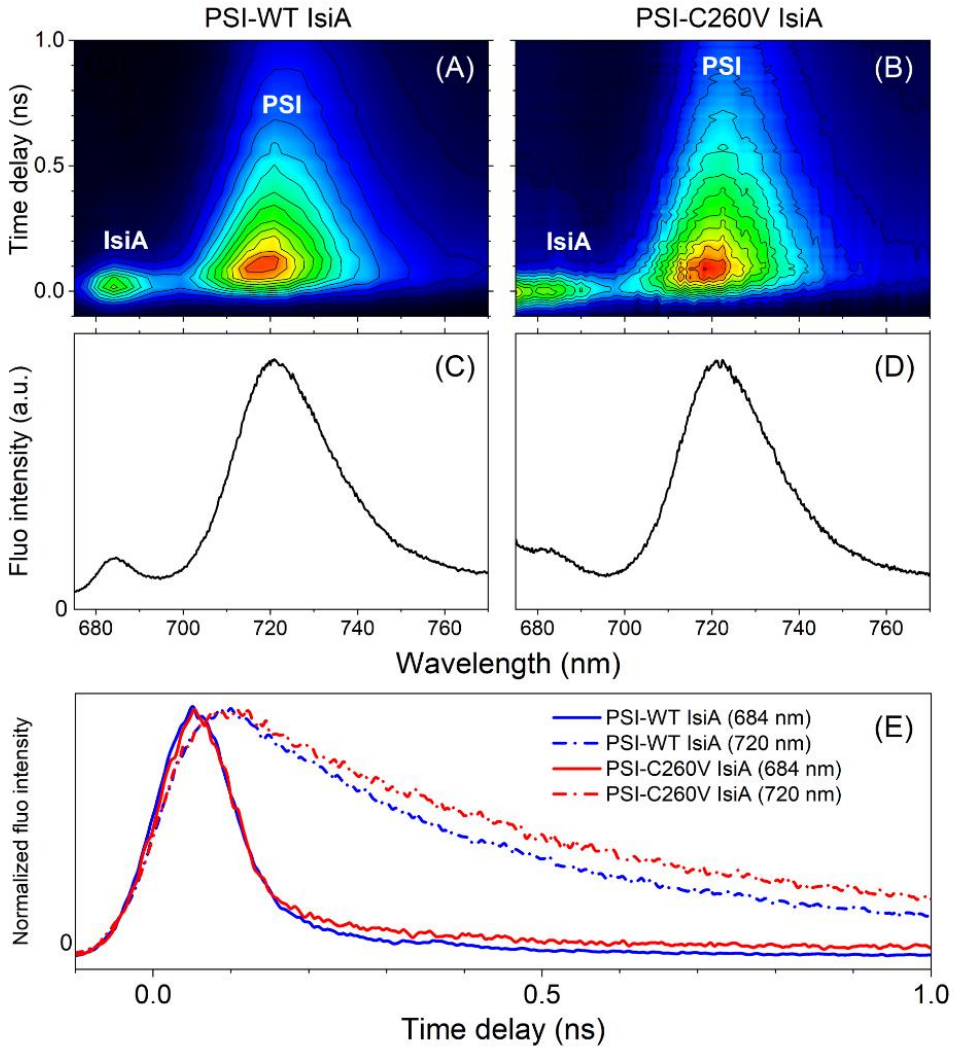

Figure 3.3 Time-resolved fluorescence of PSI-IsiA supercomplexes at 77 K. (A, B) Two dimensional, pseudo-color fluorescence decay profiles of PSI-WT and C260V IsiA supercomplexes, (C, D) Time-integrated spectra that should correspond to steady-state

fluorescence emission of both supercomplexes. (E) Comparison of IsiA-bound Chl *a* fluorescence decay in both samples. The kinetic traces are normalized to their maxima for better comparability. The samples were excited at 660 nm. Rapid decay of Chl *a* fluorescence from IsiA shows comparable and very fast energy transfer to PSI in both supercomplexes. Small differences visible in profiles (670-680 nm) and in residual long-lived signal at ~680 nm in mutant sample are associated with larger scattering of the excitation beam and possible residual contamination with free Chl *a*.

3.3.4 Change of the pigment composition and quantification of photosynthetic proteins in the C260V mutant and WT *Synechocystis* strain

According to the spectroscopic data, the C260V IsiA is incapable of quenching excitation energy. Because IsiA is important in providing photoprotection (Havaux *et al.* 2005), this significant change should profoundly affect the physiology of the cells. Therefore, study of pigment composition and photosynthetic protein content of the mutant cells grown in different conditions was performed.

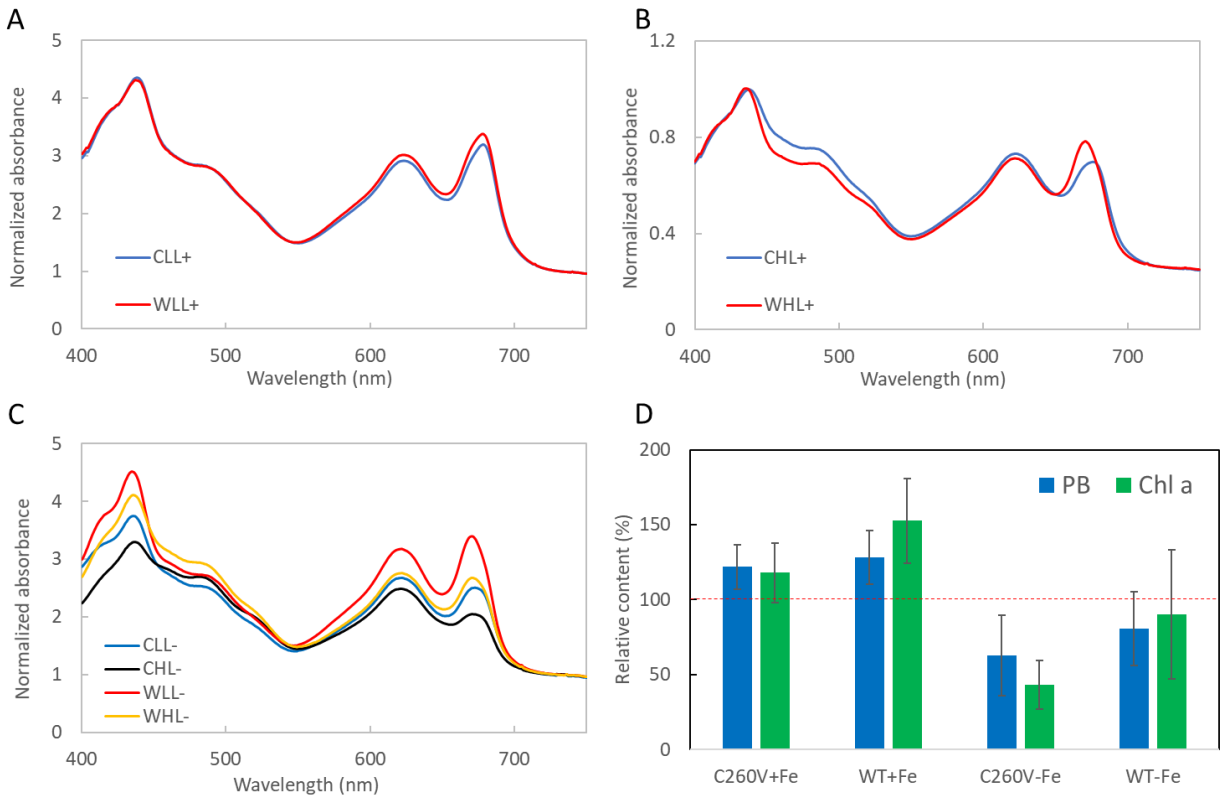

Figure 3.4 Absorption spectra of C260V (C) and wild type (W) *Synechocystis* 6803. Cultures were grown in multicultivators under (A) 200 µmol photons m^{-2} s^{-1} (low light) with sufficient iron (CLL+ and WLL+), (B) 800 µmol photons m^{-2} s^{-1} (high light) with sufficient iron (CHL+ and WHL+) and (C) under low light (LL) and high light (HL) with absence of iron. (D) The relative phycobilin and Chl *a* content per cell in C260V (C) and wild type (WT) under iron-replete and iron-depleted conditions. The whole absorption spectra were normalized to the absorption at 730 nm. The pigment content of both strains obtained under low light is shown as 100% (red dash line), and the relative content represents the phycobilin and Chl *a* content obtained from liquid culture grown under high light.

The absorption spectra of both C260V and wild type cultures grown under 200 µmol photons m^{-2} s^{-1} (low light) in BG11 (Figure 3.4A) had no noticeable difference. This was expected because there should be no *isiA* expression under this condition and, therefore, the mutation did not affect the physiology of cells under certain conditions. While cultures were grown under 800 µmol photons m^{-2} s^{-1} (high light) in BG11, the high light intensity induced *isiA* expression in both

cultures, as shown by the blue shift of Q_y absorption from 678 nm to 671 nm in the wild type and 678 nm to 676 nm in the mutant (Figure 3.4B). It is noteworthy that the different levels of blue shift were likely caused by different IsiA levels in cells, which will be discussed later. The absorption spectra show that both strains have the blue shift of Chl *a* Q_y absorption from 678 nm to 671 nm under low light and high light conditions. What interesting is that when both high light and iron stresses were applied on the C260V mutant, absorption at 671 nm is much lower, implying lower Chl *a* content on an equal OD_{730} basis. In addition, its absorbance at 671 nm, Q_y absorption band of Chl *a*, is markedly lower than its phycocyanin peak at 625 nm, suggesting a different pigment composition in the mutant strain. Because the mutant IsiA no longer quenches excitation energy, the mutant cells lose part of the capability for photoprotection, and the photosynthetic proteins, or the whole cell may be more light-sensitive.

Because the mutant appears to be more light-sensitive, the analyses were performed by comparing the data obtained from cells grown under high light with that from cells grown under low light. In iron-replete conditions, the C260V mutant had a ~20% increase in both phycobilin and Chl *a* content, while the wild type had a ~30% increase in phycobilin and ~50% increase in Chl *a* content under high light. On the other hand, in iron-depleted conditions, phycobilin and Chl *a* content in both strains pronouncedly decreased, especially the Chl *a* content in the C260V mutant, which decreased by ~55%. This suggests that the higher phycobilin to Chl *a* ratio in the C260V mutant in the iron-depleted condition under high light was due to the significantly decreased Chl *a* content caused by the high light intensity. The fact that the C260V mutant had lower Chl *a* content under high light led us to another question: what Chl *a*-binding protein did the mutant cells lose the most to cause so remarkable a decrease in Chl *a* content?

To understand how the photosynthetic proteins are affected by the lack of photoprotection provided by IsiA, we compared the photosynthetic protein content of cells grown under high light to that of cells grown under low light in iron-replete and iron-depleted conditions.

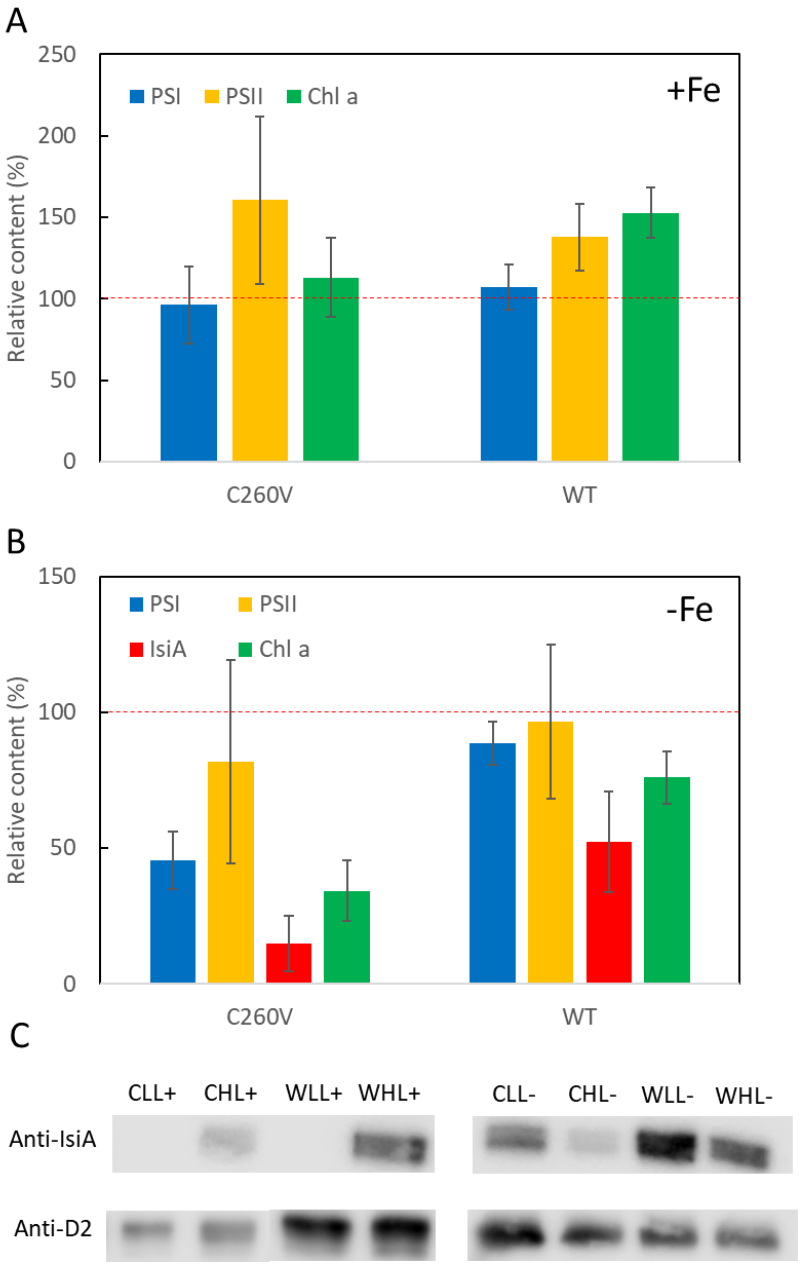

Figure 3.5 Relative photosynthetic proteins and Chl *a* content of C260V (C) and wild type (WT) *Synechocystis* 6803. PSI, SPII, IsiA and Chl *a* content in the C260V and wild type cells grown in (A) iron-replete and (B) iron-depleted conditions. The protein and Chl *a* content of both

strains obtained under low light is shown as 100% (red dash line), and the relative content represents the protein and Chl *a* content obtained from liquid culture grown under high light. (C) Immunoblotting analysis of solubilized thylakoid membranes extracted from C260V (C) and wild type (W) cells grown in iron-replete conditions under low light (CLL+ and WLL+), iron-replete conditions under high light (CHL+ and WHL+), iron-depletion under low light (CLL- and WLL-), and iron-depletion conditions under high light (CHL- and WHL-) probed by antisera specifically against IsiA and D2. Photoactive PSI content was determined based on the maximum absorbance at 705 nm of $P700^+$ in each sample. PSII and IsiA content was estimated from the chemiluminescence signals from the immunoblotting analysis. Chl *a* content was estimated by the methanol extraction method. The comparisons of protein and Chl *a* content was made on an equal cell basis.

Under iron-replete conditions, both the C260V mutant and the wild type had an increase in PSII and Chl *a* content (Figure 3.5A). Because both strains did not express *isiA* under iron-replete condition and low light, the relative IsiA content was not shown here, but both strains did produce IsiA under high light (Figure 3.5C). Interestingly, with about 50% higher PSII content, the increase of Chl *a* content in the C260V mutant due to high light was not as marked as that in the wild type. This was caused by the much higher IsiA content in the wild-type cells. Besides, under iron-depleted conditions, the PSI, IsiA and Chl *a* content of the C260V mutant significantly decreased (Figure 3.5B). On the other hand, the wild type showed a slight decrease in the PSI and PSII content and a more noticeable decrease in the IsiA content, causing the decrease in the total Chl *a* content (Figure 3.5B). These findings clearly show that the lack of quenching ability in the mutant IsiA results in the severe photodamage of PSI as well as IsiA itself under iron-depleted conditions and intense light.

3.3.5 Growth of C260V mutant and wild type *Synechocystis* strain under high light and iron stress

To elucidate how this single amino change in IsiA affects the growth of cells under various conditions, the C260V mutant and wild type *Synechocystis* 6803 strains were grown in multicultivators, and the growth of cultures was monitored (Figure 3.6A and B). Although the growth rates of both strains are not significantly different from each other, the difference in their growth patterns is clear. The lag phase was missing in the mutant and made the mutant grow faster at the early growth stage. Under iron-replete condition and strong light, the mutant strain grew faster and reached higher OD_{730} in three days compared to the wild type. This suggested that with sufficient iron, the lack of photoprotection provided by IsiA did not hinder but accelerated the growth of mutant cells. However, in iron-depleted conditions, no noticeable difference was observed in the growth curves of both strains under both high light and low light conditions (data not shown). This may be caused by a trace amount of iron remaining in the cells before inoculated into multicultivators. Therefore, to solve this issue, other growth experiments were conducted with the addition of an iron-chelator, DFB, to create the severe iron-deficient conditions. In this stricter iron-deficient condition, the mutant grown under high light started fast without a lag phase, and then bleached out after about 30 h. Under low light, the mutant still grew without the lag phase and then grew as well as the mutant without bleaching out. These results showed that the C260V mutant is more light-sensitive than the wild type in strict iron-limited conditions.

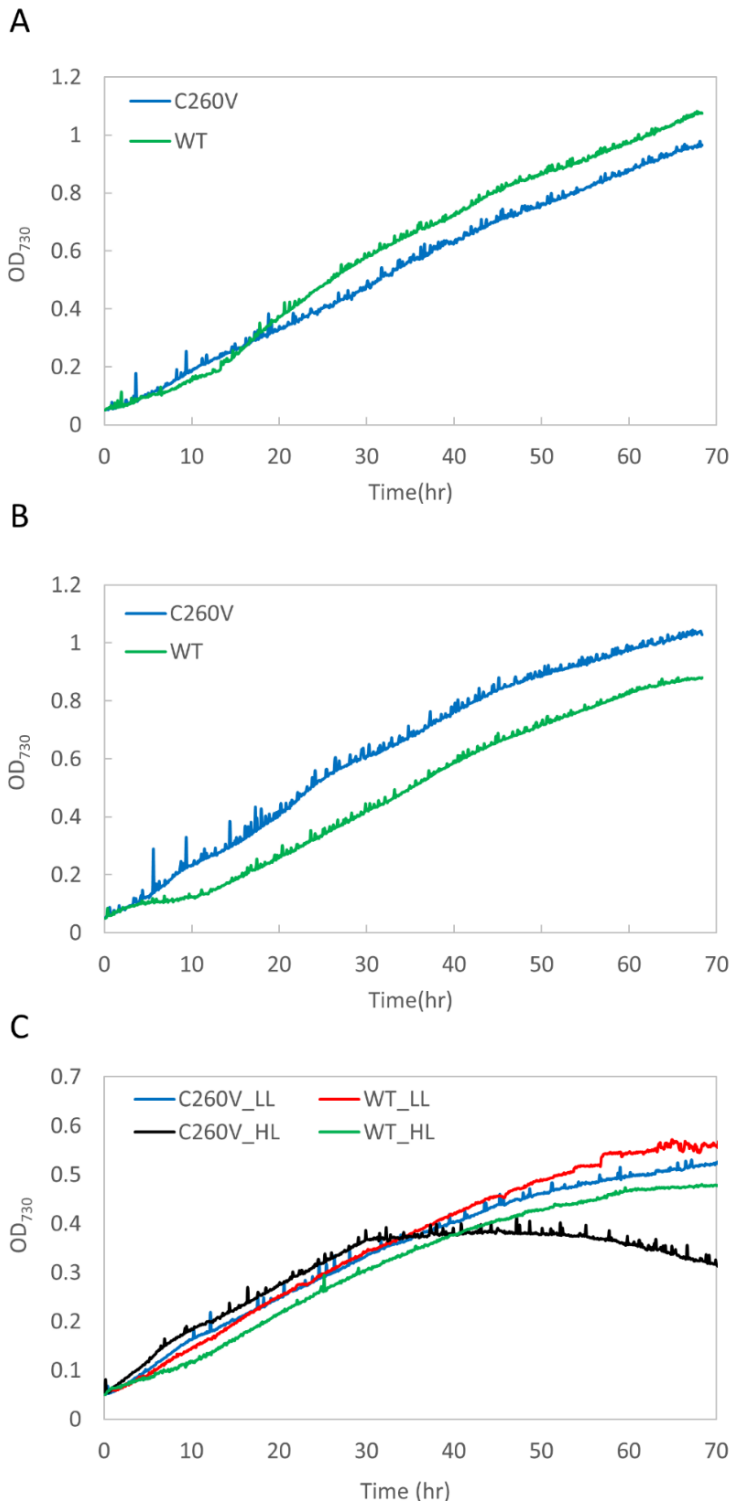

Figure 3.6 Comparison of growth pattern of C260V and wild type (WT) *Synechocystis* strains. Growth curves of C260V and wild type in iron-replete conditions under (A) 200 µmol photons m^{-2} s^{-1} (low light, LL), (B) 800 µmol photons m^{-2} s^{-1} (high light, HL), and (C) iron-depleted conditions (with the addition of iron chelator) under low light and high light.

3.4 Discussion

3.4.1 Energy transfer in the mutant C260V IsiA

It has been well established that IsiA not only serves as an light-harvesting antenna for PSI (Burnap *et al.* 1993; Andrizhiyevskaya *et al.* 2002a; Melkozernov *et al.* 2003; Ryan-Keogh *et al.* 2012), but also plays a significant role in providing photoprotection (Ihalainen *et al.* 2005; Havaux *et al.* 2005; Yeremenko *et al.* 2004; Park *et al.* 1999; Sandstrom *et al.* 2001; van der Weij-de Wit *et al.* 2007). Furthermore, some studies suggested that IsiA stores Chl *a* molecules in iron-depleted conditions, and once the cells obtain iron, IsiA releases the Chl *a* molecules which are used for the synthesis of photosynthetic proteins (Riethman and Sherman 1988; Guikema 1985; Sarcina and Mullineaux 2004). However, partially due to the unavailability of an IsiA crystal structure at high resolution, the interaction of IsiA with photosynthetic proteins, especially PSI, is not understood. Our previous study proposed that IsiA uses the cysteine-mediated mechanism to quench excitation energy (Chen *et al.* 2017; Orf *et al.* 2016). In this study, site-directed mutagenesis was performed to replace the unique cysteine in IsiA with a valine. The essentially identical absorption spectra of C260V and WT IsiA (and likewise WT PSI-IsiA and PSI-C260V IsiA) show that the C260V IsiA maintains the binding pockets for Chl *a* and binds Chl *a* molecules well, suggesting that the C260V IsiA is properly folded. In addition, the Chl *a* Q_y absorption bands of both WT and C260V IsiA have the maximum at 670.8 nm, and that of both WT and mutant PSI-IsiA have the maximum at 673.8 nm (Figure 3.1 C and D), in good agreement with previous studies (Bibby *et al.* 2001b; Boekema *et al.* 2001). These results suggest that we successfully obtained the well-folded free C260V IsiA and PSI-C260V IsiA.

Unlike FMO protein, where the cysteine-mediated quenching process was first demonstrated (Orf *et al.* 2016), IsiA has only one cysteine, which makes this cysteine in IsiA even more essential in the quenching process. It was reported that the Chl *a* fluorescence lifetime of IsiA becomes longer with the addition of reducing agents (Chen *et al.* 2017) owing to the conversion of the thiyl radical to the thiol group in IsiA under reducing environments that prevent the excitation energy quenching by the interaction between the thiyl radical and the excited Chl *a* molecule (Orf *et al.* 2016). In the mutant C260V IsiA, the cysteine is replaced with valine, and, therefore, no quenching was expected in the mutant IsiA even under oxidizing conditions. Our results show that the Chl *a* fluorescence lifetime of the C260V IsiA is even longer than that of the wild type IsiA under reducing conditions (Figure 3.2), demonstrating no quenching in the C260V mutant.

In the PSI-IsiA supercomplex, IsiA functions as an accessary antenna that absorbs light energy and transfers the energy to the reaction center of PSI. Our results are consistent with the previous studies, showing that the energy transfer from the IsiA ring to PSI is rapid and efficient (Melkozernov *et al.* 2003; Ryan-Keogh *et al.* 2012; Andrizhiyevskaya *et al.* 2002a). Moreover, excited at 660 nm, the mutant PSI-C260V IsiA and the wild type PSI-IsiA have identical fluorescence decay traces at 684 nm and 720 nm (Figure 3.3), indicating the same energy transfer process in both samples. These findings suggest that the mutant C260V IsiA is still capable of absorbing and transferring excitation energy to PSI and serves as an accessary antenna for PSI.

3.4.2 Physiological changes in the mutant C260V cells

Previous studies showed that IsiA is essential for the survival of *Synechocystis* sp. PCC 6803 and *Synechococcus* sp. PCC 7942 in iron-deficient conditions and under high light (Park *et al.* 1999; Burnap *et al.* 1993; Wang *et al.* 2010; Havaux *et al.* 2005). Although the functions of

IsiA have not been completely revealed, it has been suggested that the cells cannot survive without IsiA mainly due to the absence of photoprotection provided by IsiA (Park *et al.* 1999; Burnap *et al.* 1993; Wang *et al.* 2010; Havaux *et al.* 2005). Our spectroscopic data show that the mutant C260V IsiA no longer quenches excitation energy but still functions as a light-harvesting antenna for PSI. It is interesting that this mutant C260V IsiA affects the physiology of the mutant cells. Because we are interested in the effects of the abolishment of excitation energy quenching in the C260V IsiA on the mutant cells, the data analyses were focused on the comparisons between low and high light conditions.

Under iron-replete conditions

Under low light with sufficient iron, the absorption spectra of the C260V mutant and the wild type are almost identical (Figure 3.4A), and no IsiA was present in both cultures (Figure 3.4B). Under high light, even with sufficient iron, IsiA was induced by high light, which was confirmed by the blue shift of Chl *a* Q_y absorption from 678 nm to 671 nm in the wild type and 678 nm to 676 nm in the mutant C260V strain. The induction of IsiA was also confirmed the immunoblotting analysis shown in Figure 3.5C. As for the cellular pigment content, both phycobilin and Chl *a* content increases in both strains under high light. The changes of phycobilin content owing to high light in both strains are almost identical. In the contrast, the wild type had a much more significant increase in the Chl *a* content under high light, which suggests that the C260V mutation essentially affects the cellular Chl *a* content under different light conditions. The change of Chl *a* content should correspond to a change of the Chl *a*-binding protein. Our results show that the significant increase in the Chl *a* content in the wild type under high light should be attributed to the substantial expression of IsiA (Figure 3.5A and C). The C260V mutant only showed a slight increase in the Chl *a* content under the same condition, which is probably because

there is much lower IsiA content. Given that the C260V IsiA cannot quench the excitation energy, it is likely that the lower IsiA content in C260V mutant under high light is caused by photodamage. Besides, both strains had a higher PSII to PSI ratio under high light, as is consistent with previous studies (Kopečná *et al.* 2012; Murakami and Fujita 1991; Hihara *et al.* 1998). These findings show that with only one amino acid substitution in IsiA, the pigment and photosynthetic protein composition in mutant cells has achieved a new balance.

The growth rates of both strains under low light are nearly identical, but distinct growth patterns were observed. Instead of growing slowly right after inoculated into the multicultivators, the C260V mutant cells started fast without a lag phase. Under high light conditions, the C260V mutant grew even faster than the wild type (Figure 3.6B). The manipulation of photoprotection has been considered as one of the best approaches to improve photosynthesis (Murchie and Niyogi 2011). It was shown in plants and algae that by accelerating the recovery from photoprotection or removing some photoprotective mechanisms, the growth yield can be substantially improved (Hubbart *et al.* 2018; Kromdijk *et al.* 2016; Berteotti *et al.* 2016). However, it was reported that the *Synechocystis* 6803 mutant strain with the *isiA* gene being deleted cannot survive high light even with sufficient iron. In this study, the excitation energy quenching process in C260V IsiA was abolished, but the mutant IsiA may still provide photoprotection to cells at some level. In addition, the mutant C260V IsiA can serve as the light-harvesting antenna for PSI, which could potentially direct light energy to photochemical quenching and improve cells growth.

Under iron-depleted conditions

In iron-depleted conditions, both strains clearly show a blue shift of Chl *a* Q_y absorption, indicating the presence of IsiA under low and high light conditions (Figure 3.4C). It was reported

that cells grown in iron-depleted conditions have a significant decrease in Chl *a* content (Burnap *et al.* 1993; Sherman and Sherman 1983; Guikema and Sherman 1983) compared with the cells grown in iron-replete conditions, which is consistent with our results (data not shown). Here, we compared the absorption spectra of cells grown in iron-depleted conditions under low and high light conditions. Our results show a significant decrease in the Chl *a* Q_y absorption in the C260V mutant grown under high light (Figure 3.4C). The reduction in the Chl *a* Q_y absorption indicates the lower Chl *a* content in the C260V mutant cells, which was also reported in an *isiA* deletion strain grown under similar conditions (Burnap *et al.* 1993). It was proposed that one purpose IsiA serves is to maintain the cellular Chl *a* content in iron-deficient environments, and help the cells to recover once iron becomes available (Riethman and Sherman 1988; Guikema 1985; Sarcina and Mullineaux 2004; Schrader *et al.* 2011). Our results also show that, compared with the C260V mutant, wild type cells are able to maintain their cellular Chl *a* content, and only had a slight decrease in Chl *a* content under high light. Furthermore, the decrease in the photoactive PSI and IsiA content in the C260V mutant under high light was more significant compared with wild type. This suggests that the significant loss of Chl *a* in the mutant corresponds to the loss of PSI and IsiA. Because the C260V IsiA is unable to quench light energy, it is likely that the loss of PSI and IsiA under high light is due to severe photodamage. Nonetheless, with the lower IsiA and PSI content, the growth of the C260V mutant in YBG11-Fe under low and high light condition was not distinctly different from that of the wild type (data not shown). This may result from the remaining iron in cells even after washed three times with YBG11-Fe. To understand how this mutation affects the growth of the mutant C260V cells in strict iron-depleted conditions, DFB, an iron-chelator, was added into YBG11-Fe, and the growth of both strains was monitored in this medium. In this strict iron-depleted condition, under high light, the C260V mutant started fast, and

then bleached out after 30 h (Figure 3.6C). This suggests that the C260V mutant is more light-sensitive in iron-depleted conditions and that the fully functional IsiA is required for the cells to survive high light and iron-depleted environments.

3.4.3 Significance of IsiA in cyanobacteria

Although the *isiA* gene is well conserved among the cyanobacterial strains included in an earlier study (Chen *et al.* 2018), after decades of effort, the IsiA puzzle has still not been fully elucidated. Although it has been determined that IsiA serves as a light-harvesting antenna for PSI and provides photoprotection under stress conditions, the detailed mechanisms of those processes remain unclear. We proposed that IsiA uses the cysteine-mediated mechanism to quench excitation energy, a process that was first found in FMO protein in green-sulfur bacteria (Chen *et al.* 2017; Orf *et al.* 2016). In this study, the C260V mutation abolished the excitation energy quenching in IsiA, showing the critical role this unique cysteine plays in the quenching process. Our results also show that under strict iron-depleted conditions and high light, the mutant bleached out after 30 h, suggesting that the C260V mutant is more light-sensitive in iron-depleted conditions. This suggests that with the cysteine in IsiA, the wild type is more capable of surviving in such extreme environments. In addition, the amino acid sequence alignment of IsiA in representative strains shows that the cysteine residue is highly conserved in the 'AYFCAVN' motif (Figure 3.7), again, highlighting its importance in cyanobacteria. Interestingly, one of the two *Calothrix* strains included in this study has a serine residue instead of the conserved cysteine. The natural habitat of these two strains is reported to be different. Although *Calothrix* 6303 was isolated from a fresh water lake, *Calothrix* 7507 was sampled from an acidic peat bog, a niche unlikely to experience intense light stress. A different quenching mechanism might be at play in this strain. Our findings also show that the C260V IsiA is still capable of serving as a light-harvesting antenna for PSI.

Faster growth was observed in the C260V mutant in the presence of iron under high light. This suggests that the single amino acid change may not interfere with the other IsiA functions and in fact, light energy use may become more efficient in the mutant cells due to the removal of part of the energy quenching processes.

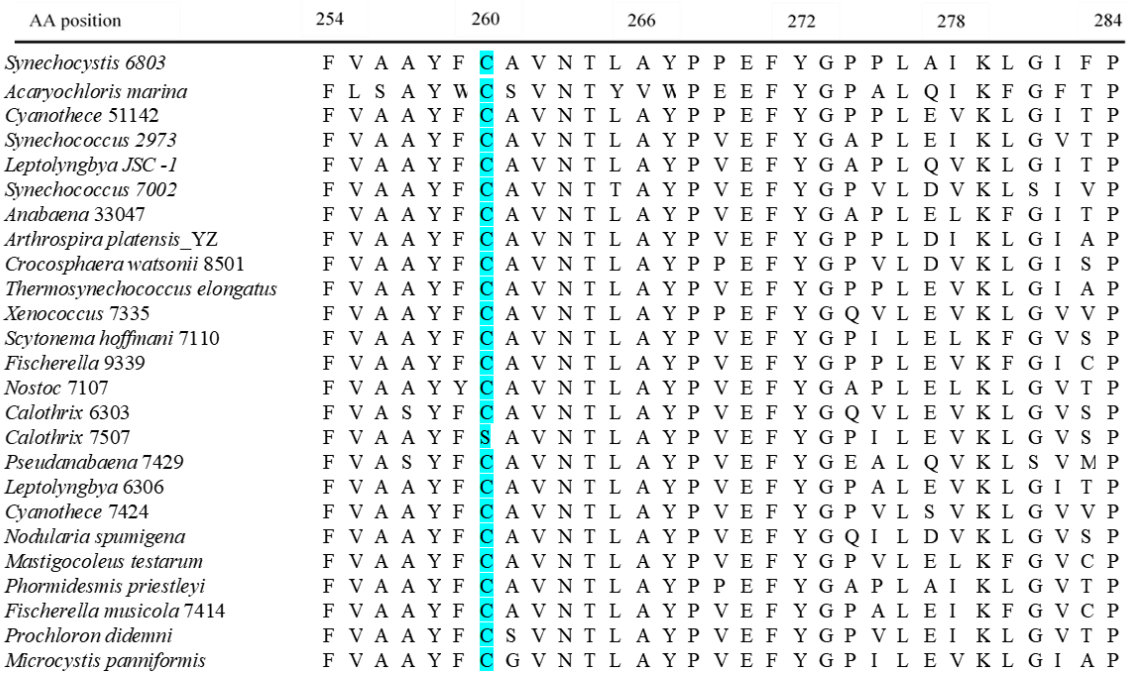

Figure 3.7 IsiA protein sequence alignment showing the conserved cysteine (C260) residue in 25 representative cyanobacterial strains.

3.5 Methods

Mutant construction

The plasmid of the C260V-His strain was constructed by replacing the kanamycin resistance gene in the plasmid of IsiA-His strain (Chen *et al.* 2017) with a gentamicin resistant gene and introducing the site mutation in one of the homologous arms. This plasmid was

constructed by Gibson assembly (Gibson *et al.* 2009), using the DNA fragments amplified by PCR. The resulting plasmid pSL2973 was verified by sequencing. The IsiA-His strain was transformed and the transformants were selected for growth on gentamicin. Segregation of the C260V-His strain was confirmed by PCR.

For the C260V strain, the mutation was introduced with the CRISPR/Cpf1 system reported previously (Ungerer and Pakrasi 2016). The editing plasmid was constructed by cloning the annealed oligos, the gRNA targeting the *isiA* sequence, into the AarI site on the pSL2680 vector. The repair template was constructed by Gibson assembly that cloned two 900 bps homology regions, including the mutation at the PAM sequence and the cysteine coding sequence, into the KpnI site on the editing vector. The resulting plasmid, pSL2854, was verified by sequencing. It was then transferred to *Synechocystis* 6803 wild type cells using the *E. coli* strain containing the pRL443 and pRL623 plasmid by the tri-parental conjugation method (Golden *et al.* 1987). The resulting colonies were repatched three times onto BG11 plates containing 10 μg/mL kanamycin. Mutations were verified by sequencing. The verified colonies were grown to stationary phase in BG11 without antibiotics and diluted 1000 times and grown to stationary phase again. This process was repeated several times to cure the editing plasmid. BG11 plates with and without kanamycin were used to screen the kanamycin-sensitive colonies, which had lost the editing plasmid. These kanamycin-sensitive patches are the markerless C260V mutants.

Culture growth conditions and thylakoid membrane preparation

Wild type and C260V *Synechocystis* sp. PCC 6803 cells were grown phototrophically in BG11 under continuous illumination with the intensity of 30 μmol photons m^{-2} s^{-1} at 30 °C. After 5 days, cells were harvested and washed three times with YBG11-Fe, a modified medium without

the addition of iron (Chen *et al.* 2017; Shcolnick *et al.* 2007). The washed cells were adjusted to the same optical density to 0.05 at 730 nm (OD_{730}= 0.05), inoculated in a multicultivator, and grown under 200 (low light) and 800 (high light) μmol photons m^{-2} s^{-1}. For iron-starved liquid cultures, BG11 was replaced with YBG11-Fe with or without the addition of deferoxamine (DFB) to the final concentration of 50 mM depending on the experimental settings. The OD_{730} was continuously recorded every 10 minutes over the course of the growth experiments. After three days grown in the multicultivator, the cells of each liquid culture were harvested and counted. One milliliter of the each culture was used to obtain the absorption spectra, and the rest of the cultures were divided based on the same cell number and resuspended in RB (50 mM morpholineethanesulfonic acid [MES]–NaOH [pH 6.0], 10 mM $MgCl_2$, 5 mM $CaCl_2$, 25% glycerol) and then stored at −80 °C for future use.

The cells were thawed on ice prior to the thylakoid membrane extraction. Cells were broken by bead-beating as described previously (Kashino *et al.* 2002; Bricker *et al.* 1998) with following modifications. The thawed cells and 0.17 mm glass beads were loaded into a prechilled Eppendorf tube with a 1:1 ratio of cell suspension to glass beads. Cells were then broken using 10 break cycles, each cycle consisting of 1 min of homogenization on a Vortex mixer, followed by 1 min of cooling. Cell homogenates were centrifuged in a SS34 rotor at 30 000 × g for 15 min and washed with RB once. The resulting pellet was then resuspended in RB and solubilized with β-D-dodecyl maltoside (DDM) to a final concentration of 1% DDM, and incubated on ice in dark with gentle stirring for 30 min. The sample was then centrifuged in a SS34 rotor at 30,000 × g for 30 min and the resulting supernatant, the solubilized thylakoid membranes, was stored at −80 °C for future use.

Cell counting

Cell cultures were grown in MC-1000 multicultivators in BG11 and YBG11-Fe under 200 and 800 μmol photons m^{-2} s^{-1} as mentioned above. The cells were harvested after three days, and diluted to OD_{730} = 0.01. Twenty milliliters of the diluted sample were taken, and its cell number was counted with an automated cell counter (Cellometer Vision; Nexcelom). The cell number was automatically counted by the Cellometer with manually curation which improve the accuracy of counts. Since the relationship between OD730 and cell number is different in different strains under different conditions all liquid cultures were counted as mentioned above to achieve the higher accuracy.

Photoactive PSI content

Cell cultures were grown in MC-1000 multicultivators in BG11 and YBG11-Fe under 200 and 800 μmol photons m^{-2} s^{-1} as mentioned above. Cells were harvested after three days, and adjusted to same cell numbers. With the addition of 10 μM 3-(3,4-dichlorophenyl)-1,1-dimethylurea (DCMU) and 20 μM dibromothymoquinone (DBMIB), which block linear and cyclic electron flow, the absorbance at 705 nm of $P700^+$ in each sample was recorded for 5 s under saturating light on a JTS-10 pump probe spectrophotometer. The $P700^+$ molar extinction coefficient of 70 mM^{-1} cm^{-1} was used to estimate the photoactive PSI content from the maximum absorbance.

SDS-PAGE and immunoblot analysis

Solubilized thylakoid membranes of C260V and wild type *Synechocystis* sp. PCC 6803 were prepared as mentioned above. The solubilized thylakoid membranes were fractionated by denaturing sodium dodecyl sulfate polyacrylamide gel electrophoresis (SDS-PAGE) and analyzed by protein immunoblot as described in previous studies (Laemmli 1970; Zak *et al.* 2001).

Fractionated proteins were blotted onto polyvinylidene difluoride (PVDF) membranes. IsiA and D2 were identified by the specific antisera and visualized by using enhanced chemiluminescence reagents (WestPico; Pierce) on an Odyssey Fc imager (LI-COR Biosciences, USA). The relative protein content was estimated by Image Studio (LI-COR Biosciences, USA) based on the chemiluminescence signals of samples.

Pigment content estimation

Cell cultures were grown in MC-1000 multicultivators in BG11 and YBG11-Fe under 200 and 800 μmol photons m^{-2} s^{-1} at 30 °C as mentioned above. One milliliter cell culture was taken and its Chl *a* content was estimated by the methanol extraction method (Porra *et al.* 1989).

The absorption spectra of cultures were obtained using a DW2000 spectrophotometer (OLIS, USA). Phycobilin content in the cultures were estimated using the equation as follows (Arnon *et al.* 1974; Collier and Grossman 1992; Murton *et al.* 2017):

$$\text{Phycobilin content}\left({}^{mg}/_{ml}\right) = 0.139 \times (A_{620} - A_{730}) - 0.0355 \times (A_{678} - A_{730}) \qquad (3.1)$$

Protein complex purification

C260V-His liquid culture was grown in YBG11-Fe with the addition of 5 mM deferoxamine under illumination with the intensity of 30 μmol photons m^{-2} s^{-1} at 30 °C for two weeks to induce *isiA* expression as described in our previous study (Chen *et al.* 2017). The solubilized thylakoid membranes were prepared as shown above, and then used to purify PSI-IsiA and IsiA protein complexes. The C260V mutant IsiA and PSI-IsiA supercomplexes were purified by using nickel affinity chromatography and rate-zonal centrifugation (Chen *et al.* 2017). After 18 h of ultracentrifugation, protein fractions were collected. The first green and fourth green bands

from the top of the gradient was determined by Western blot and spectroscopy that contains IsiA and PSI-IsiA supercomplexes, respectively.

Steady-state and time-resolved spectroscopy

Steady-state absorption spectra were recorded using UV-1800 spectrophotometer from Shimadzu. Time-resolved fluorescence (TRF) experiments were carried out using two different setups. For recording of image of fluorescence profiles of PSI-IsiA supercomplexes at 77 K a setup based on Hamamatsu (Japan) universal streak camera described in detail previously (Niedzwiedzki *et al.* 2013) was used. Single wavelength traces of IsiA samples fluorescence decay at room temperature were recorded using a standalone Simple-Tau 130 time-correlated single photon counting (TCSPC) system from Becker&Hickl (Germany). Both setups were coupled to an ultrafast laser system (Spectra-Physics, USA) described in detail previously (Dilbeck *et al.* 2016). The frequency of the excitation pulses was set to 8 MHz, corresponding to ~120 ns between subsequent pulses. To minimize the detection of scattered light from the excitation beam a long-pass 665 nm filter was placed at the entrance slit of the spectrograph/monochromator. The integrity of the samples was examined by monitoring the real-time photon count rate over the time course of the experiment. It was constant, which indicated the absence of sample photodegradation. The samples were resuspended to an absorbance of $\leq$0.1 at the Chl *a* Q_y band and the emission signal was recorded at a right angle with respect to the excitation beam. The excitation beam set to 640 nm, with photon intensity of ~10^{10} photons/cm^2 per pulse was depolarized and focused on the sample in a circular spot of ~1 mm diameter.

Amino acid alignment

Twenty-five cyanobacterial strains, representative of unicellular, filamentous, diazotrophic and non-diazotrphic cyanobacteria, were chosen based on their sequence similarity (blastp) with the IsiA protein of *Synechocystis* 6803. The sequences were obtained from the JGI/IMG microbial database and aligned with ClustalW within MEGA 7 (Kumar *et al.* 2016). The cysteine residue (highlighted) in the AYFCAVN motif is conserved across the examined cyanobacterial strains harboring the IsiA protein.

3.6 Reference

Andrizhiyevskaya EG, Frolov D, van Grondelle R, Dekker JP (2004) Energy transfer and trapping in the Photosystem I complex of *Synechococcus* PCC 7942 and in its supercomplex with IsiA. *BBA-Bioenergetics* 1656 (2-3):104-113. doi:10.1016/j.bbabio.2004.02.002

Andrizhiyevskaya EG, Schwabe TM, Germano M, D'Haene S, Kruip J, van Grondelle R, Dekker JP (2002a) Spectroscopic properties of PSI-IsiA supercomplexes from the cyanobacterium *Synechococcus* PCC 7942. *Biochimica et biophysica acta* 1556 (2-3):265-272

Andrizhiyevskaya EG, Schwabe TM, Germano M, D'Haene S, Kruip J, van Grondelle R, Dekker JP (2002b) Spectroscopic properties of PSI-IsiA supercomplexes from the cyanobacterium *Synechococcus* PCC 7942. *Biochim Biophys Acta* 1556 (2-3):265-272

Arnon DI, McSwain BD, Tsujimoto HY, Wada K (1974) Photochemical activity and components of membrane preparations from blue-green algae. I. Coexistence of two photosystems in relation to chlorophyll *a* and removal of phycocyanin. *Biochimica et biophysica acta* (BBA)-Bioenergetics 357 (2):231-245

Berera R, van Stokkum IH, d'Haene S, Kennis JT, van Grondelle R, Dekker JP (2009) A mechanism of energy dissipation in cyanobacteria. *Biophysical journal* 96 (6):2261-2267. doi:10.1016/j.bpj.2008.12.3905

Berera R, van Stokkum IH, Kennis JT, van Grondelle R, Dekker JP (2010) The light-harvesting function of carotenoids in the cyanobacterial stress-inducible IsiA complex. *Chemical Physics* 373 (1):65-70

Berteotti S, Ballottari M, Bassi R (2016) Increased biomass productivity in green algae by tuning non-photochemical quenching. *Scientific reports* 6:21339

Bibby TS, Nield J, Barber J (2001a) Iron deficiency induces the formation of an antenna ring around trimeric photosystem I in cyanobacteria. *Nature* 412 (6848):743-745. doi:10.1038/35089098

Bibby TS, Nield J, Barber J (2001b) Three-dimensional model and characterization of the iron stress-induced CP43'-photosystem I supercomplex isolated from the cyanobacterium *Synechocystis* PCC 6803. *The Journal of biological chemistry* 276 (46):43246-43252. doi:10.1074/jbc.M106541200

Bibby TS, Zhang Y, Chen M (2009) Biogeography of photosynthetic light-harvesting genes in marine phytoplankton. *PloS one* 4 (2):e4601. doi:10.1371/journal.pone.0004601

Boekema EJ, Hifney A, Yakushevska AE, Piotrowski M, Keegstra W, Berry S, Michel KP, Pistorius EK, Kruip J (2001) A giant chlorophyll-protein complex induced by iron deficiency in cyanobacteria. *Nature* 412 (6848):745-748. doi:10.1038/35089104

Bricker TM, Morvant J, Masri N, Sutton HM, Frankel LK (1998) Isolation of a highly active photosystem II preparation from *Synechocystis* 6803 using a histidine-tagged mutant of CP 47. *Biochimica et biophysica acta (BBA)-Bioenergetics* 1409 (1):50-57

Burnap RL, Troyan T, Sherman LA (1993) The highly abundant chlorophyll-protein complex of iron-deficient *Synechococcus* sp PCC 7942 (CP43) is encoded by the *isiA* gene. *Plant Physiol* 103 (3):893-902. doi:Doi 10.1104/Pp.103.3.893

Chen H-Y, Bandyopadhyay A, Pakrasi H (2018) Function, regulation and distribution of IsiA, a membrane-bound chlorophyll *a*-antenna protein in cyanobacteria. *Photosynthetica* 56 (1):322-333

Chen HS, Liberton M, Pakrasi HB, Niedzwiedzki DM (2017) Reevaluating the mechanism of excitation energy regulation in iron-starved cyanobacteria. *Biochimica et biophysica acta* 1858 (3):249-258. doi:10.1016/j.bbabio.2017.01.001

Collier JL, Grossman A (1992) Chlorosis induced by nutrient deprivation in *Synechococcus* sp. strain PCC 7942: not all bleaching is the same. *J. Bacteriol.*174 (14):4718-4726

Dilbeck PL, Tang Q, Mothersole DJ, Martin EC, Hunter CN, Bocian DF, Holten D, Niedzwiedzki DM (2016) Quenching capabilities of long-chain carotenoids in light harvesting-2 complexes from *Rhodobacter sphaeroides* with an engineered carotenoid synthesis pathway. *J. Phys. Chem. B.* 120 (24):5429–5443. doi:10.1021/acs.jpcb.6b03305

Feng X, Neupane B, Acharya K, Zazubovich V, Picorel R, Seibert M, Jankowiak R (2011a) Spectroscopic study of the CP43' complex and the PSI-CP43' supercomplex of the cyanobacterium *Synechocystis* PCC 6803. *The journal of physical chemistry B* 115 (45):13339-13349. doi:10.1021/jp206054b

Feng X, Neupane B, Acharya K, Zazubovich V, Picorel R, Seibert M, Jankowiak R (2011b) Spectroscopic study of the CP43’ complex and the PSI – CP43’ supercomplex of the cyanobacterium *Synechocystis* PCC 6803. *J. Phys. Chem. B.* 115 (45):13339-13349

Gibson DG, Young L, Chuang R-Y, Venter JC, Hutchison III CA, Smith HO (2009) Enzymatic assembly of DNA molecules up to several hundred kilobases. *Nature methods* 6 (5):343

Golden SS, Brusslan J, Haselkorn R (1987) [12] Genetic engineering of the cyanobacterial chromosome. In: *Methods in enzymology*, vol 153. Elsevier, pp 215-231

Guikema JA (1985) Fluorescence induction characteristics of *Anacystis nidulans* during recovery from iron-deficiency. *J. Plant. Nutr.* 8 (10):891-908. doi:Doi 10.1080/01904168509363393

Guikema JA, Sherman LA (1983) Chlorophyll protein organization of membranes from the cyanobacterium *Anacystis nidulans*. *Arch. Biochem. Biophys.* 220 (1):155-166. doi:Doi 10.1016/0003-9861(83)90396-X

Havaux M, Guedeney G, Hagemann M, Yeremenko N, Matthijs HC, Jeanjean R (2005) The chlorophyll-binding protein IsiA is inducible by high light and protects the cyanobacterium *Synechocystis* PCC6803 from photooxidative stress. *FEBS letters* 579 (11):2289-2293. doi:10.1016/j.febslet.2005.03.021

Hihara Y, Sonoike K, Ikeuchi M (1998) A novel gene, *pmgA*, specifically regulates photosystem stoichiometry in the cyanobacterium *Synechocystis* species PCC 6803 in response to high light. *Plant Physiol* 117 (4):1205-1216

Hubbart S, Smillie IR, Heatley M, Swarup R, Foo CC, Zhao L, Murchie EH (2018) Enhanced thylakoid photoprotection can increase yield and canopy radiation use efficiency in rice. *Communications biology* 1 (1):22

Ihalainen JA, D'Haene S, Yeremenko N, van Roon H, Arteni AA, Boekema EJ, van Grondelle R, Matthijs HC, Dekker JP (2005) Aggregates of the chlorophyll-binding protein IsiA (CP43') dissipate energy in cyanobacteria. *Biochemistry* 44 (32):10846-10853. doi:10.1021/bi0510680

Jordan P, Fromme P, Witt HT, Klukas O, Saenger W, Krauss N (2001) Three-dimensional structure of cyanobacterial photosystem I at 2.5 Å resolution. *Nature* 411 (6840):909-917. doi:10.1038/35082000

Kashino Y, Lauber WM, Carroll JA, Wang Q, Whitmarsh J, Satoh K, Pakrasi HB (2002) Proteomic analysis of a highly active photosystem II preparation from the cyanobacterium *Synechocystis* sp. PCC 6803 reveals the presence of novel polypeptides. *Biochemistry* 41 (25):8004-8012. doi:10.1021/bi026012+

Kopečná J, Komenda J, Bučinská L, Sobotka R (2012) Long-term acclimation of the cyanobacterium *Synechocystis* sp. PCC 6803 to high light is accompanied by an enhanced production of chlorophyll that is preferentially channeled to trimeric photosystem I. *Plant Physiol* 160 (4):2239-2250

Kromdijk J, Głowacka K, Leonelli L, Gabilly ST, Iwai M, Niyogi KK, Long SP (2016) Improving photosynthesis and crop productivity by accelerating recovery from photoprotection. *Science* 354 (6314):857-861

Kumar S, Stecher G, Tamura K (2016) MEGA7: Molecular evolutionary genetics analysis version 7.0 for bigger datasets. *Molecular biology and evolution* 33 (7):1870-1874. doi:10.1093/molbev/msw054

La Roche J, van der Staay GW, Partensky F, Ducret A, Aebersold R, Li R, Golden SS, Hiller RG, Wrench PM, Larkum AW, Green BR (1996) Independent evolution of the prochlorophyte and

green plant chlorophyll *a/b* light-harvesting proteins. *Proceedings of the National Academy of Sciences of the United States of America* 93 (26):15244-15248

Laemmli UK (1970) Cleavage of structural proteins during the assembly of the head of bacteriophage T4. *Nature* 227 (5259):680

Laudenbach D, Reith M, Straus N (1988) Isolation, sequence analysis, and transcriptional studies of the flavodoxin gene from *Anacystis nidulans* R2. *J. Bacteriol.*170 (1):258-265

Laudenbach DE, Straus NA (1988) Characterization of a cyanobacterial iron stress-induced gene similar to *psbC*. *Journal of bacteriology* 170 (11):5018-5026

Li H, Singh AK, McIntyre LM, Sherman LA (2004) Differential gene expression in response to hydrogen peroxide and the putative PerR regulon of *Synechocystis* sp. strain PCC 6803. *Journal of bacteriology* 186 (11):3331-3345. doi:10.1128/JB.186.11.3331-3345.2004

Martin JH, Fitzwater SE (1988) Iron-deficiency limits phytoplankton growth in the northeast Pacific subarctic. *Nature* 331 (6154):341-343. doi:Doi 10.1038/331341a0

Melkozernov AN, Bibby TS, Lin S, Barber J, Blankenship RE (2003) Time-resolved absorption and emission show that the CP43' antenna ring of iron-stressed *Synechocystis* sp. PCC6803 is efficiently coupled to the photosystem I reaction center core. *Biochemistry* 42 (13):3893-3903. doi:10.1021/bi026987u

Moore C, Mills M, Arrigo K, Berman-Frank I, Bopp L, Boyd P, Galbraith E, Geider R, Guieu C, Jaccard S (2013) Processes and patterns of oceanic nutrient limitation. *Nature geoscience* 6 (9):701

Murakami A, Fujita Y (1991) Regulation of photosystem stoichiometry in the photosynthetic system of the cyanophyte *Synechocystis* PCC 6714 in response to light-intensity. *Plant and cell physiology* 32 (2):223-230

Murchie EH, Niyogi KK (2011) Manipulation of photoprotection to improve plant photosynthesis. *Plant Physiol* 155 (1):86-92

Murton J, Nagarajan A, Nguyen AY, Liberton M, Hancock HA, Pakrasi HB, Timlin JA (2017) Population-level coordination of pigment response in individual cyanobacterial cells under altered nitrogen levels. *Photosynthesis research* 134 (2):165-174

Niedzwiedzki DM, Jiang J, Lo CS, Blankenship RE (2013) Low-temperature spectroscopic properties of the peridinin−chlorophyll *a*−protein (PCP) complex from the coral symbiotic dinoflagellate *Symbiodinium*. *J. Phys. Chem. B.* 117:11091–11099

North R, Guildford S, Smith R, Havens S, Twiss M (2007) Evidence for phosphorus, nitrogen, and iron colimitation of phytoplankton communities in Lake Erie. *Limnology and Oceanography* 52 (1):315-328

Orf GS, Saer RG, Niedzwiedzki DM, Zhang H, McIntosh CL, Schultz JW, Mirica LM, Blankenship RE (2016) Evidence for a cysteine-mediated mechanism of excitation energy regulation in a photosynthetic antenna complex. *Proceedings of the National Academy of Sciences of the United States of America* 113 (31):E4486-4493. doi:10.1073/pnas.1603330113

Pakrasi HB, Riethman HC, Sherman LA (1985) Organization of pigment proteins in the photosystem II complex of the cyanobacterium *Anacystis nidulans* R2. *Proceedings of the National Academy of Sciences* 82 (20):6903-6907

Park YI, Sandstrom S, Gustafsson P, Oquist G (1999) Expression of the *isiA* gene is essential for the survival of the cyanobacterium *Synechococcus* sp. PCC 7942 by protecting photosystem II from excess light under iron limitation. *Molecular Microbiology* 32 (1):123-129

Porra R, Thompson W, Kriedemann P (1989) Determination of accurate extinction coefficients and simultaneous equations for assaying chlorophylls a and b extracted with four different solvents: verification of the concentration of chlorophyll standards by atomic absorption spectroscopy. *Biochimica et biophysica acta* (BBA)-Bioenergetics 975 (3):384-394

Riethman HC, Sherman LA (1988) Immunological characterization of iron-regulated membrane proteins in the cyanobacterium *Anacystis nidulans* R2. *Plant physiology* 88 (2):497-505

Ryan-Keogh TJ, Macey AI, Cockshutt AM, Moore CM, Bibby TS (2012) The cyanobacterial chlorophyll-binding-protein IsiA acts to increase the *in vivo* effective absorption cross-section of PSI under iron limitation(1). *Journal of phycology* 48 (1):145-154. doi:10.1111/j.1529-8817.2011.01092.x

Sandstrom S, Park YI, Oquist G, Gustafsson P (2001) CP43 ', the *isiA* gene product, functions as an excitation energy dissipator in the cyanobacterium *Synechococcus* sp PCC 7942. *Photochem. Photobiol.* 74 (3):431-437. doi:Doi 10.1562/0031-8655(2001)074<0431:Ctigpf>2.0.Co;2

Sarcina M, Mullineaux CW (2004) Mobility of the IsiA chlorophyll-binding protein in cyanobacterial thylakoid membranes. *The Journal of biological chemistry* 279 (35):36514-36518. doi:10.1074/jbc.M405881200

Schrader PS, Milligan AJ, Behrenfeld MJ (2011) Surplus photosynthetic antennae complexes underlie diagnostics of iron limitation in a cyanobacterium. *PloS one* 6 (4). doi:ARTN e1875310.1371/journal.pone.0018753

Shcolnick S, Shaked Y, Keren N (2007) A role for *mrgA*, a DPS family protein, in the internal transport of Fe in the cyanobacterium *Synechocystis* sp. PCC6803. *Biochimica et biophysica acta* 1767 (6):814-819. doi:10.1016/j.bbabio.2006.11.015

Sherman DM, Sherman LA (1983) Effect of iron-deficiency and iron restoration on ultrastructure of *Anacystis nidulans*. *J. Bacteriol.*156 (1):393-401

Ungerer J, Pakrasi HB (2016) Cpf1 is a versatile tool for CRISPR genome editing across diverse species of cyanobacteria. *Scientific reports* 6:39681

van der Weij-de Wit CD, Ihalainen JA, van de Vijver E, D'Haene S, Matthijs HC, van Grondelle R, Dekker JP (2007) Fluorescence quenching of IsiA in early stage of iron deficiency and at cryogenic temperatures. *Biochimica et biophysica acta* 1767 (12):1393-1400. doi:10.1016/j.bbabio.2007.10.001

Vinnemeier J, Kunert A, Hagemann M (1998) Transcriptional analysis of the *isiAB* operon in salt-stressed cells of the cyanobacterium *Synechocystis* sp. PCC 6803. *FEMS Microbiology letters* 169 (2):323-330

Vrede T, Tranvik LJ (2006) Iron constraints on planktonic primary production in oligotrophic lakes. *Ecosystems* 9 (7):1094-1105

Wang Q, Hall CL, Al-Adami MZ, He Q (2010) IsiA is required for the formation of photosystem I supercomplexes and for efficient state transition in *Synechocystis* PCC 6803. *PloS one* 5 (5):e10432. doi:10.1371/journal.pone.0010432

Yeremenko N, Kouril R, Ihalainen JA, D'Haene S, van Oosterwijk N, Andrizhiyevskaya EG, Keegstra W, Dekker HL, Hagemann M, Boekema EJ, Matthijs HC, Dekker JP (2004) Supramolecular organization and dual function of the IsiA chlorophyll-binding protein in cyanobacteria. *Biochemistry* 43 (32):10308-10313. doi:10.1021/bi048772l

Yousef N, Pistorius EK, Michel KP (2003) Comparative analysis of *idiA* and *isiA* transcription under iron starvation and oxidative stress in *Synechococcus* elongatus PCC 7942 wild-type and selected mutants. *Archives of Microbiology* 180 (6):471-483. doi:10.1007/s00203-003-0618-4

Zak E, Norling B, Maitra R, Huang F, Andersson B, Pakrasi HB (2001) The initial steps of biogenesis of cyanobacterial photosystems occur in plasma membranes. *Proceedings of the National Academy of Sciences* 98 (23):13443-13448

4. Chapter Four: Introduction of an excitation energy quenching process into CP43

4.1 Abstract

CP43 is a Chl *a*-binding membrane protein functioning as a light-harvesting system of photosystem II (PSII). It closely associates with D1 and D2, where reaction center of PSII locates, and facilitates excitation energy transfer from the exterior antennae to the reaction center of PSII. Interestingly, sharing a similar structure with CP43, IsiA was determined to quench excitation energy via a cysteine-mediated mechanism, which was not found in CP43. Amino acid sequence analysis showed that no cysteine locates in close proximity to any of the Chl *a* and the cysteine playing the critical role in IsiA is replaced with a valine in CP43. In this study, site-directed mutagenesis was used to introduce the cysteine-mediated quenching process into CP43, leading to the mutant *Synechocystis* phenotypes with 25% lower maximum quantum yield in comparison with the wild type. The CP43 mutant can not grow photoautotrophically, and a low oxygen evolution rate was observed in this mutant, suggesting a less efficient PSII caused by the introduction of the excitation energy quenching process.

4.2 Introduction

CP43 is a Chl *a*-binding membrane protein, encoded by the *psbC* gene, which serves as an intrinsic antenna for photosystem II (PSII). In PSII, CP43 and CP47 proteins surround D1 and D2, where the reaction center of PSII locates (Zouni *et al.* 2001; Umena *et al.* 2011), and transfer excitation energy from the exterior antenna to the reaction center core. The crystal structure of CP43 is available at high resolution which shows that it binds 13 Chl *a* and has six transmembrane helices (Umena *et al.* 2011). Belonging to the same chlorophyll-binding 6-transmembrane helical protein superfamily, CP43 is highly homologous with IsiA, an iron stress-induced Chl *a*-binding protein (Burnap *et al.* 1993; Bibby *et al.* 2001). Although IsiA has been determined providing

photoprotection by quenching excitation energy as heat (Ihalainen *et al.* 2005; Orf *et al.* 2016; Chen *et al.* 2017), no excitation energy quenching process with CP43 directly involved has been proposed. Because efficiently transfer excitation energy to the reaction center core is one of the most essential function CP43 serves, it is not surprising that CP43 lacks any excitation energy quenching mechanism, which may distract energy flux toward the reaction center core and lower the quantum efficiency of PSII. However, with an extra quenching mechanism in CP43, it may provide photoprotection and help cells survive high light stress.

A cysteine-mediated quenching mechanism has been proposed being involved in the excitation energy quenching process in the Fenna-Matthews-Olson (FMO) complex (Orf *et al.* 2016) and the IsiA aggregate (Chen *et al.* 2017). In this mechanism, the cysteine residue plays a critical role that dissipates the excitation energy in oxidizing environments via an excited-state electron-transfer event with the participation of excited (bacterio)chlorophylls and thiyl radicals at the cysteine residues (Chen *et al.* 2017; Orf *et al.* 2016). Sharing a similar structure with IsiA, CP43 has a valine (Val277) that locates in close proximity to the Chl a_{29} as the Cys260 in IsiA (Figure 4.1). In this study, site-directed mutagenesis was performed, by which the Val277 in CP43 was replaced with a cysteine, resulting in the V277C-His47 *Synechocystis* strain. A 25% lower quantum efficiency of PSII in the V277C-His47 strain was observed, which suggests the defective energy transfer chain to the reaction center of PSII. In addition, the CP43 mutant is unable to grow photoautotrophically, and a low oxygen evolution rate was observed in this mutant, showing a significant change in the efficiency of photosynthetic reactions caused by a single amino acid substitution that may suggest the introduction of an extrinsic quenching process to CP43.

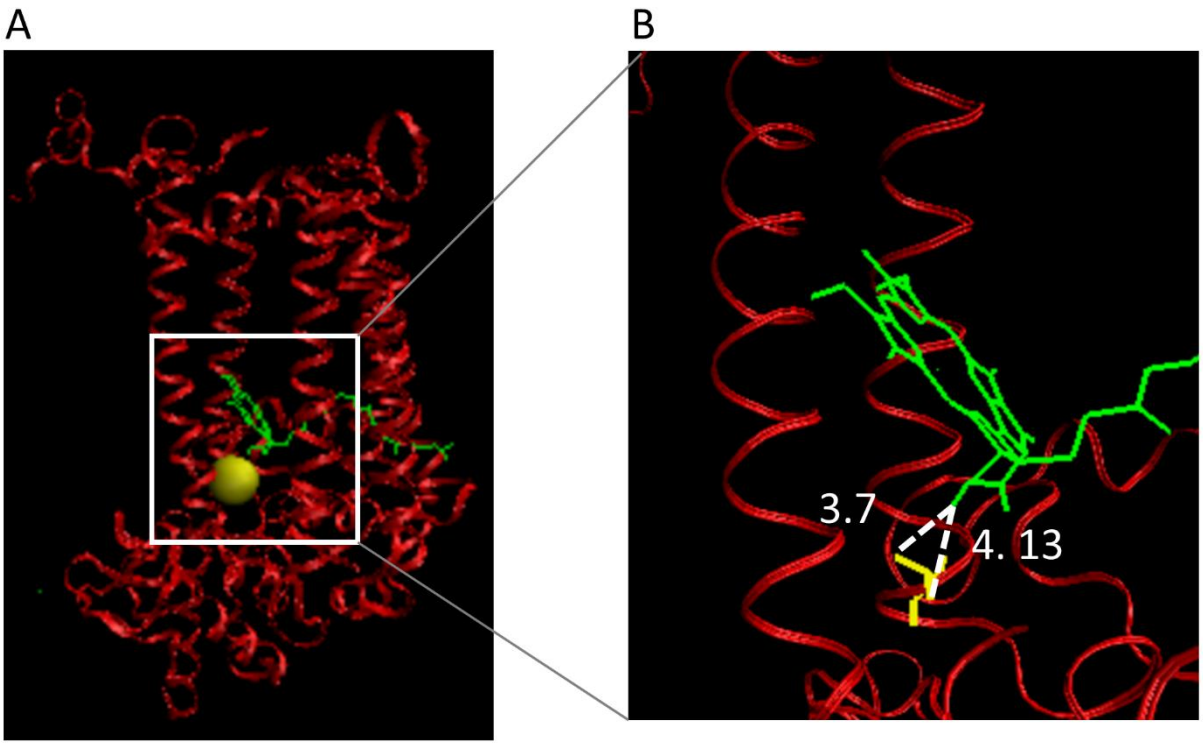

Figure 4.1 The Val290 in CP43 crystal structure. (A) The membrane side view of CP43 and (B) the close view of Val290 as well as Chl a_{29}. Val290 is showed in yellow, and the Chl a_{29} is in green. The distance between the Chl a_{29} and the Val290 is estimated and shown in white.

4.3 Results and Discussion

To understand if the cysteine-mediated quenching mechanism can be introduced into CP43, site-directed mutagenesis was performed by the CRISPR/Cpf1 system (Ungerer and Pakrasi 2016), resulting in the V277C-His47 mutant. In this V277C-His47 mutant, the valine, V277, was replaced with a cysteine which was demonstrated playing a critical role in the cysteine-mediated quenching process in IsiA (Chen *et al.* 2017). Given that the valine and Chl a_{29} are in close proximity (Umena *et al.* 2011), CP43 shares a similar structure with IsiA, and the oxidizing environment in PSII, it is likely that by replacing the valine with a cysteine, the mutant CP43 may quench excitation energy, leading to the lower quantum efficiency in PSII.

Before confirming the mutation in the V277C transformants, the colonies were examined by FluorCam (PSI, Cezch Republic), a fluorometer used to measure the fluorescence parameters. The results are shown in Table 4.1, which indicate that the colonies 3, 7 and 8 have the low quantum efficiency of PSII (F_v/F_m). Interestingly, the mutation in colonies 1, 3, and 7 were checked by sequencing, and the results show that the one with a normal F_v/F_m, colony 1, is a false positive. On the other hand, colonies 3 and 7, which have about 25% lower F_v/F_m compared with the wild type, were confirmed to be the correct V277C-His47 phenotypes. These preliminary results suggest that the V277C mutation in CP43 significantly affects energy transfer in PSII and therefore leads to the reduction in the quantum efficiency of PSII. Colony 3 was studied in this study and termed V277C-His47 mutant strain.

Table 4.1 Photosynthetic efficiencies of selected V277C transformants.

Data†	**Colony 1**	**Colony 2**	**Colony 3**	**Colony 4**	**Colony 5**	**Colony 6**	**Colony 7**	**Colony 8**
F_m	889.51	1012.96	798.76	802.89	753.85	666.67	628.11	645.65
F_v	385.54	495.06	255.57	354.89	341.16	270.04	214.21	139.19
F_v/F_m	0.43	0.49	0.32	0.44	0.45	0.40	0.34	0.21

† F_m, maximum fluorescence; F_v, variable fluorescence; F_v/F_m, maximum potential quantum efficiency of photosystem II

Growth experiments were conducted to understand the effects of the V277C mutation in CP43 on the mutant cells. In the presence of 3-(3,4-dichlorophenyl)-1,1-dimethylurea (DCMU) and glucose, the plastoquinone binding site of PSII is blocked, which, therefore, inhibit photosynthesis, and the cells are forced to grow heterotrophically. Under this condition, the V277C CP43 mutant grew as well as the His47 strain (Figure 4.2). Both strains grew well in the presence of glucose, and stopped growing once the glucose was completely consumed. On the other hand, without the addition of glucose, the V277C-His47 mutant did not grow in BG11. As mentioned above, the V277C-His47 mutant appears to have a lower quantum efficiency of PSII compared with the wild type. As a result, this mutant may not grow photoautotrophically.

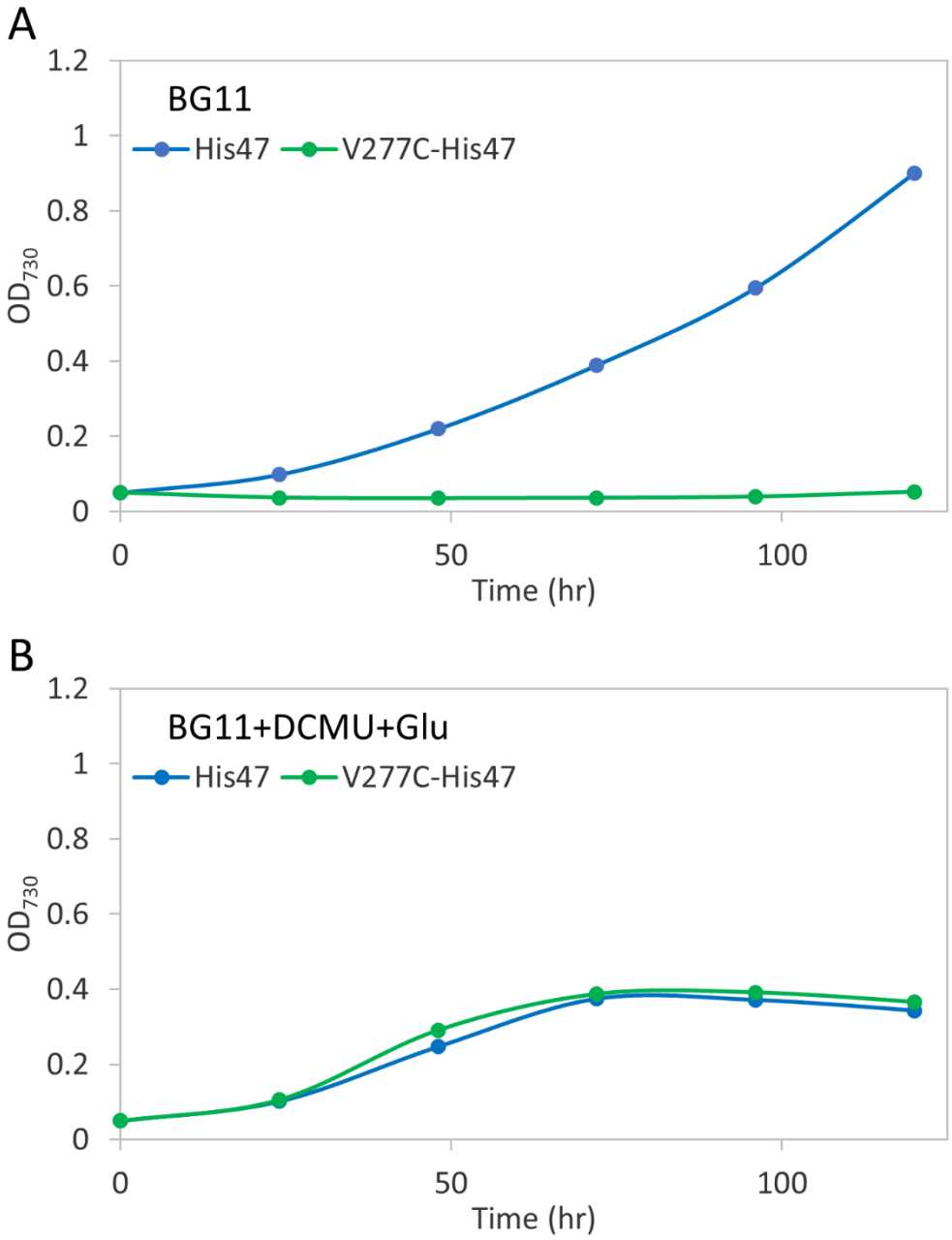

Figure 4.2 The growth curves of the V277C-His47 mutant and the His47 strain in (A) BG11 and in (B) BG11 in the presence of 20 µM DCMU and 5 mM glucose.

Furthermore, the PSII-mediated oxygen evolution rates of both the V277C-His47 and the His47 strains under different light conditions were recorded. The results show that with the mutant CP43, the PSII of the V277C-His47 strain can still split water and produce oxygen. However, the

lower maximum oxygen evolution rate found in the mutant indicates the lower photosynthesis efficiency owing to the substitution of the valine with a cysteine (Figure 4.3).

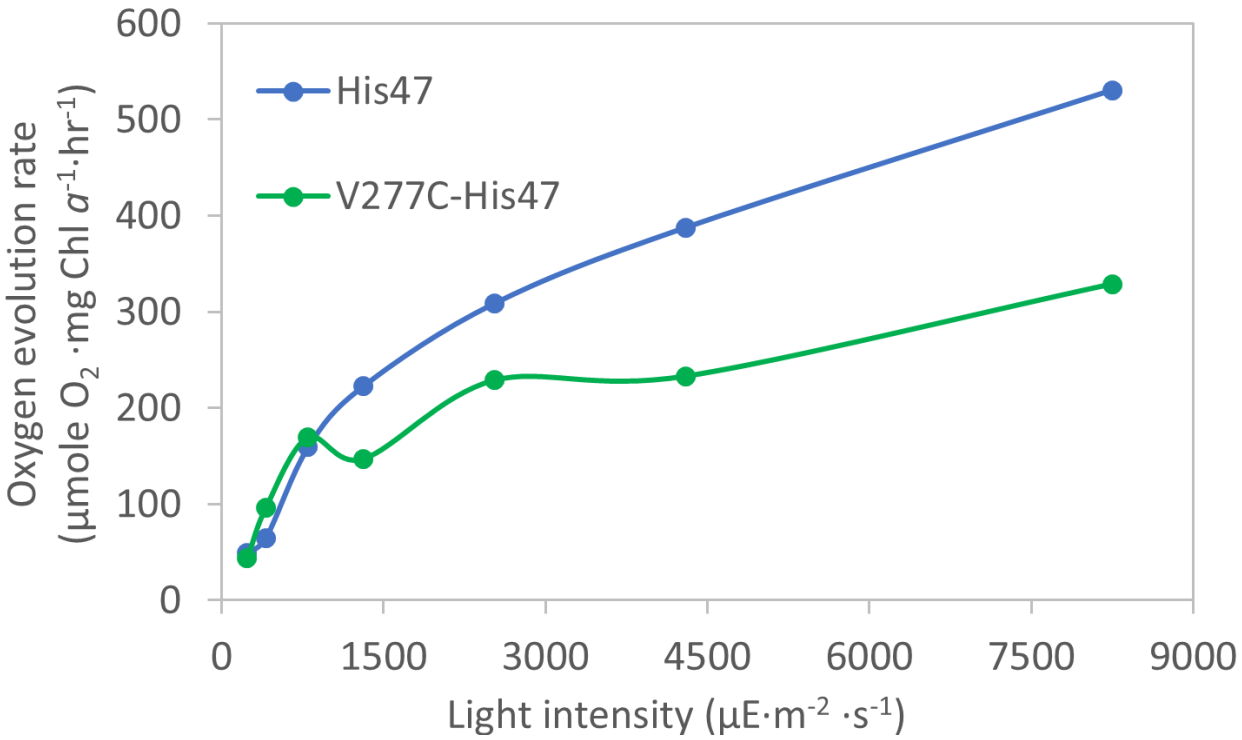

Figure 4.3 The PSII-mediated oxygen evolution rates of the His47 strain and the V277C-His47 mutant under different light conditions.

4.4 Methods

Construction of strains

Site-directed mutagenesis was performed by the CRISPR/Cpf1 system as described in previous studies (Ungerer and Pakrasi 2016). The editing plasmid with all the DNA features needed, including the gRNA and the repair template, was transformed into the His47 strain (Bricker *et al.* 1998) using the *E. coli* strain containing the pRL443 and pRL623 plasmid by the tri-parental conjugation method (Golden *et al.* 1987). In this His47 strain, a hexahistidyl tag was

added on the C-terminus of the CP47 protein. This strain has been well characterized and can be used to purify active PSII (Bricker *et al.* 1998). Since no significant physiological difference was observed between this His47 strain and the wild type *Synechocystis* sp. PCC 6803 strain, in this study, the V277C-His47 was compared with the His47 strain.

The transformants were re-patched three times onto BG11 plates containing 5 mM glucose and 5 μg/mL gentamycin for selection. Eight colonies were picked and patched and pre-screened by measuring the photosynthesis parameters. The V277C-His47 mutant was confirmed by sequencing. This mutant was grown in BG11 with 50 mM glucose, 5 μg/mL gentamycin as well as 20 μM DCMU, which prevents random mutations.

Growth experiments

To understand how the single amino acid substitution in CP43, V277C, affects the growth of cells, the growth of both the His47 and V277C-His47 strains were monitored. Both liquid cultures were pre-cultured in BG11 with 50 mM glucose, 5 μg/mL gentamycin and 20 μM DCMU for five days. The cells were then harvested and washed three times with BG11. The washed cells were adjusted to OD730 0.05 in BG11 for phototrophic growth and in BG11 with 5 mM glucose 20 μM DCMU for heterotrophic growth in a 12-well plate under the illumination of 30 μmol photons m^{-2} s^{-1} at 30 °C. One hundred and fifty milliliters liquid culture in each well was taken out every 24 hr and the OD_{730} was measured with a plate reader.

Measurements of photosynthesis parameters

Eight V277C-His47 transformants were patched on a BG11 containing 50 mM glucose and 5 μg/mL gentamycin and grown for a week. The whole plate was placed in the Closed FluorCam

FC 800-C (PSI, Czech Republic) for two minutes for dark acclimation. The plate was then imaged and the images with the Chl *a* fluorescence signals were analyzed with the FluorCam7 software (PSI, Czech Republic) and the photosynthesis parameters (F_o, F_v and F_m) were determined.

PSII-mediated oxygen evolution

Cells cultures were grown in BG11 for a week under the illumination of 30 μmol photons m^{-2} s^{-1} at 30 °C. The cells were harvested and adjusted to an equal Chl *a* content for the measurement of oxygen evolution rate. The light induced PSI-mediated oxygen evolution rate was measured with a Clark type electrode as described in our previous publication (Ungerer *et al.* 2018).

4.5 Reference

Bibby TS, Nield J, Barber J (2001) Three-dimensional model and characterization of the iron stress-induced CP43'-photosystem I supercomplex isolated from the cyanobacterium *Synechocystis* PCC 6803. *The Journal of biological chemistry* 276 (46):43246-43252. doi:10.1074/jbc.M106541200

Bricker TM, Morvant J, Masri N, Sutton HM, Frankel LK (1998) Isolation of a highly active photosystem II preparation from *Synechocystis* 6803 using a histidine-tagged mutant of CP 47. *Biochimica et biophysica acta (BBA)-Bioenergetics* 1409 (1):50-57

Burnap RL, Troyan T, Sherman LA (1993) The highly abundant chlorophyll-protein complex of iron-deficient *Synechococcus* Sp PCC7942 (Cp43) is encoded by the *isiA* gene. *Plant Physiol* 103 (3):893-902. doi:Doi 10.1104/Pp.103.3.893

Chen HS, Liberton M, Pakrasi HB, Niedzwiedzki DM (2017) Reevaluating the mechanism of excitation energy regulation in iron-starved cyanobacteria. *Biochimica et biophysica acta* 1858 (3):249-258. doi:10.1016/j.bbabio.2017.01.001

Golden SS, Brusslan J, Haselkorn R (1987) [12] Genetic engineering of the cyanobacterial chromosome. In: *Methods in enzymology*, vol 153. Elsevier, pp 215-231

Ihalainen JA, D'Haene S, Yeremenko N, van Roon H, Arteni AA, Boekema EJ, van Grondelle R, Matthijs HC, Dekker JP (2005) Aggregates of the chlorophyll-binding protein IsiA (CP43') dissipate energy in cyanobacteria. *Biochemistry* 44 (32):10846-10853. doi:10.1021/bi0510680

Orf GS, Saer RG, Niedzwiedzki DM, Zhang H, McIntosh CL, Schultz JW, Mirica LM, Blankenship RE (2016) Evidence for a cysteine-mediated mechanism of excitation energy regulation in a photosynthetic antenna complex. *Proceedings of the National Academy of Sciences of the United States of America* 113 (31):E4486-4493. doi:10.1073/pnas.1603330113

Umena Y, Kawakami K, Shen J-R, Kamiya N (2011) Crystal structure of oxygen-evolving photosystem II at a resolution of 1.9 Å. *Nature* 473 (7345):55

Ungerer J, Lin PC, Chen HY, Pakrasi HB (2018) Adjustments to photosystem stoichiometry and electron transfer proteins are key to the remarkably fast growth of the cyanobacterium *Synechococcus elongatus* UTEX 2973. *MBio* 9 (1). doi:10.1128/MBio.02327-17

Ungerer J, Pakrasi HB (2016) Cpf1 is a versatile tool for CRISPR genome editing across diverse species of cyanobacteria. *Scientific reports* 6:39681

Zouni A, Witt H-T, Kern J, Fromme P, Krauss N, Saenger W, Orth P (2001) Crystal structure of photosystem II from *Synechococcus* elongatus at 3.8 Å resolution. *Nature* 409 (6821):739

5. Chapter Five: Conclusion and future directions

5.1 Conclusion

The functions of IsiA have been studied for decades, yet the mysteries have not been fully revealed. In this work, the excitation energy quenching in IsiA was studied by time-resolved spectroscopy as well as other protein assays. In addition, the physiological changes of cells caused by the modification of the photoprotective mechanism in IsiA were also identified, suggesting the significant role IsiA plays in photosynthesis.

In this study, pure PSI-IsiA supercomplexes and IsiA aggregates were successfully isolated from the iron-starved *Synechocystis* mutant strains, which have polyhistidine-tags attached to PsaF or IsiA, by affinity chromatography followed by sucrose gradient ultracentrifugation. The protein samples with the least contamination enables us to study energy transfer in IsiA and PSI-IsiA supercomplexes. In Chapter 2, we demonstrated that the carotenoids in IsiA do not serve as energy quencher, nor supports Chl *a* for light-harvesting. Based on the time-resolved spectroscopic results, we proposed that IsiA quenches excitation energy by a cysteine-mediated quenching mechanism, which was originally demonstrated in the FMO protein (Orf *et al.* 2016).

In Chapter 3, site-directed mutagenesis was performed, resulting in the IsiA mutant strains, in which the critical cysteine residue is replaced with a valine. With this single amino acid substitution, IsiA no longer quenches excitation energy, whereas it still serves the light-harvesting purpose for PSI. Interestingly, the C260V IsiA mutant grows faster than the wild type in the presence of sufficient iron under high light. Because the mutant IsiA is unable to quench excitation energy but still capable of serving as an antenna for PSI, the faster growth rate may result from the more efficient use of light energy in the C260V IsiA mutant compared with that of the wild type.

These findings provide a promising approach for improving photosynthesis and increasing the biomass yield.

The work in Chapter 3 determined that by manipulating photoprotective mechanisms in cyanobacteria, the higher biomass yield can be achieved. In Chapter 4, we attempted to introduce this cysteine-mediated quenching process into CP43, an intrinsic antenna protein of PSII, to serve photoprotection purposes. Our results show that with a cystine residue placed at the critical position near to a Chl *a*, the mutant cells have a 25% lower quantum efficiency of PSII in comparison to the wild type and can not grow photoautotrophically. Further investigation is needed to characterize this CP43 mutant phenotype, but our results already show a potential in introducing an extrinsic photoprotective mechanism into targeted proteins.

5.2 Future directions

5.2.1 Extending the understanding of IsiA

In this work, we focused on understanding the excitation energy quenching in IsiA and the significance of this quenching process on cell growth. Nonetheless, it has been demonstrated that IsiA serves multiple functions (Park *et al.* 1999; Riethman and Sherman 1988; Burnap *et al.* 1993), which have not been fully understood. One issue that hinders our progress of understanding IsiA is the missing of IsiA crystal structure at high resolution. Recently, the mature single-particle cryo-electron microscopy technique was used to obtain the phycobilisome, a 16.8 MDa antenna protein complex, structure at 3.5Å (Zhang *et al.* 2017). This technique may be used to obtain the structure of PSI-IsiA supercomplexes and IsiA aggregates at higher resolution. The crystal structures of PSI-IsiA and IsiA are useful information that helps to study the protein-protein interactions in PSI-IsiA and IsiA aggregates.

The results from field studies and laboratory experiments suggest that IsiA is the dominant Chl *a*-binding protein in iron-deficient environments (Burnap *et al.* 1993; Schrader *et al.* 2011). Furthermore, some studies suggested that the IsiA aggregates are even more abundant compared with PSI-IsiA supercomplexes (Feng *et al.* 2011; Ryan-Keogh *et al.* 2012). However, it is not understood why cyanobacterial cells spend significant amount of energy producing IsiA aggregates under iron-deficient conditions. In addition, the *in vivo* quantification of PSI-IsiA supercomplexes and IsiA aggregates is missing, and where IsiA locates in the thylakoid membranes is not revealed. By using hyperspectral confocal fluorescence microscopy in combination with electron microscopy, the protein complexes in cells can be identified and visualized based on their distinct fluorescence emission signals (Collins *et al.* 2012). This technology can be used to determine the localization of PSI, PSII, PSI-IsiA, and IsiA aggregates, and quantify these protein complexes *in vivo*. This information is critical for understanding the roles PSI-IsiA supercomplexes and IsiA aggregates play in the cells.

5.2.2 Applying the knowledge on improving photosynthesis

Fast growth is a significant evolutionary advantage that helps organisms to compete with others. In an engineer point of view, growing fast means producing desired products or simply growing biomass fast. Therefore, fast-growing strain has always been needed. For phototrophs, one approach to achieve higher growth rate, is to improve the quantum efficiency of photosynthesis. By improving photosynthesis, the light energy can be converted to chemical energy more efficiently, which consequently increases the overall metabolism and results in the higher growth rate (Zelitch 1975; Evans 2013). To improve photosynthesis, some attempted reducing photorespiration (Hagemann and Bauwe 2016) or improving Rubisco kinetics (Parry *et al.* 2012; Whitney *et al.* 2011), some turned to the expansion of the *Photosynthetica*lly active

radiation spectrum (Blankenship and Chen 2013), others focused on manipulation of photoprotection (Murchie and Niyogi 2011). Lately, owing to the deeper understanding on the photoprotective mechanisms, several studies have shown the potential of improving photosynthesis and biomass yield by accelerating the relaxation of photoprotection (Kromdijk *et al.* 2016; Hubbart *et al.* 2018) and reducing the capability of photoprotection (Berteotti *et al.* 2016).

The cysteine-mediated quenching mechanism in IsiA has been studied in this work. With the understanding of the critical players in the quenching process, we successfully abolished this quenching process and retained the light-harvesting function for PSI, which improved the growth rate of mutant cells under high light. Furthermore, this quenching process highly depends on the local redox potential. By controlling the local redox potential in cells, we may be able to tune the level of photoprotection under fluctuating light and improve the efficiency of photosynthesis. In addition, our study on introducing this cysteine-mediated quenching mechanism into CP43 in Chapter 4 show another possibility of manipulating the photoprotective mechanism in antenna protein. Further investigation is needed to verify the cysteine-mediated quenching process in the mutant CP43 as well as understand the physiological significance of the introduction of an extrinsic photoprotective mechanism into CP43.

5.3 Reference

Berteotti S, Ballottari M, Bassi R (2016) Increased biomass productivity in green algae by tuning non-photochemical quenching. *Scientific reports* 6:21339

Blankenship RE, Chen M (2013) Spectral expansion and antenna reduction can enhance photosynthesis for energy production. *Current opinion in chemical biology* 17 (3):457-461

Burnap RL, Troyan T, Sherman LA (1993) The highly abundant chlorophyll-protein complex of iron-deficient *Synechococcus* sp PCC 7942 (CP43) is encoded by the *isiA* gene. *Plant Physiol* 103 (3):893-902. doi:Doi 10.1104/Pp.103.3.893

Collins AM, Liberton M, Jones HDT, Garcia OF, Pakrasi HB, Timlin JA (2012) Photosynthetic pigment localization and thylakoid membrane morphology are altered in *Synechocystis* 6803 phycobilisome mutants. *Plant Physiol* 158 (4):1600-1609. doi:10.1104/pp.111.192849

Evans JR (2013) Improving photosynthesis. *Plant Physiol* 162 (4):1780-1793

Feng X, Neupane B, Acharya K, Zazubovich V, Picorel R, Seibert M, Jankowiak R (2011) Spectroscopic study of the CP43' complex and the PSI-CP43' supercomplex of the cyanobacterium *Synechocystis* PCC 6803. *The journal of physical chemistry B* 115 (45):13339-13349. doi:10.1021/jp206054b

Hagemann M, Bauwe H (2016) Photorespiration and the potential to improve photosynthesis. Current opinion in chemical biology 35:109-116

Hubbart S, Smillie IR, Heatley M, Swarup R, Foo CC, Zhao L, Murchie EH (2018) Enhanced thylakoid photoprotection can increase yield and canopy radiation use efficiency in rice. Communications biology 1 (1):22

Kromdijk J, Głowacka K, Leonelli L, Gabilly ST, Iwai M, Niyogi KK, Long SP (2016) Improving photosynthesis and crop productivity by accelerating recovery from photoprotection. *Science* 354 (6314):857-861

Murchie EH, Niyogi KK (2011) Manipulation of photoprotection to improve plant photosynthesis. *Plant Physiol* 155 (1):86-92

Orf GS, Saer RG, Niedzwiedzki DM, Zhang H, McIntosh CL, Schultz JW, Mirica LM, Blankenship RE (2016) Evidence for a cysteine-mediated mechanism of excitation energy regulation in a photosynthetic antenna complex. *Proceedings of the National Academy of Sciences of the United States of America* 113 (31):E4486-4493. doi:10.1073/pnas.1603330113

Park YI, Sandstrom S, Gustafsson P, Oquist G (1999) Expression of the *isiA* gene is essential for the survival of the cyanobacterium *Synechococcus* sp. PCC 7942 by protecting photosystem II from excess light under iron limitation. Molecular *Microbiology* 32 (1):123-129

Parry MA, Andralojc PJ, Scales JC, Salvucci ME, Carmo-Silva AE, Alonso H, Whitney SM (2012) Rubisco activity and regulation as targets for crop improvement. Journal of Experimental Botany 64 (3):717-730

Riethman HC, Sherman LA (1988) Immunological characterization of iron-regulated membrane proteins in the cyanobacterium *Anacystis nidulans* R2. *Plant physiology* 88 (2):497-505

Ryan-Keogh TJ, Macey AI, Cockshutt AM, Moore CM, Bibby TS (2012) The cyanobacterial chlorophyll-binding-protein IsiA acts to increase the *in vivo* effective absorption cross-section of PSI under iron limitation(1). *Journal of phycology* 48 (1):145-154. doi:10.1111/j.1529-8817.2011.01092.x

Schrader PS, Milligan AJ, Behrenfeld MJ (2011) Surplus photosynthetic antennae complexes underlie diagnostics of iron limitation in a cyanobacterium. *PloS one* 6 (4):e18753. doi:10.1371/journal.pone.0018753

Whitney SM, Houtz RL, Alonso H (2011) Advancing our understanding and capacity to engineer nature's CO_2-sequestering enzyme, rubisco. *Plant Physiol* 155 (1):27-35

Zelitch I (1975) Improving the Efficiency of Photosynthesis. *Science* 188 (4188):626-633

Zhang J, Ma J, Liu D, Qin S, Sun S, Zhao J, Sui S-F (2017) Structure of phycobilisome from the red alga *Griffithsia pacifica*. *Nature* 551 (7678):57

Appendix 1: Characterization of IsiA and PSI-IsiA supercomplexes

Introduction

Energy transfer in PSI-IsiA and IsiA has been investigated for decades (Andrizhiyevskaya *et al.* 2002; Melkozernov *et al.* 2003; Berera *et al.* 2009; Berera *et al.* 2010; Ryan-Keogh *et al.* 2012), yet the mechanism of energy transfer as well as energy quenching has not been fully understood. To study energy transfer in both protein complexes, pure protein samples are needed, especially for IsiA-only sample. As discussed in Chapter 1, the energy quenching process in IsiA has been studied, and a quenching process was proposed which attributes the energy dissipation in IsiA to a carotenoid- Chl *a* interaction (Berera *et al.* 2009; Berera *et al.* 2010). However, our spectroscopic results in Chapter 2 showed no energy transfer between the carotenoids and Chls in IsiA. After revisited the previous studies, we demonstrated that this disagreement is due to the PSI contamination in the IsiA sample in previous studies (Berera *et al.* 2009; Berera *et al.* 2010). This again showed the necessity of having the pure protein samples for studying energy transfer in IsiA. In this study, we showed the characterization of PSI-IsiA and IsiA protein samples purified from PsaF-His and IsiA-His strains, which are not shown in other Chapters above.

Results and discussion

The iron-starved PsaF-His and IsiA-His cultures were harvested and broken. The thylakoid membranes were solubilized with mild detergents, and protein samples were purified by affinity chromatography. Multiple protein bands were obtained from the resulting elutions by sucrose gradient ultracentrifugation (Figure 1). Because the His-tag is attached to different proteins in PsaF-His and IsiA-His, the elutions contain different compositions of protein complexes. The protein samples purified from PsaF-His contain PSI and PSI-IsiA. On the other hand, protein samples obtained from IsiA-His contain IsiA and PSI-IsiA. In this study, the analyses were focused

on the green band 4 from PsaF-His, which mainly contains PSI-IsiA, and green band 1 from IsiA-His, which only has IsiA aggregates.

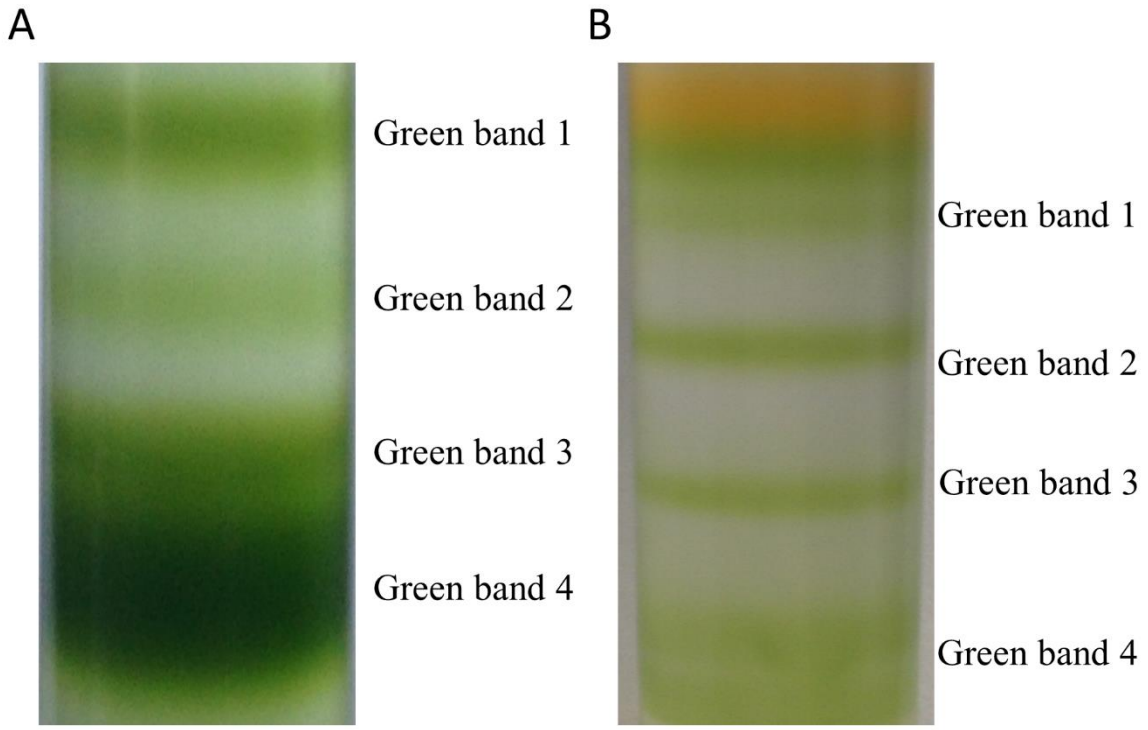

Figure 1. Protein bands obtained by sucrose gradient ultracentrifugation. Protein samples were purified by nickel affinity chromatography from solubilized thylakoid membranes from the iron-starved (A) PsaF-His and (B) IsiA-His cells.

The green band 4 obtained from PsaF-His has the highest molecular weight which suggest that it mainly contains the PSI_3-$IsiA_{18}$ supercomplex. Other green bands were determined that have PSI monomer, PSI trimer as well as other lower molecular weight PSI_x-$IsiA_y$ supercomplexes (data not shown). The steady-state fluorescence emission spectrum of the PSI-IsiA supercomplex, green band 4, is shown in Figure 2. It has a huge peak at 718 nm and a small bump at 682 nm, and these results are consistent with previous studies (Bibby *et al.* 2001; Andrizhiyevskaya *et al.* 2002). On the other hand, the green band 1 obtained from IsiA-His was determined to contain only IsiA-

aggregates in Chapter 2. In its steady-state fluorescence emission spectrum, there is only one huge peak at 682 nm, which is consistent with previous studies (Bibby *et al.* 2001), too. Interestingly, the IsiA fluorescence spectra shown in some studies have a small bump at about 718 nm (Andrizhiyevskaya *et al.* 2002; Melkozernov *et al.* 2003; Ihalainen *et al.* 2005), indicating the PSI contamination in their IsiA sample. This may lead to the wrong conclusion if the samples were used as "IsiA-only" samples to perform experiments.

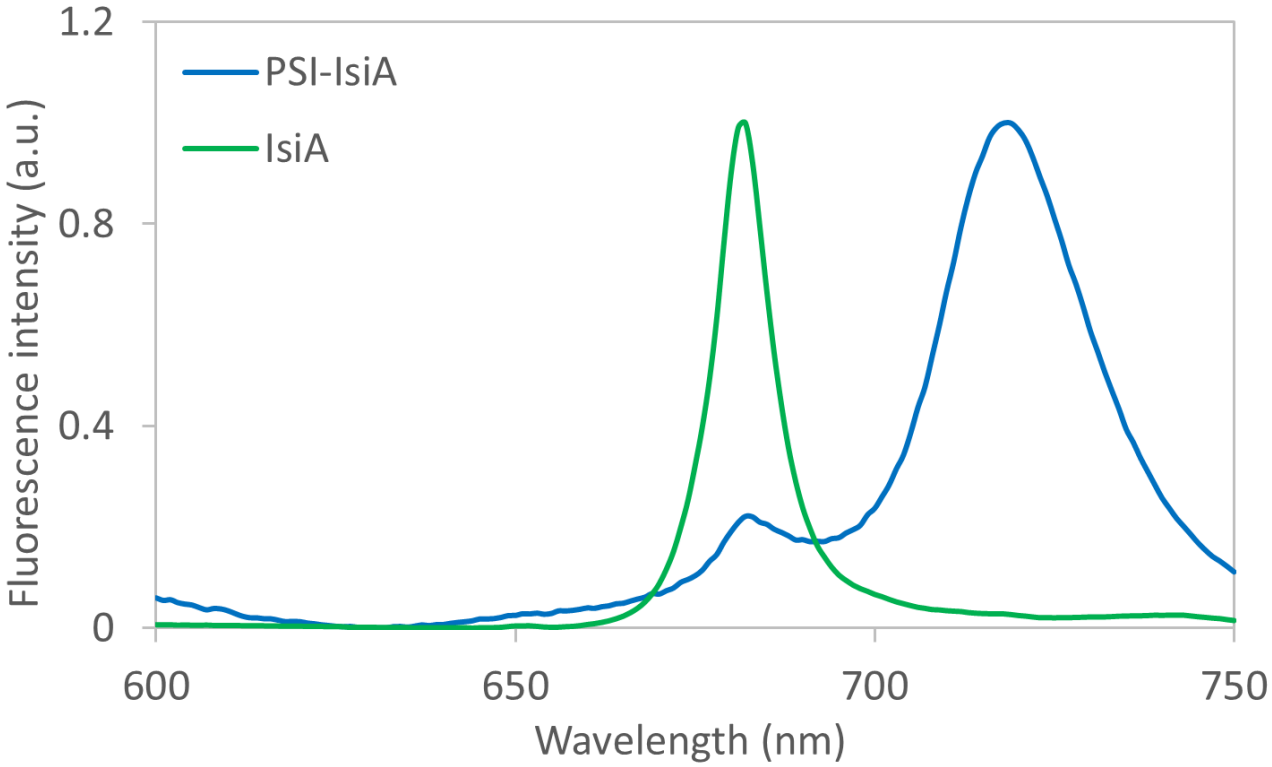

Figure 2. Steady-state fluorescence emission spectra of PSI-IsiA and IsiA excited at 435 nm at 77K.

The results of high resolution clear native polyacrylamide gel electrophoresis (hrCN-PAGE) showed that the green band 4 obtained from PsaF-His has many bands at the high molecular weight region (Figure 3A). Those bands were examined by 2D-SDS analysis and the

results showed that they are various forms of PSI-IsiA aggregates or PSI_x-$IsiA_y$ supercomplexes (Figure 3B). In addition, PSI trimers, monomers and ATP synthases were also found in this green band. In the IsiA sample, multiple bands with approximately 50 kDa difference between each were found. This 50 kDa difference is close to the molecular weight of one IsiA copy with the co-factors. Therefore, it is likely that this sample contains various IsiA complexes which consist of 2 to 12 IsiA copies.

The PSI-IsiA sample contains various forms of PSI-IsiA supercomplexes which may not be the best sample to study for understanding the detailed mechanism of energy transfer in PSI-IsiA. Nonetheless, because the ATP synthase is not involved in excitation energy transfer and PSI trimer and monomers do not affect the fluorescence emission of PSI-IsiA supercomplexes, we were still able to observe the efficient and rapid energy transfer from IsiA to PSI. On the other hand, in our IsiA sample, it contains only IsiA but with different numbers of IsiA copies. For the purpose of studying excitation energy quenching in individual IsiA copy, with different numbers of IsiA copies does not affect the results. The only concern is the PSI-IsiA supercomplex contamination, which was ruled out by the assays described in Chapter 2 and 3.

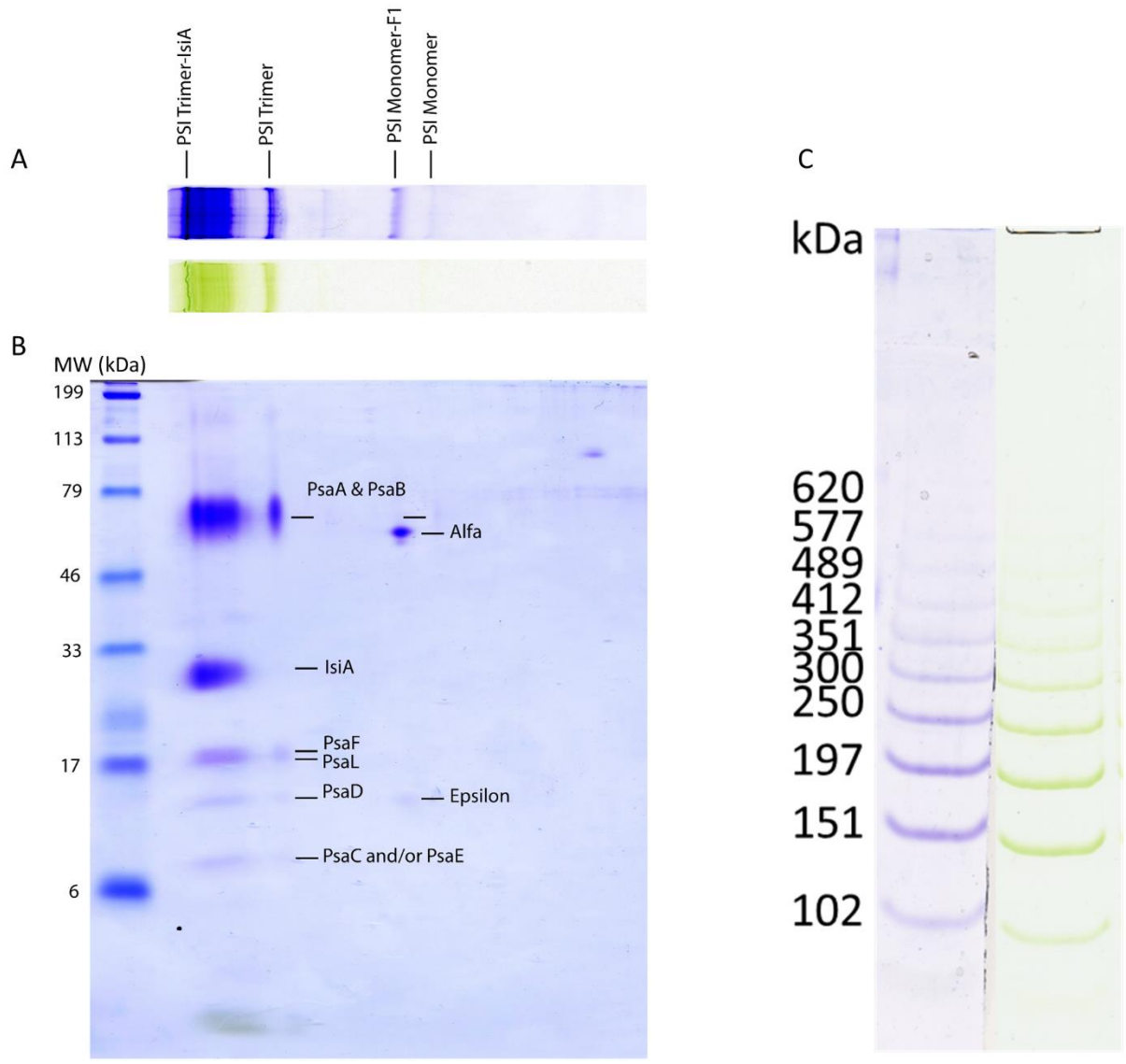

Figure 3. The (A) hrCN-PAGE and (B) 2D-SDS PAGE analyses of the PSI-IsiA sample as well as the (C) hrCN-PAGE analysis of the IsiA sample.

Methods and materials

Growth conditions and protein purification

PsaF-His and IsiA-His strains, which have a polyhistidine tag at the C-terminus of PsaF and IsiA, respectively, were grown in YBG11-Fe medium to induce the expression of *isiA*. The

cells were grown under the light intensity of 30 μmol photons m^{-2} s^{-1} at 30 ˚C and harvested after 7 to 12 days of growth when the IsiA Chl *a* fluorescence became dominant.

The cells were broken by the bead-beater technique and the solubilized thylakoid membranes were prepared as described in Chapter 2. The protein complexes were purified from the solubilized thylakoid membranes by affinity chromatography. The resulting protein mixtures in the elutions, were further separated by sucrose gradient ultracentrifugation, as described in Chapter 2.

hrCN-PAGE and 2D-SDS PAGE

Both gels were Bis-Tris gels prepared as described in previous study (Wittig *et al.* 2007). The 4 – 12% acrylamide gel was used for hrCN-PAGE and the 10% acrylamide gel was used for 2D-SDS PAGE. Both gels were stained by the Coomassie Blue G-250 dye to visualize protein bands.

77K Steady-state fluorescence emission spectra

The protein samples were prepared as described above. The fluorescence emission spectra were obtained at 77K with the Chl *a* excited at 435 nm by a SPEX Fluoromax 2 spectrofluorometer.

Reference

Andrizhiyevskaya EG, Schwabe TM, Germano M, D'Haene S, Kruip J, van Grondelle R, Dekker JP (2002) Spectroscopic properties of PSI-IsiA supercomplexes from the cyanobacterium *Synechococcus* PCC 7942. *Biochimica et biophysica acta* 1556 (2-3):265-272

Berera R, van Stokkum IH, d'Haene S, Kennis JT, van Grondelle R, Dekker JP (2009) A mechanism of energy dissipation in cyanobacteria. *Biophysical journal* 96 (6):2261-2267. doi:10.1016/j.bpj.2008.12.3905

Berera R, van Stokkum IH, Kennis JT, van Grondelle R, Dekker JP (2010) The light-harvesting function of carotenoids in the cyanobacterial stress-inducible IsiA complex. *Chemical Physics* 373 (1):65-70

Bibby TS, Nield J, Barber J (2001) Three-dimensional model and characterization of the iron stress-induced CP43'-photosystem I supercomplex isolated from the cyanobacterium *Synechocystis* PCC 6803. *The Journal of biological chemistry* 276 (46):43246-43252. doi:10.1074/jbc.M106541200

Ihalainen JA, D'Haene S, Yeremenko N, van Roon H, Arteni AA, Boekema EJ, van Grondelle R, Matthijs HC, Dekker JP (2005) Aggregates of the chlorophyll-binding protein IsiA (CP43') dissipate energy in cyanobacteria. *Biochemistry* 44 (32):10846-10853. doi:10.1021/bi0510680

Melkozernov AN, Bibby TS, Lin S, Barber J, Blankenship RE (2003) Time-resolved absorption and emission show that the CP43' antenna ring of iron-stressed *Synechocystis* sp. PCC 6803 is efficiently coupled to the photosystem I reaction center core. *Biochemistry* 42 (13):3893-3903. doi:10.1021/bi026987u

Ryan-Keogh TJ, Macey AI, Cockshutt AM, Moore CM, Bibby TS (2012) The cyanobacterial chlorophyll-binding-protein IsiA acts to increase the *in vivo* effective absorption cross-section of PSI under iron limitation(1). *Journal of phycology* 48 (1):145-154. doi:10.1111/j.1529-8817.2011.01092.x

Wittig I, Karas M, Schägger H (2007) High resolution clear native electrophoresis for in-gel functional assays and fluorescence studies of membrane protein complexes. *Molecular & Cellular Proteomics* 6 (7):1215-1225

Appendix 2: Adjustments to photosystem stoichiometry and electron transfer proteins are key to the remarkably fast growth of the cyanobacterium *Synechococcus elongatus* UTEX 2973

AMERICAN SOCIETY FOR MICROBIOLOGY | mBio®

RESEARCH ARTICLE

Adjustments to Photosystem Stoichiometry and Electron Transfer Proteins Are Key to the Remarkably Fast Growth of the Cyanobacterium *Synechococcus elongatus* UTEX 2973

Justin Ungerer,[a] Po-Cheng Lin,[b] Hui-Yuan Chen,[b] Himadri B. Pakrasi[a,b]

[a]Department of Biology, Washington University, St. Louis, Missouri, USA

[b]Department of Energy, Environmental and Chemical Engineering, Washington University, St. Louis, Missouri, USA

ABSTRACT At the genome level, *Synechococcus elongatus* UTEX 2973 (*Synechococcus* 2973) is nearly identical to the model cyanobacterium *Synechococcus elongatus* PCC 7942 (*Synechococcus* 7942) with only 55 single nucleotide differences separating the two strains. Despite the high similarity between the two strains, *Synechococcus* 2973 grows three times faster, accumulates significantly more glycogen, is tolerant to extremely high light intensities, and displays higher photosynthetic rates. The high homology between the two strains provides a unique opportunity to examine the factors that lead to increased photosynthetic rates. We compared the photophysiology of the two strains and determined the differences in *Synechococcus* 2973 that lead to increased photosynthetic rates and the concomitant increase in biomass production. In this study, we identified inefficiencies in the electron transport chain of *Synechococcus* 7942 that have been alleviated in *Synechococcus* 2973. Photosystem II (PSII) capacity is the same in both strains. However, *Synechococcus* 2973 exhibits a 1.6-fold increase in PSI content, a 1.5-fold increase in cytochrome b_6f content, and a 2.4-fold increase in plastocyanin content on a per cell basis. The increased content of electron carriers allows a higher flux of electrons through the photosynthetic electron transport chain, while the increased PSI content provides more oxidizing power to maintain upstream carriers ready to accept electrons. These changes serve to increase the photosynthetic efficiency of *Synechococcus* 2973, the fastest growing cyanobacterium known.

IMPORTANCE As the global population increases, the amount of arable land continues to decrease. To prevent a looming food crisis, crop productivity per acre must increase. A promising target for improving crop productivity is increasing the photosynthetic rates in crop plants. Cyanobacteria serve as models for higher plant photosynthetic systems and are an important test bed for improvements in photosynthetic productivity. In this study, we identified key factors that lead to improved photosynthetic efficiency and increased production of biomass of a cyanobacterium. We suggest that the findings presented herein will give direction to improvements that may be made in other photosynthetic organisms to improve photosynthetic efficiency.

KEYWORDS cyanobacteria, electron transport, photosynthesis, *Synechococcus*

The global population is increasing, while the demand for biofuels consumes more and more arable land that would otherwise be used for agriculture. These trends create a looming food crisis that will be realized within the next 50 years. In order to avoid such a crisis, global food production must increase even though the amount of farm land is decreasing. Over the past 50 years, production per hectare has more than doubled due to advances in controlling nutrition, pests, disease, and drought and

Received 14 December 2017 **Accepted** 3 January 2018 **Published** 6 February 2018

Citation Ungerer J, Lin P-C, Chen H-Y, Pakrasi HB. 2018. Adjustments to photosystem stoichiometry and electron transfer proteins are key to the remarkably fast growth of the cyanobacterium *Synechococcus elongatus* UTEX 2973. mBio 9:e02327-17. https://doi.org/10.1128/mBio.02327-17.

Editor Stephen J. Giovannoni, Oregon State University

Address correspondence to Himadri B. Pakrasi, Pakrasi@wustl.edu.

This article is a direct contribution from a Fellow of the American Academy of Microbiology. Solicited external reviewers: Robert Burnap, Oklahoma State University; Louis Sherman, Purdue University.

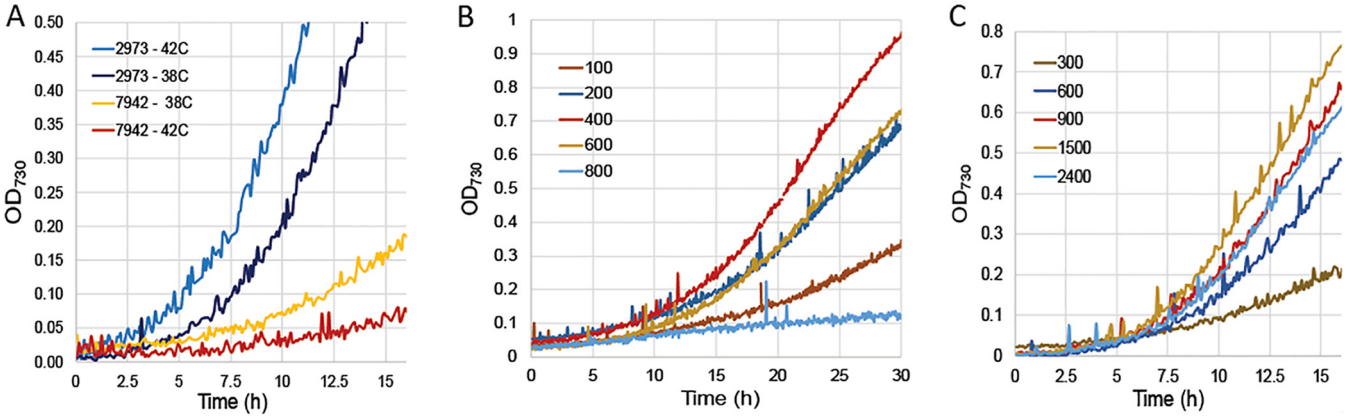

FIG 1 Growth of *Synechococcus* 7942 and *Synechococcus* 2973 under various conditions. (A) Comparison of growth at 38°C versus 42°C. *Synechococcus* 7942 was grown with 400 μmol m^{-2} s^{-1} light and 5% CO_2, and *Synechococcus* 2973 was grown with 900 μmol m^{-2} s^{-1} light and 5% CO_2. (B) Growth of *Synechococcus* 7942 at various light intensities at 38°C and 5% CO_2. (C) Growth of *Synechococcus* 2973 at various light intensities at 38°C and 5% CO_2. Light intensity in panels B and C is given in μmol m^{-2} s^{-1}. Notice the difference in the scale of the *x* axis in panel B versus panels A and C.

increases in the amount of biomass partitioned into grain. Unfortunately, these problems are essentially solved which leaves little room for improvement in these areas in the future. Plants operate at ~1% of the theoretical maximum for solar energy capture and conversion which suggests that improvements to photosynthesis is a promising path for improving crop yields in the future.

Cyanobacteria are the ancient ancestors of the chloroplast and serve as a genetically tractable model for the study of photosynthesis. One model cyanobacterium, *Synechococcus elongatus* PCC 7942 (*Synechococcus* 7942), has a recently discovered relative, *Synechococcus elongatus* UTEX 2973 (*Synechococcus* 2973), that is nearly genetically identical but exhibits photosynthesis rates more than twofold higher. The two strains differ by only 55 single nucleotide polymorphisms (SNPs), a 7.5-kb deletion/insertion, and a 188-kb inversion; however, *Synechococcus* 2973 produces biomass at three times the rate of *Synechococcus* 7942 (see below). Unlike many model strains, *Synechococcus* 2973 is capable of biomass production at rates that are comparable to heterotrophs such as the yeast *Saccharomyces cerevisiae*. The extremely close relatedness of the two cyanobacterial strains offers an excellent system to examine how a slower-growing, less-productive model organism can be transitioned into a fast-growing and highly productive strain. We set out to compare the photophysiology of the two strains to elucidate which specific changes lead to the increased productivity of *Synechococcus* 2973. Such a comparison will give direction to the changes that must be made to improve the photosynthetic rates of other model and industrial relevant cyanobacteria and eventually higher plants.

RESULTS

Growth of *Synechococcus* 2973 and *Synechococcus* 7942. Despite being genetically similar, the two *Synechococcus* strains display significant phenotypic differences such as optimum growth conditions and maximum growth rates under such conditions. In our previous study, we reported that *Synechococcus elongatus* UTEX 2973 grew best at 500 μmol m^{-2} s^{-1} light (20), which was the maximum intensity that our bioreactor could achieve. With an upgraded bioreactor (MC-1000HL; Photon Systems Instruments, Brno, Czech Republic), we returned to examine a wider range of growth conditions. We found that *Synechococcus elongatus* PCC 7942 grows best at 38°C and exhibits reduced growth at 42°C (Fig. 1A). In contrast, the optimum growth temperature for *Synechococcus* 2973 is 42°C, and it grows slightly slower at 38°C (Fig. 1A). Another characteristic difference between the two strains is their capacity for light tolerance and maximum growth rates under optimum conditions. *Synechococcus* 7942 achieves its maximum growth rate, a 4.9-h doubling time, at 400 μmol m^{-2} s^{-1} light,

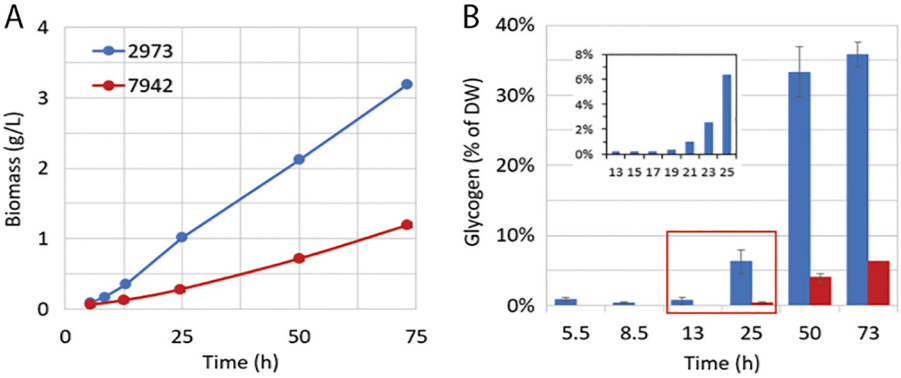

FIG 2 Biomass accumulation (A) and glycogen content (B) of *Synechococcus* 2973 and *Synechococcus* 7942. The inset graph in panel B presents glycogen synthesis between 13 and 25 h. DW, dry weight (cell weight).

5% CO_2, and 38°C (Fig. 1B). Increasing light intensity above 400 μmol m^{-2} s^{-1} slows growth due to photoinhibition. In contrast, *Synechococcus* 2973 achieves the remarkable doubling time of 1.5 h at 1,500 μmol m^{-2} s^{-1} light, 5% CO_2, and 42°C (Fig. 1C). Furthermore, *Synechococcus* 2973 does not appear to suffer from significant photoinhibition at light intensities that far exceed natural sunlight, up to 2,400 μmol m^{-2} s^{-1} (Fig. 1C).

Although they are closely related, *Synechococcus* 2973 and *Synechococcus* 7942 are two different strains. As such, they grow well under different conditions, and therefore, there is no single growth condition that both strains can be cultured under for direct comparison. Under the maximum light intensity that *Synechococcus* 7942 grows at (400 μmol m^{-2} s^{-1} light), both strains grow at similar rates, and we would not be able to investigate the rapid growth phenotype of *Synechococcus* 2973. If we grow both strains at higher light intensities, then *Synechococcus* 7942 becomes photoinhibited, and we would be comparing a strain experiencing severe photodamage to a healthy one. Therefore, to compare the two strains in this study, we chose conditions that work well for each strain. To limit the variables that are different in the growth conditions, we chose 38°C as the growth temperature because both strains grow well at this temperature. However, *Synechococcus* 7942 was cultured at 300 μmol m^{-2} s^{-1} light, while *Synechococcus* 2973 was cultured at 900 μmol m^{-2} s^{-1} light. The cyanobacteria grown under both light conditions were supplemented with 5% CO_2.

Glycogen accumulation. *Synechococcus* 2973 demonstrates high growth rates under high light and high CO_2 conditions. To understand more about carbon utilization by this fast-growing strain, we compared the time course of biomass and glycogen accumulation that occurs after log-phase growth has transitioned to linear growth at an optical density at 730 nm (OD_{730}) of ~0.4. *Synechococcus* 2973 undergoes a protracted period of linear growth where it reached densities much higher than our bioreactor can record. During this time, *Synechococcus* 2973 accumulates biomass steadily at a rate of 1.1 g $liter^{-1}$ day^{-1} (Fig. 2A), which is nearly three times higher than the rate shown by *Synechococcus* 7942, which accumulates biomass at a rate of 0.45 g $liter^{-1}$ day^{-1}. During the fast growth phase of *Synechococcus* 2973 (before 12 h), the glycogen content is extremely low (<1% of cell weight [dry weight {DW}]) (Fig. 2B). After that time, cells enter a linear growth phase (Fig. 2A). The glycogen content drastically increases between 19 and 25 h, changing 21-fold from 0.3% to 6.3% of DW (Fig. 2B, inset graph; also see Fig. S1 in the supplemental material). The amount of glycogen increases from 6% of DW (66 mg $liter^{-1}$) to 33% of DW (693 mg $liter^{-1}$) within the next 24-h span (24 h to 48 h) and ultimately reaches 1.1 g $liter^{-1}$ (36% of DW) by day 3 (Fig. 2B). These results reveal that *Synechococcus* 2973 directs all of its fixed carbon into growth during log phase and then rapidly transitions into directing the high flux of carbon into storage during the linear growth phase. As for *Synechococcus* 7942, the biomass and glycogen contents accumulated at much lower rates. The glycogen

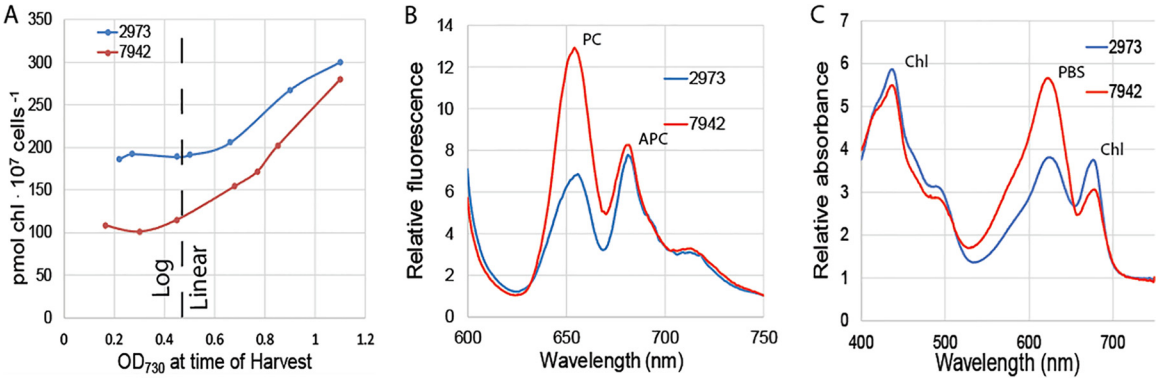

FIG 3 Pigment content of *Synechococcus* 2973 versus *Synechococcus* 7942. (A) Chlorophyll content as a function of culture density. As indicated, log growth occurs when the OD_{730} of the cell culture was below 0.4 and linear growth occurs when the OD_{730} of the cell culture was above 0.4. (B) 77 K fluorescence of *Synechococcus* 2973 versus *Synechococcus* 7942 with excitation at 590 nm. PC, phycocyanin; APC, allophycocyanin. (C) Absorption spectra of *Synechococcus* 2973 versus *Synechococcus* 7942. PBS, phycobilisome.

content is negligible during the first day of growth, and it is less than 10% (75 mg liter^{-1}) of DW at day 3 (Fig. 2B).

Pigment content. In this study, we performed several experiments that are typically normalized to chlorophyll content. When harvesting cells at similar densities, we observed large differences in chlorophyll content between samples for the two *Synechococcus* strains. The differences in chlorophyll content were also apparent in absorbance scans (Fig. 3C). If the strains differ in chlorophyll content, then normalization to chlorophyll will be an invalid method of comparison. We compared chlorophyll (Chl) content in the two strains and found that *Synechococcus* 2973 has 190 ± 7 pmol Chl 10^7 cells^{-1} s^{-1} compared to 112 ± 9 pmol Chl 10^7 cells^{-1} s^{-1} in *Synechococcus* 7942 during log-phase growth (Fig. 3A) (1). Our results show that during log-phase growth, *Synechococcus* 2973 has a 1.7-fold-higher chlorophyll content per cell compared to *Synechococcus* 7942; however, the chlorophyll content becomes more similar as the cultures enter linear growth, differing by only 1.1-fold near stationary phase. We also noted that in both strains, chlorophyll content per cell remains constant during log growth but increases as a function of culture density during linear growth. This highlights the importance of harvesting cultures during log phase when normalizing to chlorophyll content, as chlorophyll is variable during linear growth. Over the course of this study, normalization was calculated based on cell number to avoid errors caused by the different chlorophyll levels between the two strains.

Synechococcus 2973 is significantly less blue than *Synechococcus* 7942 (Fig. S2), indicating that *Synechococcus* 2973 exhibits an altered pigment composition. To examine the pigment compositions of the two strains, we determined room temperature absorption spectra from 400 nm to 750 nm. The absorbance scans were taken of cultures with equal cell numbers and normalized at 750 nm. We observed increased absorbance at 680 nm in *Synechococcus* 2973 that resulted from its increased chlorophyll content (Fig. 3C). We also observed significantly reduced phycobilisome absorbance at 625 nm, indicating that *Synechococcus* 2973 exhibits decreased phycobilisome content (Fig. 3C). We examined the difference using low-temperature fluorescence at 77 K with excitation at 590 nm to excite phycobilins and normalized at 750 nm. Phycocyanin (PC) exhibits a fluorescence maximum at 665 nm, and allophycocyanin (APC) exhibits a fluorescence maximum at 682 nm (2). We found that *Synechococcus* 2973 exhibits a significantly reduced phycocyanin fluorescence relative to *Synechococcus* 7942, while allophycocyanin fluorescence remains unchanged (Fig. 3B). In *Synechococcus* 2973, the ratio of relative fluorescence of PC/APC was 0.88, while it was 1.55 in *Synechococcus* 7942. Interestingly, the decrease in phycobilisome absorbance is a result of fewer or shorter rods (PC) rather than a reduction in the number of phycobilisome complexes, as indicated by the same fluorescence from the APC cores in both strains.

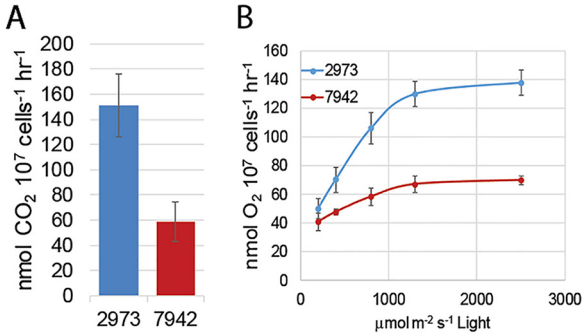

FIG 4 Photosynthetic parameters of *Synechococcus* 2973 and *Synechococcus* 7942. (A) CO_2 uptake rates. (B) Whole-chain O_2 evolution at various light intensities.

Photosynthetic parameters. We set about characterizing the photosynthetic parameters that contribute to rapid autotrophic growth. To generate biomass at a higher rate than *Synechococcus* 7942, *Synechococcus* 2973 must acquire more fixed carbon. We compared CO_2 uptake rates for the two strains and found that *Synechococcus* 2973 takes up carbon at a rate of 151 nmol CO_2 10^7 cells^{-1} h^{-1} versus 59 nmol CO_2 10^7 cells^{-1} h^{-1} for *Synechococcus* 7942 (Fig. 4A). It follows then that *Synechococcus* 2973 is also likely to exhibit higher photosynthetic rates to support higher carbon fixation rates. We compared whole-chain O_2 evolution rates for the two strains using a Clarke electrode and found that *Synechococcus* 2973 also exhibits a twofold-higher maximum rate of O_2 evolution, 139 ± 24 nmol O_2 10^7 cells^{-1} h^{-1} versus 74 ± 9 nmol O_2 10^7 cells^{-1} h^{-1} for *Synechococcus* 7942 (Fig. 4B). Under low light, the two strains differed by only 24% which mirrors the similar growth rates that are observed at low light intensities. As light intensity increases, the photosynthetic electron transport rate of *Synechococcus* 2973 increases much more rapidly than that of *Synechococcus* 7942, culminating in a twofold difference in the O_2 evolution rate. We also examined respiratory O_2 uptake in both strains. It was found that *Synechococcus* 2973 exhibits a 2.4-fold-higher rate of respiratory O_2 uptake (14.3 nmol O_2 10^7 cells^{-1} h^{-1} versus 5.9 nmol O_2 10^7 cells^{-1} h^{-1}). However, respiratory O_2 uptake is only about 10% of photosynthetic O_2 evolution and does not contribute significantly to total oxygen evolution rates.

PSII activity. We hypothesized that *Synechococcus* 2973 would have increased photosystem II (PSII) content to support the higher rate of photosynthetic O_2 evolution that we recorded (Fig. 4B). Western blot analysis was used to compare the PSII content in the two strains. Equal cell numbers of each strain were harvested, and the chlorophyll content, which varied in the two strains, was measured. After the membranes were purified, we adjusted the samples to the same chlorophyll ratio that was measured in whole cells to maintain equal cell numbers for comparison. The Western blot indicates that both strains contain similar amounts of PSII on a per cell basis (Fig. 5A). Since both strains have similar PSII contents, we hypothesized that the PSII centers in *Synechococcus* 2973 must be more active than those in *Synechococcus* 7942. We next interrogated PSII activity directly by measuring PSII-mediated O_2 evolution in the presence of saturating FeCN and 2,6-dichloro-*p*-benzoquinone (DCBQ) which accept electrons directly from PSII (2). Interestingly, we found that both strains had similar maximum capacities for PSII, as indicated by the similar rates of PSII-mediated O_2 evolution (Fig. 5B).

Comparing whole-chain to PSII-mediated O_2 evolution rates of the two strains shows that *Synechococcus* 2973 operates photosynthesis at close to its maximum capacity, while *Synechococcus* 7942 shows a significant inhibition of O_2 evolution under real-world conditions. This suggests that *Synechococcus* 7942 has a photosynthetic bottleneck in the electron transport chain (ETC) downstream of PSII that is alleviated in *Synechococcus* 2973. If electron transport out from PSII is decreased due to a lack of carriers or acceptors, there will be a bottleneck because the cells cannot transfer electrons through the ETC fast enough to keep up with PSII. If no oxidized carrier is

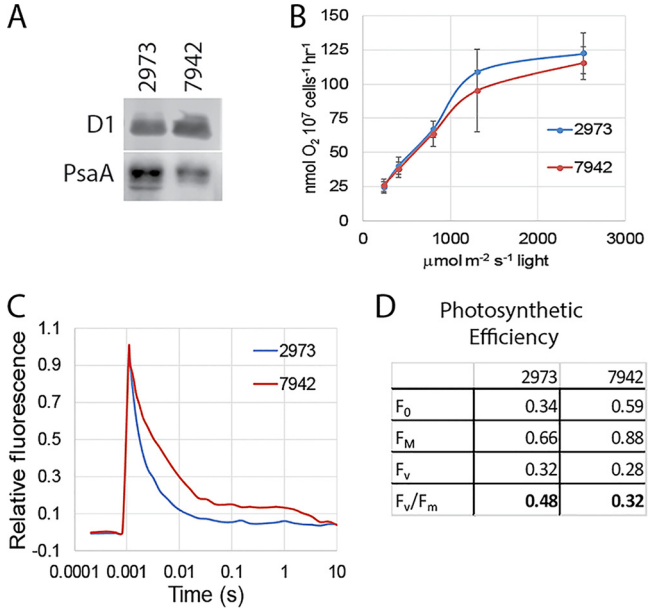

	2973	7942
F_0	0.34	0.59
F_M	0.66	0.88
F_v	0.32	0.28
F_v/F_m	**0.48**	**0.32**

FIG 5 Function of PSII. (A) Western blot loaded based on equal cell number and probed with antibodies against PSII (D1) or PSI (PsaA). (B) PSII-mediated O_2 evolution with DCMU and DBMIB. (C) Q_A^- reoxidation kinetics of *Synechococcus* 2973 versus *Synechococcus* 7942. (D) Photosynthetic efficiencies of *Synechococcus* 2973 versus *Synechococcus* 7942.

available to accept electrons from PSII, the reaction center will remain in the closed state for longer periods of time, and oxygen evolution will be decreased. While in the closed state, PSII reaction centers will release excess energy through chlorophyll fluorescence, and as PSII is reoxidized by plastoquinone, the reaction centers will reopen, and fluorescence will decrease (3). We used an FL-200 dual modulation PAM fluorometer (Photon Systems Instruments, Brno, Czech Republic) to compare primary quinone electron acceptor of reaction center II (Q_A^-) reoxidation kinetics of the two strains. After double normalization at minimum fluorescence (F_0) and maximum fluorescence (F_m), we found that the rate of Q_A^- reoxidation is significantly higher in *Synechococcus* 2973 (halftime of 1.6 ms) compared to *Synechococcus* 7942 (halftime of 3.1 ms) (Fig. 5C). This suggests that *Synechococcus* 2973 has a higher whole-chain O_2 evolution rate because it is better able to move electrons out of PSII as indicated by the increased rate of Q_A^- reoxidation.

Using the unnormalized fluorescence data, we found that variable fluorescence (F_v) was similar in both strains, which further supports both strains having similar PSII content. We also calculated the photosynthetic efficiency (F_v/F_m) of PSII for each strain (4). The F_v/F_m value obtained from *Synechococcus* 2973 is 0.48 $\pm$ 0.03, while the value obtained from *Synechococcus* 7942 is 0.32 $\pm$ 0.05 (Fig. 5D). Both strains had similar maximum capacities for PSII; however, *Synechococcus* 2973 operates PSII more efficiently under real-world conditions as indicated by whole-chain O_2 evolution and photosynthetic efficiency values. We suggest here that a downstream bottleneck in the ETC in *Synechococcus* 7942 causes a backup of electron flow which slows turnover of PSII, because reaction centers are stuck in the closed state for longer periods of time.

In *Synechococcus* 7942, the PSI/PSII ratio varies from 2 to 3.5 (5–7), and there are 96 chlorophyll molecules per PSI center compared to 35 chlorophyll molecules per PSII center; thus, most of the chlorophyll is found associated with PSI (8–10). Therefore, we hypothesized that the increased chlorophyll content would be associated with an increase in PSI content in *Synechococcus* 2973. We measured photoactive PSI content to estimate total PSI content per cell. A JTS-10 pump probe spectrophotometer (BioLogic Science Instruments) was used to measure maximum A_{705} of fully oxidized PSI after a saturating light pulse in the presence of dibromothymoquinone (DBMIB) and

TABLE 1 PSI content of *Synechococcus* 2973 and *Synechococcus* 7942

Synechococcus strain	PSI content (pmol/10^7 cells)	Chlorophyll content (pmol/10^7 cells)	No. of chlorophyll molecules/PSI
2973	1.95	189	96.9
7942	1.19	119	100

3-(3′,4′-dichlorophenyl)-1,1-dimethylurea (DCMU) to block cyclic and linear electron flow. A molar extinction coefficient for $P700^+$ of 70 mM^{-1} cm^{-1} was used to obtain the concentration of photo-oxidizable PSI in the sample (10). *Synechococcus* 2973 was found to have 1.95 ± 0.2 pmol PSI per 10^7 cells, while *Synechococcus* 7942 has 1.19 ± 0.2 pmol PSI per 10^7 cells (Table 1). Therefore, *Synechococcus* 2973 has 1.6-fold more PSI per cell, which suggests that the 1.7-fold increase in chlorophyll in *Synechococcus* 2973 results exclusively from increased PSI content. We also compared the PSI contents of the two strains by Western blotting and quantitated 1.7-fold-more PSI in *Synechococcus* 2973 than in *Synechococcus* 7942 by this method (Fig. 5A). Not all PSI centers may be photo-oxidizable, thus we validated our estimate by calculating the number of chlorophyll molecules per PSI center based on our measurement of the total amount of chlorophyll and number of PSI centers obtained. We calculated that *Synechococcus* 2973 had 97 chlorophyll molecules per PSI center, while *Synechococcus* 7942 had 100 chlorophyll molecules per PSI center (Table 1). There should be 96 chlorophyll molecules per PSI center plus a small amount of chlorophyll in PSII. Taking the PSI/PSII ratio into consideration, our estimation of PSI content is within 10% of the expected value based on chlorophyll content.

Cytochrome *f* and plastocyanin kinetics. We have demonstrated that *Synechococcus* 2973 displays a higher photosynthetic rate than *Synechococcus* 7942 and that the increased rate is due to an ETC bottleneck downstream of PSII being alleviated. It is likely that increased PSI content leads to more efficient flow of electrons through the ETC by oxidizing upstream ETC carriers so that they may accept more electrons. To examine this in more detail, we studied cytochrome *f* and plastocyanin redox kinetics using a highly sensitive JTS-10 pump probe spectrophotometer.

For cytochrome *f*, absorption decreases as a function of oxidation. An initial drop in absorption upon illumination is due to $P700^+$ pulling electrons off cytochrome *f* (through plastocyanin), followed by a rise in absorption at ~150 ms after illumination that is caused by the arrival of electrons from PSII. Absorption then falls again, as PSI draws off electrons faster than PSII can replenish them until the light is turned off, at which time cytochrome *f* returns to the dark-adapted state. We subjected samples that were adjusted to equal cell numbers to determine the oxidation-reduction kinetics of the cytochrome complex in the two cyanobacterial strains (Fig. 6A). Due to the

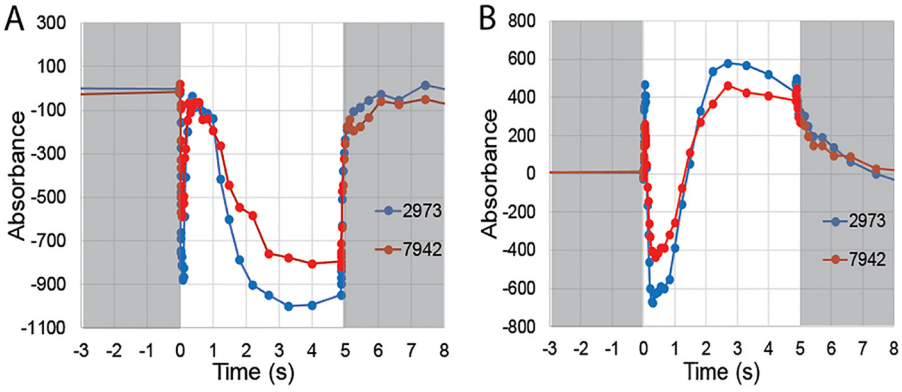

FIG 6 Cytochrome b_6f and plastocyanin oxidation-reduction kinetics in *Synechococcus* 2973 and *Synechococcus* 7942. (A) Cytochrome *f* kinetics. (B) Plastocyanin kinetics. Dark (gray background) and light (white background) conditions are indicated in the figure.

increased PSI content of *Synechococcus* 2973, we observed a stronger initial oxidation of the cytochrome *f* pool upon illumination in this strain. Both strains have similar PSII contents, and both return the cytochrome *f* pool to the resting state with the initial pulse of electrons; however, the cytochrome pool became more oxidized once again after ~2-s illumination in *Synechococcus* 2973, because the increased concentration of $P700^+$ has stronger oxidizing power for the plastocyanin pool, which in turn oxidizes the cytochrome *f* pool. Careful examination of these data reveals a bottleneck in the ETC. Immediately upon illumination, the oxidizing power of PSI generates a more oxidized cytochrome *f* pool in *Synechococcus* 2973. This creates a larger hole for the electrons to flow into and allows more influx of electrons from PSII. The initial pulse of electrons is sufficient to fully rereduce the cytochrome *f* pool in both strains; however, in *Synechococcus* 2973, the oxidized cytochrome *f* pool must accept more electrons to reach the fully reduced state. Since both strains have equal capacities for PSII, but the cytochrome *f* pool in *Synechococcus* 2973 can accept more electrons, higher electron flux through cytochrome *f* would be allowed in *Synechococcus* 2973.

From the same series of experiments, we also determined the kinetics of plastocyanin oxidation and reduction (Fig. 6B) (11, 12). In the case of plastocyanin, absorption increases with oxidation and decreases with reduction. An initial rise in absorption upon illumination is due to $P700^+$ oxidizing the plastocyanin pool. As the initial burst of electrons arrives from PSII through cytochrome *f*, the absorption drops to below the initial level. Finally, the absorption increases again, as $P700^+$ removes electrons from the plastocyanin pool faster than they are replenished. Comparing cytochrome *f* and plastocyanin kinetics of the two strains at 300 ms after illumination reveals more about the bottleneck in the ETC. Plastocyanin is more deeply oxidized immediately upon illumination; it is more deeply reduced by electrons arriving from PSII 300 ms after illumination. At 300 to 800 ms, the cytochrome *f* pool is fully rereduced and cannot accept additional electrons in either strain, but the plastocyanin pool is more deeply reduced by the initial burst of electrons from PSII; thus, more electrons are passing through cytochrome *f* into plastocyanin in *Synechococcus* 2973 under steady-state conditions. Therefore, we conclude that the bottleneck in the ETC occurs as the electrons are passing through cytochrome *f*.

We repeated the experiment on cytochrome *f* and plastocyanin kinetics in the presence of the inhibitors DCMU, DBMIB, and methyl viologen (Fig. S3). This set of inhibitors prevents electrons from flowing into cytochrome *f* and plastocyanin while allowing both pools to become fully oxidized by PSI. After 2.5 s of saturating light, we collected the maximum absorbance and applied extinction coefficients of 18 mM cm^{-1} and 4.7 mM cm^{-1} for cytochrome *f* and plastocyanin, respectively, to determine the concentration of each within the cell (Fig. S2) (11, 13). We found that *Synechococcus* 2973 has 1.38 ± 0.1 pmol cytochrome *f* per 10^7 cells, while *Synechococcus* 7942 has only 0.86 ± 0.1 pmol cytochrome *f* per 10^7 cells. The plastocyanin contents were 2.21 ± 0.3 pmol per 10^7 cells and 1.07 ± 0.2 pmol per 10^7 cells for *Synechococcus* 2973 and *Synechococcus* 7942, respectively. Therefore, on a cellular basis, *Synechococcus* 2973 shows a 1.5-fold increase in cytochrome *f* and a 2.2-fold increase in plastocyanin. Increased contents of carriers in the electron transport chain allows higher flux of electrons through the ETC to complement the increased PSI capacity, which leads to higher photosynthetic rates in *Synechococcus* 2973.

DISCUSSION

Synechococcus 2973 and *Synechococcus* 7942 are nearly genetically identical strains. However, *Synechococcus* 2973 exhibits a 3-fold-higher growth rate and a 2.5-fold-higher rate of glycogen accumulation, which are the result of a 2.5-fold increase in carbon uptake and 1.9-fold-higher rate of O_2 evolution, indicating higher photosynthetic rates in *Synechococcus* 2973. Both strains have similar PSII contents, and as such, the maximum photosynthetic capacity of PSII is the same in both strains. The higher photosynthetic rate is the result of a 1.5-fold increase in photosynthetic efficiency in *Synechococcus* 2973. The increase is attributable to a 1.9-fold increase in the rate

that electrons exit PSII (Q_A^- reoxidation), a 1.6-fold increase in PSI content, a 1.5-fold increase in cytochrome *f* content, and a 2.2-fold increase in plastocyanin content. It is worth noting that all the aforementioned fold increases in *Synechococcus* 2973 correlate well with each other.

Both strains share the same capacity of PSII; however, *Synechococcus* 2973 displays a higher flux of electrons from water to CO_2 as indicated by its higher carbon fixation rate and higher rate of whole-chain oxygen evolution. *Synechococcus* 7942 displays a marked bottleneck in the ETC that reduces flux from CO_2 to water, reduces photosynthetic efficiency, and decreases photosynthetic rates under real-world conditions. This bottleneck is alleviated in *Synechococcus* 2973. The specific location of the bottleneck occurs as the electrons pass through the cytochrome b_6f complex. Since both strains have the same capacity of PSII as indicated by PSII-mediated O_2 evolution, both strains should be capable of sending a similar number of electrons from PSII under saturating light. However, this is not the case under real-world conditions. *Synechococcus* 2973 shows a higher flux of electrons out of PSII as indicated by the faster Q_A^- reoxidation kinetics. Although the potential electron flux from PSII is similar for both strains, *Synechococcus* 2973 has a larger pool of downstream ETC carriers waiting to receive the electrons, which allows higher photosynthetic electron flux in the strain. An initial pulse of electrons fully returns cytochrome *f* back to the reduced state in both *Synechococcus* strains; however, *Synechococcus* 2973 accepts more reducing equivalents to reach the resting state, because the oxidized cytochrome *f* pool is larger. Since the same number of electrons could leave PSII in both strains, but more electrons can be accepted by cytochrome *f* in *Synechococcus* 2973, we conclude that the unaccepted electrons back up in the ETC in *Synechococcus* 7942. The lack of available oxidized carriers in the ETC limits the electrons from moving on from PSII. The reduced flux of electrons out of PSII was duly noted in our measurements of Q_A^- reoxidation kinetics. The backed-up electrons cause the PSII reaction centers to remain in the closed state for longer periods of time, which reduces the photosynthetic efficiency and results in a lower rate of O_2 evolution under real-world conditions. It is likely that this also increases the propensity of photodamage in *Synechococcus* 7942, making it sensitive to high light intensities.

Synechococcus 2973 overcomes the bottleneck by displaying both increased levels of electron carriers in the ETC and increased PSI content, which serves to pull more electrons through the ETC. Although we were not able to address plastoquinone levels, we conclude that they are sufficiently high to not impede electron flow, because we observed that the cytochrome *f* pool becomes fully rereduced to the dark-adapted state by the initial pulse of electrons from PSII in both strains. In *Synechococcus* 2973, the increased levels of cytochrome *f* and plastocyanin serve to allow a larger volume of electron flux through the ETC. The increased level of PSI serves to oxidize the increased levels of electron carriers so that they can accept electrons. Together, these two features result in increased light-driven electron transfer rates which drive a higher rate of carbon fixation, thus increasing photosynthetic efficiency in *Synechococcus* 2973. The ability of *Synechococcus* 2973 to empty electrons out of PSII more efficiently and rapidly would also serve to reduce photodamage by reducing the propensity for charge recombination that exists while reaction centers are stuck in the closed state. Therefore, the more efficient electron transport chain would increase light tolerance by reducing the rate of photodamage in *Synechococcus* 2973. It is interesting that *Synechococcus* 7942 has the PSII capacity to support a much higher rate of photosynthesis, but the lack of downstream carriers creates a bottleneck in the ETC that suppresses the photosynthetic rate. It has also been previously shown that overexpression of plastocyanin from *Anabaena* in *Synechococcus* 7942 increases electron transport ~2.5-fold (14). Cyanobacteria are recognized for their high PSI/PSII ratio in conjunction with high photosynthetic efficiencies compared to higher plants. In this study, we found that further increasing this ratio by 1.7-fold generated a significant boost in photosynthetic efficiency as well as productivity. *Synechococcus* 2973 operates PSII at near maximum capacity, while *Synechococcus* 7942 and other widely used cyanobacteria such as *Synechocystis* sp. strain PCC 6803 operate PSII at well below their maximum capacity. It is also worth

noting that *Synechococcus* 2973 seems specifically adapted to a high light environment. It shows a significant reduction in phycobilisome antennae, which are less important under saturating light but useful under low light. Phycobilisomes are costly to make, and their reduction may free up resources for the increased production of other photosynthetic components such as more PSI and higher levels of ETC carriers. Interestingly, the observations reported here are predicted by the autotrophic replicator model (ARM) where the autotrophic growth rate is formulated as a proteome allocation optimization problem. This model predicts that increased growth rate would be associated with increased allocation of proteins to photosynthetic electron transport at the expense of protein resources being allocated to light-harvesting complexes (15).

The results presented in this study suggest a strategy for improving photosynthetic efficiency and ultimately productivity in these and other cyanobacteria. It is commonly accepted that RuBisCO activity is the limiting factor in photosynthesis. Here we show that electron flux through the photosynthetic electron transport chain, and hence energy production, limits the photosynthetic rate in *Synechococcus* 7942. Future work will be needed to identify which of the 55 single nucleotide differences between the two organisms lead to the marked changes in the photosynthetic apparatus that we report here.

MATERIALS AND METHODS

Strains and growth conditions. *Synechococcus elongatus* UTEX 2973 (*Synechococcus* 2973) and *Synechococcus elongatus* PCC 7942 (*Synechococcus* 7942) were maintained on BG11 agar plates at 38°C with 125 μmol m^{-2} s^{-1} light. *Synechococcus* 2973 was routinely grown in BG11 liquid medium at 38°C with 900 μmol m^{-2} s^{-1} light and 5% CO_2 in an MC-1000 multicultivator (Photon Systems Instruments, Czech Republic). *Synechococcus* 7942 was routinely grown in BG11 liquid medium at 38°C with 400 μmol m^{-2} s^{-1} light and 5% CO_2 in an MC-1000 multicultivator. For growth curves, strains were grown under the conditions indicated. The multicultivator was used to simultaneously grow eight cultures under different conditions and record the optical density at 730 nm (OD_{730}) of the cultures every 5 min over the course of the growth experiment. Growth rates (K') were calculated using Microsoft Excel by fitting an exponential curve to the logarithmic section of the growth data (typically OD_{720} of <0.3) and using the slope, m, as K' ($y = ke^{mx}$). Doubling times were then calculated as ln(2)/K'.

Glycogen determination. Cultures were collected by centrifugation, and the pellets were resuspended with 300 μl KOH (30% [wt/vol]) each and incubated at 95°C for 90 min. Glycogen was precipitated by adding 1.2 ml absolute ethanol, and the samples were kept on ice for 2 h. Glycogen was collected by centrifugation at full speed (16K $\times$ *g*) for 5 min. The pellets were washed twice with 1 ml absolute ethanol. The washed pellets were dried at 60°C for 15 min until the remaining ethanol was evaporated. The dried samples were resuspended in 300 μl sodium acetate solution (100 mM, pH 4.75). Then, glycogen was digested to glucose by amyloglucosidase (4 U/assay) for 25 min at 55°C. After digestion, the insoluble pellets were removed by centrifugation, and the supernatants were used for determining the glycogen content using a glucose (HK) assay kit (Sigma, USA). Samples that were not treated with amyloglucosidase were included to determine the background glucose content. By subtraction of the background glucose content, the actual glycogen concentration was determined.

Thylakoid membrane preparation. The *Synechococcus* 2973 and *Synechococcus* 7942 preparations with same cell numbers were harvested and broken by bead-beating technique (16). Thylakoid membranes were resuspended in RB (50 mM morpholineethanesulfonic acid [MES]–NaOH [pH 6.0], 10 mM $MgCl_2$, 5 mM $CaCl_2$, 25% glycerol) and mixed with β-D-dodecyl maltoside (DDM) to a final concentration of 1% DDM, and then incubated on ice in the dark for 30 min. Solubilized membranes were isolated by ultracentrifugation at gradually increasing speed from 120 to 27,000 $\times$ *g* at 4°C for about 20 min. The solubilized membranes were then stored at −80°C for further use.

SDS-PAGE and immunoblot analysis. The solubilized membranes of *Synechococcus* 2973 and *Synechococcus* 7942 were loaded on an equal cell number basis. Proteins were analyzed by SDS-PAGE as described previously (17). For the immunoblot analysis, the SDS-polyacrylamide gels were blotted onto polyvinylidene difluoride (PVDF) membranes. The membranes were then incubated with PsaA- and D1-specific primary antibodies, respectively, and then incubated with secondary antibodies (horseradish peroxidase [HRP]). The target proteins were detected and visualized by chemiluminescence on an ImageQuant LAS-4000 imager.

Cell counting. Cultures were grown in MC-1000 multicultivators at 38°C, 5% CO_2, and with 900 or 400 μmol m^{-2} s^{-1} light for *Synechococcus* 2973 and *Synechococcus* 7942, respectively. Twenty microliters of culture was removed at various time points during growth, and cells were counted with an automated cell counter (Cellometer Vision; Nexcelom). The counted images were manually curated to improve accuracy of the counts. The accompanying Cellometer software reported cell counts in cells per milliliter after curation. The counts were used to construct an accurate six-point standard curve of each strain for cell number versus OD_{730} reported by the multicultivator for cultures ranging in densities from OD_{730} values of 0.1 to 1.0. The relationship was found to be linear over this entire range. The standard curve was used to convert OD_{730} to cell number in later experiments.

Chlorophyll content. Cultures were grown in MC-1000 multicultivators at 38°C, 5% CO_2, and either 900 or 400 μmol m^{-2} s^{-1} light for *Synechococcus* 2973 and *Synechococcus* 7942, respectively. One milliliter of culture was removed at various time points during growth, and the chlorophyll content was determined by a methanol extraction method (1).

77 K fluorescence. Cultures were grown in MC-1000 multicultivators at 38°C, 5% CO_2, and either 900 or 400 μmol m^{-2} s^{-1} light for *Synechococcus* 2973 and *Synechococcus* 7942, respectively. The fluorescence emission spectra of phycobilisomes from whole cells of each strain were measured at 77 K with samples adjusted to equal cell number (2×10^8 cells per ml). Excitation occurred at 590 nm, and fluorescence emission was recorded between 600 nm and 750 nm and normalized at 750 nm. The measurements were made on a SPEX fluoromax 2 spectrofluorimeter and analyzed with Data Max for Windows.

Absorption spectra. Cultures were grown in MC-1000 multicultivators at 38°C, 5% CO_2, and either 900 or 400 μmol m^{-2} s^{-1} light for *Synechococcus* 2973 and *Synechococcus* 7942, respectively. Absorption spectra of *Synechococcus* 2973 and *Synechococcus* 7942 that were harvested during log phase were determined on an Olis DW-2000 spectrophotometer, and data were analyzed with Olis Globalworks software. Spectra were normalized at 750 nm to correct for differences in light scattering.

CO_2 uptake rate. *Synechococcus* 2973 and *Synechococcus* 7942 were grown in an MC-1000 multicultivator (Photon Systems Instruments) to an OD_{730} of 0.5. *Synechococcus* 2973 was grown at 900 μmol m^{-2} s^{-1} light, and *Synechococcus* 7942 was grown at 400 μmol m^{-2} s^{-1} light. Two 1-ml samples were sealed in 13-ml Hungate tubes with rubber septa and sparged with 3% CO_2 for 5 min. One tube for each strain was placed on its side on a shaker under its respective white light-emitting diode (LED) illumination (900 or 400 μE m^{-2} s^{-1}) at 38°C for 1 h after which time total CO_2 was measured by gas chromatography (GC). The second tube was measured immediately without incubation to determine initial CO_2. Total CO_2 was calculated as the sum of the dissolved plus gaseous CO_2 within a sealed system. Total CO_2 of the system was determined after injecting 100 μl of 10 N HCl into the tube to force dissolved CO_2 out of solution, followed by quantification of the headspace CO_2 content on an HP 5980 gas chromatograph under the following conditions: temperature of 100°C; carrier gas, helium at a flow rate of 40 ml min^{-1}; using a Porapak N column and thermal conductivity detector (TCD). CO_2 uptake was determined as follows: initial total CO_2 − final total CO_2.

Oxygen evolution. Cells were harvested during log growth and adjusted based on equal cell numbers. The light-induced oxygen evolution was measured for 1 min at 38°C with a custom-built Clark-type electrode (18). For the light saturation curves, different neutral density filters were placed in front of the halogen light source to achieve different light intensities. For whole-chain O_2 evolution, $NaHCO_3$ was added to 10 mM. For the measurements of PSII-mediated O_2 evolution, we added potassium ferricyanide (FeCN) to 1.2 mM and 2,6-dichloro-*p*-benzoquinone (DCBQ) to 0.6 mM.

Room temperature fluorescence kinetics. The kinetics of chlorophyll *a* (Chl *a*) fluorescence and the fluorescence parameters F_v/F_m (maximum quantum yield) of photosystem II (PSII) were measured using a double-modulation fluorescence fluorometer, FL-200 (Photon Systems Instruments, Brno, Czech Republic) (19). The instrument contained red LEDs for both actinic (20-μs) and measuring (2.5-μs) flashes and was used in the time range of 100 μs to 100 s. Data from both strains were double normalized at F_0 and F_m, which were set at a relative fluorescence of 0 and 1, respectively.

PSI content. Cultures were grown in MC-1000 multicultivators at 38°C, 5% CO_2, and either 900 or 400 μmol m^{-2} s^{-1} light for *Synechococcus* 2973 and *Synechococcus* 7942, respectively. Cells were harvested during log phase, cultures were adjusted to have equal cell numbers, and chlorophyll content was recorded. Then, 10 μM 3-(3′,4′-dichlorophenyl)-1,1-dimethylurea (DCMU) and 20 μM dibromothymoquinone (DBMIB) were added to block both linear and cyclic electron flow and changes in the absorbance at 705 nm of $P700^+$ were recorded for 5 s under saturating light on a JTS-10 pump probe spectrophotometer. A molar extinction coefficient for $P700^+$ of 70 mM^{-1} cm^{-1} was used to calculate the PSI content from the maximum absorbance.

Cytochrome *f* and plastocyanin kinetics. Cytochrome *f* and plastocyanin redox kinetics were recorded on a JTS-10 pump probe spectrophotometer (BioLogic Science Instruments, Grenoble, France). Cells were grown to mid-log phase in an MC-1000 multicultivator at 38°C, 5% CO_2, and either 900 or 400 μmol m^{-2} s^{-1} light for *Synechococcus* 2973 and *Synechococcus* 7942, respectively. After harvest, the cell samples were adjusted to equal cell numbers and then dark adapted for 3 min before measurements were taken. Absorbance changes due to cytochrome *f* and plastocyanin oxidation and reduction were probed with a measuring beam consisting of short pulses provided by a white LED, and light was filtered through a 10-nm bandwidth interference filter centered at 546 nm, 554 nm, 563 nm, and 573 nm in separate experiments. Long-pass 3-mm-thick BG39 filters were placed in front of the detectors to block the light from an actinic LED emitting in the 720-nm region. Continuous far-red actinic illumination of 5 s was interrupted by short (200-μs) dark pulses, during which detecting pulses from the white LED were delivered. The data sets collected from experiments with the four interference filters were then deconvoluted to generate cytochrome *f* and plastocyanin absorption signals.

SUPPLEMENTAL MATERIAL

Supplemental material for this article may be found at https://doi.org/10.1128/mBio.02327-17.

FIG S1, TIF file, 0.04 MB.

FIG S2, TIF file, 0.2 MB.

FIG S3, TIF file, 0.1 MB.

TABLE S1, DOCX file, 0.02 MB.

ACKNOWLEDGMENTS

This study was supported by funding from NSF (MCB-1546840) to H.B.P.

P.-C.L. collected data on glycogen accumulation, H.-Y.C. performed Western blotting. J.U. performed all other experiments and wrote the article. H.B.P. and J.U. edited the article.

We declare that we have no conflicts of interest.

REFERENCES

1. Porra RJ, Thompson WA, Kriedemann PE. 1989. Determination of accurate extinction coefficients and simultaneous equations for assaying chlorophylls a and b extracted with four different solvents: verification of the concentration of chlorophyll standards by atomic absorption spectroscopy. Biochim Biophys Acta 975:384–394. https://doi.org/10.1016/S0005-2728(89)80347-0.
2. Yu J, Wu Q, Mao H, Zhao N, Vermaas WFJ. 1999. Effects of chlorophyll availability on phycobilisomes in *Synechocystis* sp. PCC 6803. IUBMB Life 48:625–630. https://doi.org/10.1080/713803568.
3. Kalaji HM, Schansker G, Ladle RJ, Goltsev V, Bosa K, Allakhverdiev SI, Brestic M, Bussotti F, Calatayud A, Dąbrowski P, Elsheery NI, Ferroni L, Guidi L, Hogewoning SW, Jajoo A, Misra AN, Nebauer SG, Pancaldi S, Penella C, Poli D, Pollastrini M, Romanowska-Duda ZB, Rutkowska B, Serôdio J, Suresh K, Szulc W, Tambussi E, Yanniccari M, Zivcak M. 2014. Frequently asked questions about in vivo chlorophyll fluorescence: practical issues. Photosynth Res 122:121–158. https://doi.org/10.1007/s11120-014-0024-6.
4. Kromkamp J, Barranguet C, Peene J. 1998. Determination of microphytobenthos PSII quantum efficiency and photosynthetic activity by means of variable chlorophyll fluorescence. Mar Ecol Prog Ser 162:45–55. https://doi.org/10.3354/meps162045.
5. Fraser JM, Tulk SE, Jeans JA, Campbell DA, Bibby TS, Cockshutt AM. 2013. Photophysiological and photosynthetic complex changes during iron starvation in *Synechocystis* sp. PCC 6803 and *Synechococcus elongatus* PCC 7942. PLoS One 8:e59861. https://doi.org/10.1371/journal.pone.0059861.
6. Vermaas WFJ. 25 April 2001. Photosynthesis and respiration in cyanobacteria. *In* eLS. John Wiley & Sons Ltd, Chichester, United Kingdom. https://doi.org/10.1038/npg.els.0001670.
7. Matthijs HCP, van der Staay GWM, Mur LR. 1994. Prochlorophytes: the 'other' cyanobacteria?, p 49–64. *In* Bryant DA (ed), Advances in photosynthesis, vol 1. The molecular biology of cyanobacteria. Springer, Dordrecht, Netherlands. https://doi.org/10.1007/978-94-011-0227-8_3.
8. Tchernov D, Helman Y, Keren N, Luz B, Ohad I, Reinhold L, Ogawa T, Kaplan A. 2001. Passive entry of CO_2 and its energy-dependent intracellular conversion to HCO_3^- in cyanobacteria are driven by a photosystem I-generated $\Delta\mu H^+$. J Biol Chem 276:23450–23455. https://doi.org/10.1074/jbc.M101973200.
9. Umena Y, Kawakami K, Shen J-R, Kamiya N. 2011. Crystal structure of oxygen-evolving photosystem II at a resolution of 1.9 A. Nature 473:55–60. https://doi.org/10.1038/nature09913.
10. Vermaas WFJ, Timlin JA, Jones HDT, Sinclair MB, Nieman LT, Hamad SW, Melgaard DK, Haaland DM. 2008. In vivo hyperspectral confocal fluorescence imaging to determine pigment localization and distribution in cyanobacterial cells. Proc Natl Acad Sci U S A 105:4050–4055. https://doi.org/10.1073/pnas.0708090105.
11. Pierre Y, Breyton C, Kramer D, Popot J-L. 1995. Purification and characterization of the cytochrome b6f complex from *Chlamydomonas reinhardtii*. J Biol Chem 270:29342–29349. https://doi.org/10.1074/jbc.270.49.29342.
12. Bailleul B, Johnson X, Finazzi G, Barber J, Rappaport F, Telfer A. 2008. The thermodynamics and kinetics of electron transfer between cytochrome b6f and photosystem I in the chlorophyll d-dominated cyanobacterium, *Acaryochloris marina*. J Biol Chem 283:25218–25226. https://doi.org/10.1074/jbc.M803047200.
13. Yoshizaki F, Sugimura Y, Shimokoriyama M. 1981. Purification, crystallization, and properties of plastocyanin from a green alga, *Enteromorpha prolifera*. J Biochem 89:1533–1539. https://doi.org/10.1093/oxfordjournals.jbchem.a133346.
14. Geerts D, Schubert H, de Vrieze G, Borrias M, Matthijs HC, Weisbeek PJ. 1994. Expression of *Anabaena* PCC 7937 plastocyanin in *Synechococcus* PCC 7942 enhances photosynthetic electron transfer and alters the electron distribution between photosystem I and cytochrome-*c* oxidase. J Biol Chem 269:28068–28075.
15. Burnap RL. 2015. Systems and photosystems: cellular limits of autotrophic productivity in cyanobacteria. Front Bioeng Biotechnol 3:1. https://doi.org/10.3389/fbioe.2015.00001.
16. Kashino Y, Lauber WM, Carroll JA, Wang Q, Whitmarsh J, Satoh K, Pakrasi HB. 2002. Proteomic analysis of a highly active photosystem II preparation from the cyanobacterium *Synechocystis* sp. PCC 6803 reveals the presence of novel polypeptides. Biochemistry 41:8004–8012.
17. Burnap RL, Troyan T, Sherman LA. 1993. The highly abundant chlorophyll-protein complex of iron-deficient *Synechococcus* sp. PCC 7942 (Cp43′) is encoded by the *isiA* gene. Plant Physiol 103:893–902. https://doi.org/10.1104/pp.103.3.893.
18. Nedbal L, Gibas C, Whitmarsh J. 1991. Light saturation curves show competence of the water splitting complex in inactive photosystem II reaction centers. Photosynth Res 30:85–94. https://doi.org/10.1007/BF00042006.
19. Trtílek M, Kramer DM, Koblížek M, Nedbal L. 1997. Dual-modulation LED kinetic fluorometer. J Lumin 72-74:597–599. https://doi.org/10.1016/S0022-2313(97)00066-5.
20. Yu J, Liberton M, Cliften PF, Head RD, Jacobs JM, Smith RD, Koppenaal DW, Brand JJ, Pakrasi HB. 2015. *Synechococcus elongatus* UTEX 2973, a fast growing cyanobacterial chassis for biosynthesis using light and CO_2. Scientific Reports 5:8132. https://doi.org/10.1038/srep08132.